Departamento de Biología Molecular
Facultad de Ciencias
Universidad Autónoma de Madrid

Tesis Doctoral

"Functional interplay between c-Myc and Max in B lymphocyte differentiation"

Mercedes Pérez Olivares

Febrero, 2019

INDEX

ABSTRACT

ABSTRACT

All blood cell lineages are generated from hematopoietic stem cells (HSCs) which undergo a progressive differentiation process towards lineage commitment. B lymphocytes are cells of the innate immune system that differentiate via well-defined stages of maturation in a process associated with rearrangements of the B cell receptor (BCR) gene segments V(D)J. This process is tightly regulated by several transcription factors, among which is c-Myc.

The *c-myc*, *n-myc* and *l-myc* proto-oncogenes are members of the Myc family of transcription factors. These proteins contain a basic-region/helix-loop-helix/leuzine zipper (bHLH-LZ) motif at their C-terminal end, and regulate multiple cellular functions such as cell proliferation, apoptosis and differentiation. Deregulation of the expression of *myc* genes has a prominent impact in human health. In fact, it is estimated that up to 50% of all human cancers have a constitutive enhanced expression of Myc family proto-oncogenes. Among them, c-Myc is the most widely expressed and relevant in primary B lymphocytes.

Most of the literature assumes that c-Myc functions rely entirely on its ability to form heterodimers with its mandatory partner Max. However, there is evidence suggesting that c-Myc can perform some functions in a Max-independent context. Thus, the functional interplay *in vivo* between c-Myc and Max is poorly understood, due in part to the early embryonic lethality associated with germline deletion of Max and c-Myc. In this work, we have generated new *in vivo* models to study the collaboration and dependency between Max and c-Myc in early and terminal B lymphocyte differentiation.

We observed that c-Myc requires Max for normal B lymphocyte differentiation and function. However, we unexpectedly found that some key B cell biological functions such as cell differentiation, proliferation or DNA replication can be initiated in the absence of Max and c-Myc/Max. Thus, we suggest that c-Myc/Max heterodimers are not essential for the initiation of some B cell functions, but both factors are required for fine-tuning the initial response upon activation.

RESUMEN

La mayoría de las células de la sangre se generan a partir de células madre hematopoyéticas que sufren un proceso progresivo de diferenciación hasta convertirse en células de un linaje concreto. Los linfocitos B son células del sistema inmune innato que se diferencian en estadios de maduración asociados a reordenamientos en los segmentos génicos V(D)J del receptor de linfocitos B. Este proceso, se encuentra regulado por múltiples factores de transcripción, entre los que se encuentra c-Myc.

Los proto-oncogenes *c-myc*, *n-myc* y *l-myc* son miembros de familia Myc de factores de transcripción. Estas proteínas se caracterizan por tener un dominio región básica/hélice-giro-hélice/cremallera de leucina en su extremo C terminal, y regulan múltiples funciones celulares tales como la proliferación celular, la apoptosis o la diferenciación celular. De hecho, se estima que más del 50% de todos los cánceres humanos se caracterizan por tener una expresión constitutivamente elevada de los proto-oncogenes de la familia Myc. De todos ellos, c-Myc es el factor de transcripción más expresado e importarte en los linfocitos B primarios.

La mayoría de la literatura asume que las funciones de Myc dependen exclusivamente de su capacidad para formar heterodímeros con la proteína Max. Sin embargo, existen algunos trabajos que sugieren que Max podría realizar determinadas funciones en ausencia de Myc. A pesar de ello, no se conoce bien la relación entre c-Myc y Max *in vivo*, en parte debido a la letalidad embrionaria asociada a la deleción de Max y c-Myc en la línea germinal. En este trabajo, hemos generado nuevos modelos experimentales *in vivo* para estudiar la colaboración y la dependencia entre Max y c-Myc en la diferenciación temprana y tardía de linfocitos B.

Observamos que c-Myc necesita Max para la correcta diferenciación y función de los linfocitos B. Sin embargo, encontramos que algunas funciones biológicas básicas de las células B, pueden iniciarse en ausencia de Max y de c-Myc/Max. Por lo tanto, sugerimos que los heterodímeros c-Myc/Max no son esenciales para la iniciación de algunas funciones en los linfocitos B, pero ambos factores son necesarios para que se produzca una regulación precisa del la respuesta inicial tras la activación.

ABBREVIATIONS

Abbreviation	Full name
7-AAD	7-AminoActinoMycin
aa	Amino acids
ASC	Antibody-Secreting Cell
BCR	B Cell Receptor
bFGF	basic Fibroblast Growth Factor
BM	Bone Marrow
BP	Biological Process
BSA	Bovine Serum Albumin
CD	Cluster of Differentiation
CDK	Cyclin-Dependent Kinase
CKI	Cyclin-dependent Kinase Inhibitor
CldU	5-Chloro-2'-deoxyUridine
CLP	Common Lymphoid Progenitor
CSR	Class Switch Recombination
DDK	Dbf4-Dependent Kinase
DEG	Differentially Expressed Genes
DKO	Double KnockOut
DNA	DeoxyriboNucleic Acid
dNTP	DeoxyriboNucleotide TriPhosphate
EdU	5-Ethynil-2'-deoxyUridine
ESC	Embryonic Stem Cell
FBS	Fetal Bovine Serum
FC	Fold Change
FDR	False Discovery Rate
Flt3-L	FMS-related Tyrosine kinase 3 Ligand
GC	Germinal Center
GFP	Green Fluorescent Protein
GO	Gene Ontology
GTRD	Gene Transcription Regulation Database
HAT	Histone Acetyl Transferase
HDAC	Histone DeACetylase
HLH	Helix-Loop-Helix
HSC	Hematopoietic Stem Cell
IdU	5-Iodo-2'-deoxyUridine
IF	ImmunoFluorescence
Ig	Immunoglobulin
IL	InterLeukin
kDa	kiloDalton
KEGG	Kyoto Encyclopedia of Genes and Genomes
KO	KnockOut
LPS	LipoPolySaccharide

LZ	LeuzineLeucine Zipper
MALT	Mucosae-Associated Lymphoid Tissue
MAX	Myc-Associated factor X
MCM	MiniChromosome Maintenance
MF	Molecular Function
MFI	Mean Fluorescence Intensity
mRNA	messenger RiboNucleic Acid
MZ	Marginal Zone
NK	Natural Killer
NLS	Nuclear Localization Signal
OCT	Optimal Cutting Temperature
ORC	Origin Recognition Complex
PBS	Phosphate-Buffered Saline
PCR	Polymerase Chain Reaction
PFA	ParaFormAldehyde
PNA	PeaNut Agglutinin
pre-RC	pre-Replication Complex
RNA	RiboNucleic Acid
RT	Room Temperature
SCF	Stem Cell Factor
SHM	Somatic HyperMutation
TAD	TransActivation Domain
WB	Western Blot
WT	WildType

INTRODUCTION

INTRODUCTION

1. B cell differentiation

1.1. Early B cell differentiation

All blood cell lineages are generated in the foetal liver and post-natal bone marrow (BM) from hematopoietic stem cells (HSCs). These cells undergo a progressive loss of stemness and differentiation potential, and activate specific transcriptional programs towards lineage commitment (Laiosa et al., 2006).

Common lymphoid progenitors (CLPs), differentiated from HSCs, are multipotent cells that can give rise to either B, T or Natural Killer (NK) cells in different subsequent steps (Kondo et al., 1997). The generation of B lymphocytes is controlled by several transcription factors that regulate well-defined B cell differentiation stages associated with rearrangements of the B cell receptor (BCR) gene segments V(D)J (Busslinger, 2004; Nutt and Kee, 2007; Pang et al., 2014). This process is linked to the expression of surface molecules which define different B cell populations through differentiation and maturation, from pre-pro-B to naïve mature recirculating B cells (Figure I1) (Hardy and Hayakawa, 2001).

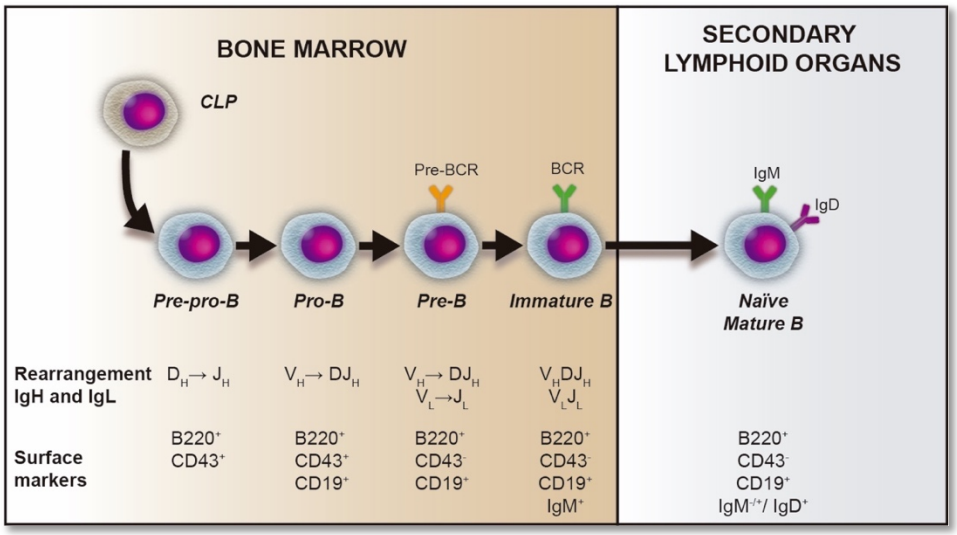

Figure I1. Early B cell differentiation in mouse BM. Surface markers and BCR status of each subpopulation are indicated.

The expression of B220 and CD43, two lineage-specific markers, on the surface of B committed cells leads to the beginning of D_H-J_H recombination at the pre-pro-B cells stage. Then, these cells give rise to pro-B cells, characterized by the expression of the CD19 surface marker and the onset of V_H-to-DJ_H rearrangement. This process, when successful, results in cell surface expression of the pre-BCR, a determinant step in the transition from the pro-B to the pre-B stage. Signalling from the pre-BCR stimulates cell expansion and induces immunoglobulin (Ig) light-chain genes recombination. Productive assembly of Ig light-chain generates immature B lymphocytes, with a complete surface IgM receptor. These developmental stages occur in an antigen-independent fashion and take place in the bone marrow, before B lymphocytes move to the periphery and are selected for self-tolerance (Hardy and Hayakawa, 2001). Newly generated B cells, undergo further differentiation to become naïve mature B cells that recirculate through secondary lymphoid organs (lymph nodes, Peyer's patches, tonsils, mucosa-associated lymphoid tissue [MALT] and spleen).

1.2. Terminal B cell differentiation

Upon encountering their specific antigen in secondary lymphoid organs, B lymphocytes are activated and begin a process called terminal B cell differentiation (Figure I2). In these organs, naïve mature B cells interact with specific antigens and auxiliary cells from the immune system to generate antibody-secreting (plasma) cells (ASC) and memory B cells. The generation of each B cell subset will depend on the nature of the antigen, dose and place of encounter in secondary lymphoid organs.

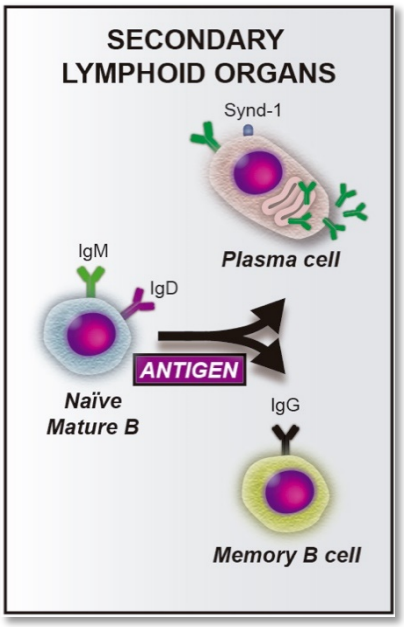

Figure I2. Terminal B cell differentiation in mouse secondary lymphoid organs.

B cells that enter the spleen from the BM are called transitional B cells, identified by the surface expression of $IgM^{hi}IgD^{+}CD23^{int}CD21^{int/hi}$ (Chung et al., 2003). These cells can either be recruited into the marginal zone (MZ) of the spleen ($IgM^{hi}IgD^{lo}CD23^{-}CD21^{hi}$), where they offer fast responses against blood pathogens and trigger the generation of plasmablast or short-lived plasma cells, or mature into follicular B cells ($IgM^{lo}IgD^{hi}CD23^{+}CD21^{int}$) in the follicles of secondary lymphoid organs. Follicles are located in the surrounding of T cell zones, and when follicular B cells encounter their antigens and receive T cell signals, they are able to form germinal centers (GCs) (Pillai and Cariappa, 2009). GCs are specialized follicular areas where proliferating antigen-specific B cells, T follicular helper cells, and follicular dendritic cells interact to give rise to high-affinity antibody-secreting plasma cells and memory B cells (Gatto and Brink, 2010).

Plasma cells are fully differentiated B cells that have acquired the ability to secrete large amounts of antibodies (Shapiro-Shelef and Calame, 2005). They do not proliferate, and are characterized by the expression of the proteoglycan syndecan-1

(or CD138), and the downregulation of B220 on their cell surface (Sanderson et al., 1989). Moreover, they can undergo additional DNA rearrangements in a process termed class switch recombination (CSR), and alternatively, the antigen affinity of antibodies can be increased by somatic hypermutation (SHM). CSR involves DNA rearrangement events in which the Ig heavy constant region is interchanged for a different one, resulting in swapping of isotype from IgM to IgD, IgG, IgE or IgA, without altering antigen specificity. Furthermore, the variable region gene sequences of both heavy and light chains can be further modified by SHM, introducing point mutations which lead to affinity maturation (Manis et al., 2002; Honjo et al., 2002). Both functions are critical for the generation of high-affinity antibodies and an effective immune response.

Memory B cells are mainly generated after T-dependent antigenic stimulation in GCs, and express class-switched Igs on their surface, but do not secrete antibodies. These cells become plasma cells or ASC, which secrete high-affinity antibodies after antigen re-challenge and provide a fast and robust secondary antibody response (Kurosaki et al., 2015).

2. c-Myc transcription factor

As previously mentioned, the process of early and terminal B cell differentiation is tightly regulated by a coordinated action of several transcription factors, among which is c-Myc (Nutt and Kee, 2007).

The *c-myc* proto-oncogene was identified in the 1970's as the human homologue of a retroviral oncogene termed *v-myc*, the transforming gene of the MC29 avian myelocytomatosis virus. The avian retrovirus MC29 induces a wide variety of tumors in chickens, including leukaemias, sarcomas, and renal and hepatic carcinomas. (Sheiness et al., 1978). The *c-myc* proto-oncogene was also found to be closely related to neoplastic transformation, being deregulated in numerous animal and human tumors, including Burkitt's lymphoma, plasmacytoma, breast carcinoma, small cell lung

cancer carcinoma, colon carcinoma, osteosarcoma and glioblastoma (Cole, 1986; DePinho et al., 1991; Spencer and Groudine, 1991). It is estimated that *c-myc* is deregulated in more than 50% of human cancers, and its deregulation is related to poor prognosis and reduced patient survival.

The Myc family of proto-oncogenes, comprising *c-myc*, *n-myc* and *l-myc*, code for c-Myc, N-Myc and L-Myc nuclear phosphoproteins, respectively. They are transcription factors that potentially regulate the expression of more than 15% of all genes from flies to humans (Orian et al., 2003; Li et al., 2003). Myc genes modulate multiple aspects of cellular physiology such as cell cycle, protein biogenesis, cell adhesion, metabolism, cell differentiation, apoptosis, and regulation of transcription and translation (Grandori et al., 2000; Meyer and Penn, 2008; Kress et al., 2015) (Figure I3). Among Myc proteins, c-Myc is the most widely expressed and relevant in primary B lymphocytes.

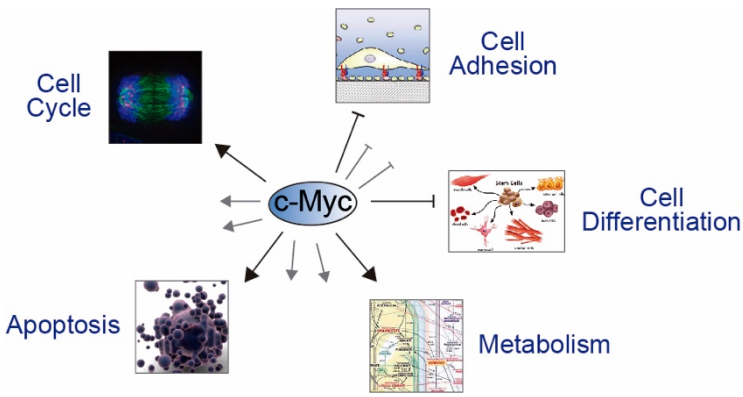

Figure I3. Simplified scheme of some of the main functions of c-Myc. Black arrows indicate promotion or suppression of the represented cell functions by c-Myc. Grey arrows indicate that some other functions of c-Myc are reported.

3. c-Myc protein

Myc family members have a basic-region/helix-loop-helix/leucine zipper (bHLH-LZ) motif at their C-terminal end, which is common to other transcription factors that specifically bind DNA consensus sequences (canonical: 5'-CACGTG-3', and non-

canonical: 5'-CANNTG-3') called E-boxes (Blackwell et al., 1990; Desbarats et al., 1996; Fernandez et al., 2003; Sabo and Amati, 2014). The HLH and leucine zipper (HLH-LZ) domains mediate protein-protein interaction, and the basic region (b) is necessary to directly mediate binding to the major groove of DNA within E-boxes. The N-terminal end harbours the transactivation domain (TAD), which is conserved in all Myc family members and is essential for the recruitment of different transcriptional co-factors to activate or repress c-Myc target genes (Figure I4).

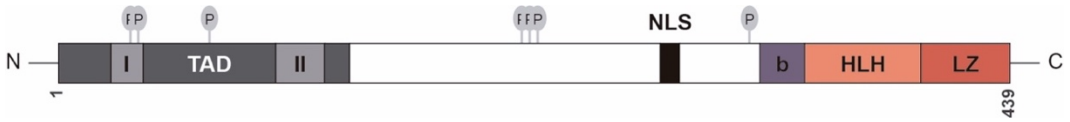

Figure I4. Schematic representation of c-Myc structure. Structural and functional domains are indicated: TAD (transactivation domain), I (Myc box I), II (Myc box II), NLS (nuclear localization signal), b (basic region), HLH (helix-loop-helix domain), LZ (leucine zipper domain). Major sites of phosphorylation are identified by grey circles containing a P. The numbers below refer to amino acids of the protein.

The bHLH-LZ domain is required to mediate interactions with its high-affinity binding partner Max. Both proteins form Myc/Max heterodimers that binds DNA in a sequence-specific manner, regulating transcription (Blackwood and Eisenman, 1991; Blackwood et al., 1991).

c-Myc is needed throughout B cell differentiation *in vivo*. In fact, deletion of *c-myc* in early B cell progenitors prevent them from progressing beyond the pre-B cell stage (Vallespinos et al., 2011). Later in B cell differentiation, mature B lymphocytes require c-Myc for cell proliferation, terminal differentiation and GC formation (Calado et al., 2012; Fernandez et al., 2013). Moreover, mature B lymphocytes lacking c-Myc show elevated levels of the cell cycle inhibitor p27, as well as greater resistance to apoptosis when compared to normal cells (Alboran et al., 2001; Alborán et al., 2004).

Oncogenic activation of *myc* occurs mainly through constitutive overexpression by different mechanisms such as insertional mutagenesis, chromosomal translocations, gene amplification or alterations of the signalling pathways that control

its expression (Soucek et al., 2008; Meyer and Penn, 2008; Dang, 2012; Whitfield et al., 2017; Chen et al., 2018). For example, in Burkitt´s lymphoma, a GC B cell tumor, c-Myc is translocated to one of the three Ig loci, and is overexpressed by regulatory elements of these loci (Gelmann et al., 1983; Schmitz et al., 2014).

4. Max protein and function

Since Max (Myc-associated Factor X) was discovered in the early 1990's (Blackwood and Eisenman, 1991; Prendergast et al., 1991) as a bHLH-LZ protein that specifically binds Myc, great efforts have been made to characterize its role in Myc functions. Disruption of the bHLH-LZ domain prevents its association with Myc (Blackwood and Eisenman, 1991). Max has been described to be the essential heterodimerization partner of Myc for most biological processes, including transcriptional activation, cell cycle progression, apoptosis and even cell transformation (Amati et al., 1992; 1993a; b). Moreover, Max is required for mouse development, since a loss of Max function *in vivo* leads to developmental arrest at an early embryonic stage (~E5.5-6.5) (Shen-Li et al., 2000).

Max is a ubiquitously expressed and highy stable protein that binds other bHLH-LZ proteins apart from Myc. It is a small protein (18 kDa) simply composed of a bHLH-LZ domain and a nuclear localization signal (NLS) (Figure I5); unlike Myc, Max lacks a transactivation domain. The current view assigns it a central role in modulating the complex Myc protein network (Kato et al., 1992).

Figure I5. Schematic representation of Max structure. Structural and functional domains are indicated: b (basic region), HLH (helix-loop-helix domain), LZ (leucine zipper domain), NLS (nuclear localization signal). Major sites of phosphorylation are identified by grey circles containing a P. The numbers below refer to amino acids of the protein.

Myc/Max heterodimers bind DNA with higher affinity than either Myc or Max homodimers alone. In fact, Myc homodimers are scarce and inactive under physiological conditions, whereas Max homodimers are active and compete for DNA binding with other E-box-binding factors. Thus, in resting conditions, Max can homodimerize or form heterodimers with Mxd family or Mga proteins, other bHLH-LZ proteins that generally antagonize Myc functions (Conacci-Sorrell et al., 2014; Link and Hurlin, 2015). Then, upon mitogen activation, Myc is rapidly induced and the balance between transcription repression and activation changes, due to the higher affinity of Max for Myc than for itself (Blackwood et al., 1991). Unlike the highly dynamic expression of Myc, levels of Max are constant, and both its mRNA and protein are found at comparable levels in quiescent and cycling cells. In fact, Max expression is not influenced by Myc levels, and it is highly stable, with a half-life of over 12 hours. Thus, these data provide a view of the regulation of the Myc network dependent on the expression patterns of Max-associated transcription factors (Blackwood et al., 1991; Kretzner et al., 1992).

4.1. Myc/Max/Mxd-Mga network

The Mxd (formerly known as Mad) family of bHLH-LZ proteins comprises Mxd1-Mxd4 and Mnt, discovered through their ability to bind Max (Zervos et al., 1993; Ayer et al., 1993; Hurlin et al., 1995; 1997). Moreover, Max binds to Mga, a large protein that contains not only a bHLH-LZ motif, but also possesses a T-domain DNA-binding motif (Hurlin et al., 2000) (Figure I6). They efficiently compete with Myc for heterodimerization with Max, and both Mxd-Max and Mga-Max heterodimers recognize the same E-boxes in DNA as Myc-Max complexes. However, they generally function as transcriptional repressors (Ayer et al., 1993) or, alternatively, they are unable to activate transcription of target genes (Zervos et al., 1993).

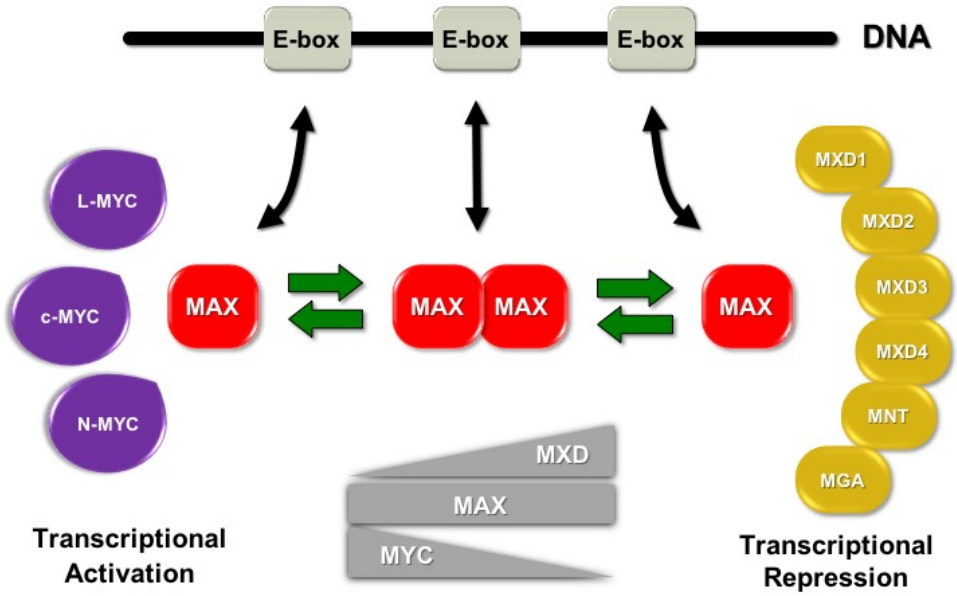

Figure I6. Myc/Max/Mxd-Mga network. The components of the Myc/Max/Mxd-Mga network are indicated. All of the complexes occur by the HLH-LZ dimerization domain, and share the ability to bind to E-boxes sequences on the DNA. However, the have opposite transcriptional activities.

The balanced expression of *myc/max/mxd-mga* network genes affect different aspects of cell behaviour, being critical for the regulation of Myc functions. As transcription factors, they control gene expression by recruiting of chromatin remodelling cofactors (Grandori et al., 2000). Myc interacts with a component of the SWI/SNF complex, which contains an ATPase activity involved in nucleosome remodelling. Myc also recruits TRRAP complexes, which act as a platform of co-activators with histone acetyl transferase (HAT) activities (McMahon et al., 2000). On the other hand, Mxd-Mga proteins recruit the mSIN3 repressor complex, with histone deacetylase (HDAC) activity, and other chromatin modifying proteins (Laherty et al., 1997). However, Max protein has not been reported to bind transcriptional cofactors, and its homodimers are not able to directly modulate promoter activity, although they compete for DNA binding on E boxes (Kretzner et al., 1992). Myc and Mxd-Mga proteins rarely co-express in the same cell, and are active with temporally and spatially different patterns (Lüscher, 2001). In this regard, the switch from Myc/Max to Mad/Max

complexes has been described to dictate monocyte to macrophage differentiation *in vitro* (Ayer and Eisenman, 1993). Moreover, a balance of Myc and Mad has been demonstrated to control cell fate determination and apoptosis *in vivo* during *Xenopus laevis* intestinal development (Okada et al., 2017).

4.2. Max-independent functions of Myc

The vast majority of the scientific literature assumes that c-Myc functions rely entirely on its ability to form heterodimers with Max protein. Germline knockouts (KO) for Max are lethal in embryos at early post-implantation (E5.5-6.5), when the dilution of maternal Max in the embryo takes place (Shen-Li et al., 2000). This occurs considerably earlier than in animals lacking c-Myc (E9.5-10.5) (Davis et al., 1993). The early lethality of Max germline KO hindered the study of Max functions *in vivo*. However, recent reports have shown the ability of Myc proteins to retain some biological functions in the absence of Max, either *in vitro* or *in vivo* (Gallant and Steiger, 2009). The PC12 rat pheochromocytoma tumor cell line contains a nonfunctional Max protein, due to a C-terminal mutation that prevents homo- or heterodimerization. Nevertheless, these cells can divide, differentiate and undergo apoptosis in the absence of Max (Hopewell and Ziff, 1995; Wert et al., 2001). c-Myc has also been shown to induce transcription of a reporter gene containing Myc/Max binding sites in this cell line (Ribon et al., 1994). Moreover, c-Myc has been described to inhibit Ras-mediated neuronal-like differentiation of UR61 cells (a PC12-derived cell line with inducible expression of the *n-ras* oncogene), by direct blockade of c-Jun upregulation (Vaqué et al., 2008). Another Max-independent function of Myc was reported using a dominant negative Myc, called Omomyc (Soucek et al., 1998), which sequesters wildtype (wt) Myc, preventing its association with Max, and enhances c-Myc-dependent apoptosis *in vitro* while repressing specific target genes (Soucek et al., 2002). Some other *in vitro* approaches raised the possibility of Max-independent functions of Myc in vertebrates, such as loss of the undifferentiated state of embryonic stem cells (ESCs)

and apoptosis (Hishida et al., 2011; Wiese and Eilers, 2011), or phosphorylation of RNA polymerase II independently of a Max-binding region (Cowling and Cole, 2007).

In *Drosophila melanogaster*, a Myc mutant lacking the Max-interaction domain still retained partial activity in endoreplication and cell competition (Steiger et al., 2008). In that article, they also demonstrated that Myc could control RNA polymerase III in the absence of Max.

Such Max-independent activities of Myc could explain the relationship between *max* loss-of-function mutations and some human cancers. The finding of germline-inactivating mutations in *max* were described to be responsible for hereditary pheochromocytoma, a rare tumor with neuroendocrine features, and correlated to its metastatic potential (Comino-Méndez et al., 2011). That was supported by the discovery of the previously described Max mutant in the PC12 cell line (Hopewell and Ziff, 1995). Inactivation of *max* is also observed in small cell lung cancer, and is mutually exclusive with alterations in *myc* (Romero et al., 2014). Moreover, in primary B lymphocytes, Max overexpression was described to reduce the rate of B lymphoma onset in *eμ-myc* transgenic mice (Lindeman et al., 1995). Altogether, these data present Max as a tumor suppressor gene that, when inactivated, can promote the development of tumors.

5. c-Myc and DNA replication

During DNA replication, DNA molecules must duplicate into two identical copies to allow a proper transmission of genetic information to each daughter cells. This process requires a strict control to ensure a precise genome duplication. First, the pre-replication complex (pre-RC) needs to be assembled onto potential replication origins, in a process known as replication licensing. This includes the recruitment of an inactive form of the helicase minichromosome maintenance 2-7 (Mcm2-7), among other pre-RC proteins (Figure I7, upper part). Then, during the cell cycle S phase, the inactive pre-RC becomes active in a process called origin firing (Figure I7, lower part) (Siddiqui et al., 2013).

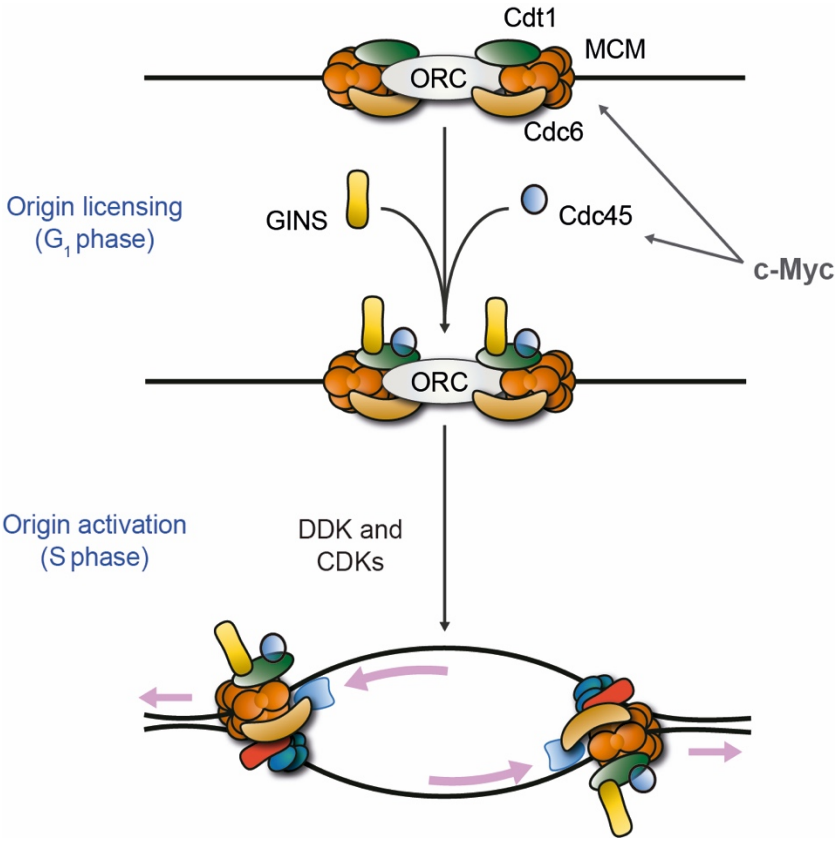

Figure I7. Role of c-Myc in origin licensing and activation. c-Myc promotes origin licensing by mediating the recruitment of pre-RC factors, including Cdt1, Cdc6, MCM helicases, Cdc45 and GINS. DDK and CDKs phosphorylation activities promotes G1/S transition and initiation of DNA synthesis.

c-Myc is induced during cell cycle entry and is critical for cell cycle G_1/S transition, balancing the expression levels of cyclins and cyclin-dependent kinases (CDKs) versus cyclin-dependent kinase inhibitors (CKIs) (Bretones et al., 2015). Replication origins are preferentially located near gene promoters, closely relating DNA replication to transcription (Aladjem and Redon, 2017). c-Myc has been previously described to regulate DNA replication through transcription-dependent and transcription-independent mechanisms (Dominguez-Sola and Gautier, 2014). c-Myc has also been reported to transcriptionally regulate Cdt1 expression, an essential component of the

pre-RC (Valovka et al., 2013). Cdt1 promotes loading of Mcm2-7 onto origins of replication during G_1 phase, together with the Cdc6 protein (Borlado and Méndez, 2008) and origin recognition complex (ORC). c-Myc also has a direct role in the control of DNA replication by direct interaction with the pre-RC proteins Cdc6 and Mcm2-7. It also promotes the recruitment of Cdc45 to chromatin (Dominguez-Sola et al., 2007), which is an essential component of the CMG complex (Cdc45/MCM/GINS) that initiates DNA replication (Aparicio et al., 2006). Productive activation of the MCM helicase during G_1/S transition to unwind DNA, requires its phosphorylation by Dbf4-dependent kinase (DDK) and by CDKs. Such phosphorylation allows the conformational change needed for the assembly of the replisome machinery (Weinreich and Stillman, 1999; Heller et al., 2011) (Figure I7).

AIMS

AIMS

1. To characterize the role of Max and the functional relationship between c-Myc and Max in early and terminal B lymphocyte differentiation using conditional mouse models.

2. To analyse the contribution of c-Myc and Max to the transcriptional program in mature B lymphocytes.

MATERIALS AND METHODS

MATERIALS AND METHODS

1. Mice

1.1. Generation of conditional *max*$^{fl/fl}$ mice and genotyping

The *max* gene contains 5 exons which encode a protein of 160 aa. To generate *max*$^{fl/fl}$ mice, we employed a gene targeting strategy using loxP sites in the mouse germline *max* locus (Thomas and Capecchi, 1987). Recombination between the two loxP sites mediated by the Cre recombinase led to deletion of the flanked exons 4 and 5 (aa: 57-160), containing the HLHZip domain and the 3' untranslated region (3'UTR).

Mice were genotyped using a polymerase chain reaction (PCR)-based analysis of tail genomic DNA with primers MaxF9 and MaxF10 (Table MM1) to amplify *max* floxed (340 base pair; bp) and wt (240 bp) alleles. Deleted *max* allele (421 bp) was amplified using MaxNull_F2 and MaxNull_R2 (Table MM1). GAPDH 5'and GAPDH 3' primers were used for DNA normalization.

To generate *max*$^{fl/fl}$*;mb-1*$^{cre/+}$*;rosa26*$^{egfp/egfp}$ mice (*MaxKO-mb1*), *max*$^{fl/fl}$ mice were first bred with *mb1-cre* "knock-in" mice (Hobeika et al., 2006), and progeny crossed to yield homozygous (*max*$^{fl/fl}$*;mb-1*$^{cre/+}$*)* and heterozygous control mice (*max*$^{fl/+}$*;mb-1*$^{cre/+}$*).* Offspring were subsequently bred with *rosa26-egfp* mice (Mao et al., 2001) and progeny crossed to obtain *max*$^{fl/fl}$*;mb-1*$^{cre/+}$*;rosa26*$^{egfp/egfp}$ and control mice (*max*$^{fl/+}$*;mb-1*$^{cre/+}$*;rosa26*$^{egfp/egfp}$*).* Mice were genotyped using hcre-DIR and hcre-REV primers (Table MM1) for the *mb-1* cre allele (500 bp), and mb-1in1 and mb-1in2 for the *mb-1* wt allele (418 bp). The *rosa26-egfp* allele was genotyped using GFPI and GFPII primers for the *egfp* allele (374 bp), and LacZ1 and LacZ2 primers for the *rosa26* wt allele (350 bp) (Table MM1).

To generate *max*$^{fl/fl}$*;cd19*$^{cre/+}$*;rosa26*$^{egfp/egfp}$ mice (*MaxKO-cd19*), *max*$^{fl/fl}$ mice were bred with *cd19-cre* mice (Rickert et al., 1995), and progeny crossbred to yield homozygous (*max*$^{fl/fl}$*;cd19*$^{cre/+}$*)* and heterozygous control mice (*max*$^{fl/+}$*;cd19*$^{cre/+}$*).* Then, mice were crossed with *rosa26-egfp* mice (Mao et al., 2001), as described above.

Cd19-cre mice were genotyped using 69R and SF4 primers for the *cd19* cre allele (269 bp), and cd19wt2 and cd19wt3 primers for the *cd19* wt allele (560 bp) (Table MM1).

1.2. Generation of c-Myc/Max DKO mice

The generation of *c-myc*$^{fl(fl}$*;mb-1*$^{cre/+}$*;rosa26*$^{egfp/egfp}$ (*MycKO-mb1*) and *c-myc*$^{fl(fl}$*;cd19*$^{cre/+}$*;rosa26*$^{egfp/egfp}$ (*MycKO-cd19*) mice has been previously described (Alboran et al., 2001; Vallespinos et al., 2011). Briefly, *c-myc*$^{fl/fl}$ mice, in which *c-myc* exons 2 and 3 are flanked by loxP sites, were bred with either *mb1-cre* mice (Hobeika et al., 2006) or *cd19-cre* mice (Rickert et al., 1995) to delete *c-myc* in developing and mature B lymphocytes, respectively. *c-myc* wt and cre alleles were amplified using c-mycFloxS and c-mycFloxA primers, and the deleted *c-myc* allele (750 bp) was amplified using Null S and Null A (Table MM1).

Table MM1. Specific primers used for PCR analysis of mice genotype

MaxF9 CTATAAGAAAAAAATCCAGAGAGGG **MaxF10** CCCAAAGTGTCAAGCAACTCACAG for *max* wt and flox alleles.	**LacZ1** GTGGTGGTTATGCCGATCG **LacZ2** TACCACAGCGGATGGTTCGG for rosa26 wt allele.
MaxNull_F2 TGAGACAAGGCGCATAACGA **MaxNull_R2** CCAGGTAAGTCGCTCTTGGT for *max* null allele.	**69R** GGACATGTTCAGGGATCGCCAGGCG **SF4** GCATAACCAGTGAAACAGCATTGCTG for *cd19* cre allele.
hcre-DIR ACCTCTGATGAAGTCAGGAAGAA **hcre-REV** GGAGATGTCCTTCACTCTGATTCT for *mb-1* wt allele.	**cd19wt2** CCTTAGGTCACAGTCCAGGT **cd19wt3** -TCACCTGTCTCTTCTGAGAA for *cd19* wt allele.
mb-1in1 CTGCGGGTAGAAGGGGGTC **mb-1in2** -CCTTGCGAGGTCAGGGAGCC for *mb-1* wt allele.	**c-mycFloxS**GCCCCTGAATTGCTAGGAAGACTG **c-mycFloxA** CCGACCGGGTCCGAGTCCCTATT for *c-myc* wt and flox alleles.
GFP I -GGCTTAAAGGCTAACCTGTG **GFP II** GGAGCGGGAGAAATGGATATG for *egfp* allele.	**Null S** TCGCGCCCCTGAATTGCTAGGAA **Null A** -TGCCCAGATAGGGAGCTGTGATACTT for *c-myc* null allele.
gapdh 5' CATCACCATCTTCCAGGAGC **gapdh 3'** CATGAGTCCTTCCACGATACC for *gapdh* allele. DNA normalization.	

Conditional double knockout mice *c-myc*$^{fl/fl}$*;max*$^{fl/fl}$*;mb1*$^{cre/+}$*;rosa26*$^{egfp/egfp}$ (*DKO-mb1*) or *c-myc*$^{fl/fl}$*;max*$^{fl/fl}$*;cd19*$^{cre/+}$*;rosa26*$^{egfp/egfp}$ (*DKO-cd19*) were generated by breeding *MaxKO-mb1* and *MaxKO-cd19* mice to *MycKO-mb1* or *MycKO-cd19* mice, respectively.

All the mice used were 8-10-weeks-old.

2. Flow cytometry and cell sorting

Single cell suspensions from mouse BM or spleen were incubated in NH_4Cl buffer to lyse erythrocytes and incubated with a suitable dilution of each anti-mouse antibody in phosphate-buffered saline (PBS) with 2% foetal bovine serum (FBS). Antibodies used were from Biolegend (B220-PE-Cy7, IgD-Alexa Fluor 647), eBioscience (CD49b-biotin, IgG1-PE, IgM-APC, GL-7-biotin), Beckman Coulter (B220-APC, Ly-6C-biotin,), BD Pharmingen (CD21-APC, CD23-PE, CD43-PE-Cy7, CD69-biotin, CD138 (Syndecan-1)-PE, IgG1-PE), Southern Biotech (IgM-PE). Biotinylated antibodies were developed with streptavidin-eFluor 450 (eBioscience), streptavidin-PE or streptavidin-APC (Beckman Coulter). BM B cell subpopulations were characterized as pro-B cells (Ly-6c$^-$CD49b$^-$B220$^+$IgM$^-$CD43$^+$), pre-B cells (Ly-6c$^-$CD49b$^-$B220$^+$IgM$^-$CD43$^-$), immature B cells (Ly-6c$^-$CD49b$^-$B220^{lo}IgM$^+$CD43$^-$), and mature B cells (Ly-6c$^-$CD49b$^-$B220^{hi}IgM$^+$CD43$^-$). Spleen B lymphocytes were identified as follicular B cells (B220$^+$CD23$^+$CD21^{int}), marginal zone B cells (B220$^+$CD23$^-$CD21^{hi}) and immature (newly formed/transitional stage 1) B cells (B220$^+$CD23$^-$CD21^{lo}). Cell death was monitored using Annexin-V-eFluor 450 or Annexin-V-APC (Immunostep) and 7-aminoactinomycin D (7-AAD; Beckman Coulter), to characterize alive (7-AAD$^-$ Annexin V$^-$), early apoptotic (7-AAD$^-$ Annexin V$^+$), late apoptotic (7-AAD$^+$ Annexin V$^+$) and necrotic (7-AAD$^+$ Annexin V$^-$) cells. Cell cycle was assessed directly measuring DNA synthesis by EdU incorporation 4 h after of intraperitoneal (i.p.) injection (200 µg; Click-iT Plus EdU (Pacific Blue picolyl azide) flow cytometry kit, ThermoFisher Scientific) for *in vivo* assays, or after 4 h *in vitro* (10µM) on activated mature B lymphocytes. Then, cells were stained with propidium iodide (Beckman Coulter) to measure DNA content.

Cell proliferation was monitored with the CellTrace Violet cell proliferation kit (ThermoFisher Scientific).

For cell sorting, freshly isolated cells from BM and spleen were stained with anti-B220-PE-Cy7 (Biolegend) and anti-IgM-PE (Southern Biotech) or anti-B220-PE-Cy7 only in PBS with 2% FBS. Cells were sorted (purity >97% was verified by flow cytometry re-analysis) based on the expression of GFP and different combinations of the previous antibodies on a FACSAria IIu sorter (BD Biosciences).

3. Cell cultures

For B cell differentiation assays *in vitro*, sorted BM $GFP^+B220^+IgM^-$ B lymphocytes were plated ($4x10^5$ cells/well) in RPMI 1640 medium (GIBCO) with 15% heat-inactivated FBS, 2-mercaptoethanol (GIBCO), penicillin/streptomycin (GIBCO) and supplemented with recombinant murine interleukin-7 (IL-7; 10ng/ml), murine stem cell factor (SCF; 10ng/ml) and recombinant Fms-related tyrosine kinase 3 ligand (rFlt3-L; 10 ng/ml) (all from Peprotech) for 4 days. For activation of mature B lymphocytes *in vitro*, sorted $B220^+$ GFP^+ splenocytes were cultured (10^5 cells/well) in RPMI 1640 medium with 15% heat-inactivated FBS, 2-mercaptoethanol, penicillin/streptomycin and activated with *Escherichia coli* lipopolysaccharide (LPS; 20 µg/ml; Sigma-Aldrich) and interleukin-4 (IL-4; 20 ng/ml; R&D Systems). Activated cells and supernatants were harvested after 3 days.

4. Immunization

T cell-dependent immunization was performed in 6- to 8-weeks-old *MaxKO-cd19, MycKO-cd19, DKO-ccd19* and heterozygous control mice with 200 µg of 2,4,6-trinitrophenyl hapten (TNP)-keyhole limpet hemocyanin (KLH) (Biosearch Technologies) in Imject Alum (ThermoFisher Scientific) at a 1:1 ratio in 0,2ml PBS,

by i.p. injection. Mice were analysed 13 days after immunization by flow cytometry and immunofluorescence. Mice injected with PBS were used as controls.

5. Tissue immunofluorescence

Freshly isolated spleens were immersed in optimal cutting temperature (OCT) compound and frozen in liquid nitrogen. Cryostat sections (10 µm) were fixed in 4% paraformaldehyde (PFA) for 10 min at room temperature (RT), and blocked with PBS containing 2% FBS, 2% bovine serum albumin (BSA) and 10% goat serum (30 min at RT). Then, sections were stained with FITC-conjugated peanut agglutinin (PNA; Vector Laboratories), Cy3-conjugated Fab fragment goat anti-mouse IgM (µ heavy chain specific; Jackson ImmunoResearch Lab.) and rabbit anti-GFP antibody (A-11122, ThermoFisher Scientific) followed by Alexa647-conjugated goat anti-rabbit IgG (Southern Biotech) at RT. Sections were then mounted in Fluoromount (Southern Biotech) and imaged on a Zeiss Axiovert LSM 510-META inverted microscope with a 20x/air objective. Images were analysed using LSM 510 software (Zeiss), and GC analysis and quantification were done using FiJi software (ImageJ, NIH). GC were identified as PNA^+ in a comparable number of follicles in the spleen tissue sections per mouse model. Colocalization analysis of PNA/GFP was used to determine the presence of GFP^+ cells within GCs in the tissue sections mentioned above. The frequency of GC GFP^+ vs GC GFP^- was calculated as (GC GFP^+/total GC) x 100 and (GC GFP^-/total GC) x 100, respectively.

6. Analysis of replication fork rate in stretched DNA fibers

Splenic $B220^+GFP^+$ B lymphocytes were isolated by cell sorting and stimulated to proliferate with 20 µg/ml LPS (Sigma-Aldrich) and 20 ng/ml IL-4 (R&D Systems). After 48 h , cells were sequentially pulse-labeled with two thymidine analogs: 50 µM CldU (20 minutes) followed by 250 µM IdU (20 min). Labelled cells were lysed in buffer containing 0.5% SDS, 200 mM Tris pH 7.4 and 50 mM EDTA, and DNA fibers were spread on microscope slides. Slides were air-dried and fixed in methanol and acetic acid (3:1) for 2 min. CldU and IdU tracks were detected by immunofluorescence with

anti-BrdU antibodies (Abcam ab1791 for CldU; Beckton-Dickinson 347580 for IdU). Fiber integrity was assessed with anti-ssDNA antibody (Millipore Mab3034). Slides were examined with a Leica DM6000 B microscope (Mourón et al., 2013; Quinet et al., 2017).

7. Preparation of whole-cell extracts and western blots

Whole-cell extracts were prepared by resuspending cells in Laemmli buffer followed by sonication (2 x 30 sec in a Branson Digital sonifier set to 20% amplitude). SDS-PAGE and immunoblotting were performed following standard protocols. Source of primary antibodies: MCM2 and MCM3 (Alvarez et al., 2015); MCM4 and MCM6 (Búa et al., 2015); pS40-MCM2 (Abcam ab133243), CDC6 (Millipore 05-550); CDC7 (Abcam ab108332); CDC45 and PSF2 (Aparicio et al., 2009); MEK2 (BD Biosciences Pharmingen 610236); SMC1 (Remeseiro et al., 2012).

8. Gene expression analysis

Sorted splenic $B220^{+}GFP^{+}$ B lymphocytes were stimulated with LPS and IL-4 for 3 days. Total RNA was extracted using the RNeasy Micro Kit (Cat No./ID: 74004, Qiagen), and cDNA was generated with avian myeloblastosis virus reverse transcriptase, using random hexamers (SuperScriptTM III First-Strand Synthesis System, Cat 18080051, ThermoFisher). For real-time quantitative PCR (qPCR), 2 µl cDNA were used with specific primers (Table MM2) and SYBR-green core reagents (5x HOT FIREPol EvaGreen qPCR Mix Plus; Solis BioDyne). qPCR was performed in an ABI Prism 7700 (Applied Biosystems) and results were analysed with SDS software v1.9 (Applied Biosystems). Relative gene expression was normalized to that of the housekeeping gene β-actin. For BM B cells, total RNA was extracted from sorted $B220^{+}IgM^{+}GFP^{+}$ B lymphocytes, and the same gene expression analysis was followed.

Table MM2. Specific primers used for qPCR analysis	
Card11_1R CCTACAAGAGGAAGTCCGCC **Card11_1F** CCAGGTACTTATCCCGCAGC for *card11* allele.	**RPL39_1R** CGGTCCCGGCCTTICTCT **RPL39_1F** GAGAAGACATGGCGAGAAGCC for *rpl39* allele.
CD72_1R CTCCAAACTGGCAGCATTCG **CD72_1F** -CGCTGGGCAGAGAAACTTCA for *cd72* allele.	**MycE2E3_1R** CAGCGACTCTGAAGAAGAGCA **MycE2E3_1F** GACCTCTTGGCAGGGGTTTG for *myce2e3* allele.
Med13l_1R GTGGGGAGATGAACCCAACC **Med13l_1F** AGTCCTTCTTCCACAACCTGC for *med13i* allele.	**Max_1R** CTCCAAGGAGAGAAGGCATCC **Max_1F** CAATGTCTTGCTGGTGCGTA for *max* allele.
SSH2_1R ACAGCCCAGAAGCATCAGC **SSH2_1F** AGCCATTCCCTCGTGGTAGA for *ssh2* allele.	**cdc7_1R** CTGACCAGACCACAGCGATT **cdc7_1F** AAAATGGGTACCGCCCACTG for *cdc7* allele.
MRPL12_1R CAAAGCCTGTGGACAAAGTAA **MRPL12_1F** ACCAGCTTCTTGGCCTGGAC for *mrpl12* allele.	**B actin_1R** AGGAGATTACTTGCTCTGGCTCCTA **B actin_1F** ACTCATCGTACTCCTGCTTGCTGAT for *beta actin* allele.

9. RNAseq library preparation, sequencing and generation of FastQ files

Barcoded RNA-Sequencing (RNA-Seq) libraries were generated from 200 ng of total RNA, using the NEB Next Ultra RNA library Prep Kit for Illumina (New England Biolabs), after poly A+ RNA selection using oligo-d$(T)_{25}$ magnetic beads. The size of the libraries was checked using an Agilent 2100 Bioanalyzer DNA 1000 chip (Agilent Technologies), and their concentration was determined using a Qubit® fluorometer (Life Technologies). Libraries were sequenced on a HiSeq2500 (Illumina) to generate 60-base single reads. FastQ files for each sample were obtained using CASAVA v1.8 software (Illumina).

10. RNA-Seq analysis

Sequencing adaptor contaminations were removed from reads using cutadapt software, and the resulting reads were mapped and quantified in the transcriptome (Ensembl GRCm38, gene-build 82) using RSEM v1.2.3 (Li and Dewey, 2011). Genes

with at least 1 count per million in at least 2 samples were considered for statistical analysis. Data were TMM (trimmed mean of M-values) normalized and transformed with the voom function for differential expression tests, using the Bioconductor packages edgeR (Robinson et al., 2010) and limma (Ritchie et al., 2015). Those genes with a Benjamini-Hochberg adjusted *p*-value ≤0.01 were considered to be differentially expressed. Batch effects were accounted for by using a random variable in the model. A functional analysis on differentially expressed genes (DEG) was performed using DAVID GO (Huang et al., 2009) and R package GOplot (Walter et al., 2015).

RNA-Sequencing data were deposited in the Gene Expression Omnibus (GEO) database (Accession number: GSE115915).

11. Statistical analysis

All the statistical analyses were performed using two-tailed unpaired Student's t-tests (Prism 6.0; GraphPad) except for DNA fiber analyses, where statistical significance was assessed using non-parametric one-way ANOVA Kruskal–Wallis test, followed by Dunn's post-test.

RESULTS

RESULTS

1. Generation of Max and c-Myc/Max conditional KO mice in B lymphocytes

To circumvent the embryonic lethality of Max germline knockouts (Shen-Li et al., 2000), we used the cre-loxP system to delete *max* from primary B lymphocytes *in vivo*. We generated homozygous mice for the max^{flox} conditional allele ($max^{fl/fl}$ mice), where two loxP sites were inserted between the 4th and 5th exons of the *max* germline locus (Figure R1), containing the HLHZip domain, required for Myc heterodimerization (Blackwood and Eisenman, 1991), and the 3'UTR.

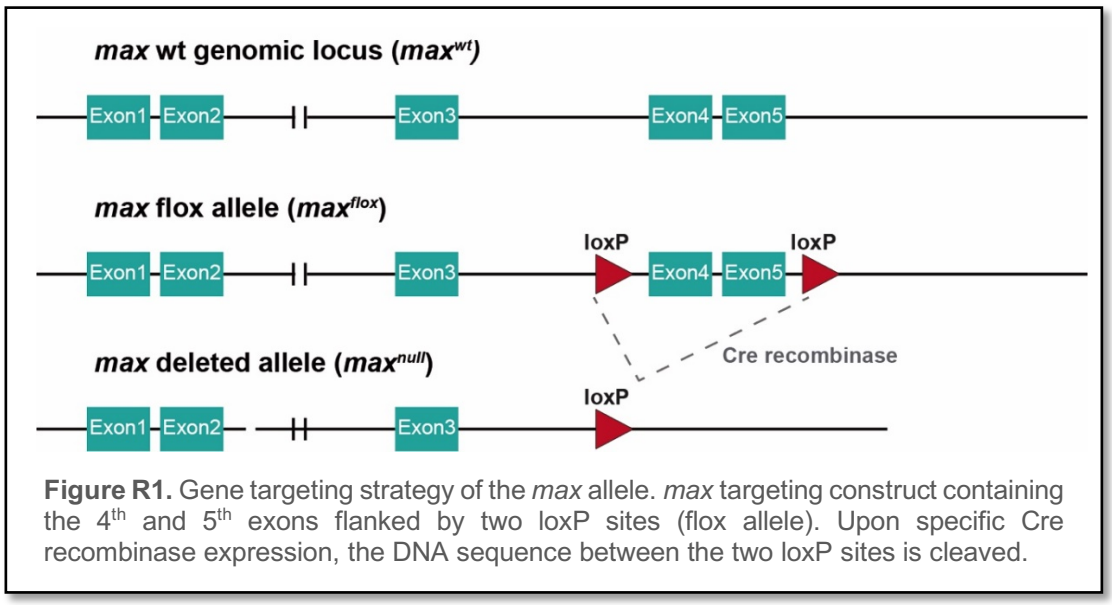

Figure R1. Gene targeting strategy of the *max* allele. *max* targeting construct containing the 4th and 5th exons flanked by two loxP sites (flox allele). Upon specific Cre recombinase expression, the DNA sequence between the two loxP sites is cleaved.

We bred these mice with *mb1-cre* "knock-in" mice (Hobeika et al., 2006) or *cd19-cre* mice (Rickert et al., 1995) to delete *max* in developing and mature B lymphocytes, respectively. In *mb1-cre* mice, the Cre recombinase is expressed under control of the promoter of *Ig-*α chain of the B cell receptor (BCR) (*mb-1* gene) at the beginning of the pro-B cell stage in the BM. On the other hand, in *cd19-cre* mice,

expression of the Cre recombinase is controlled by the promoter of the B cell lineage-specific *cd19* gene, which is expressed from the pre-B cell stage.

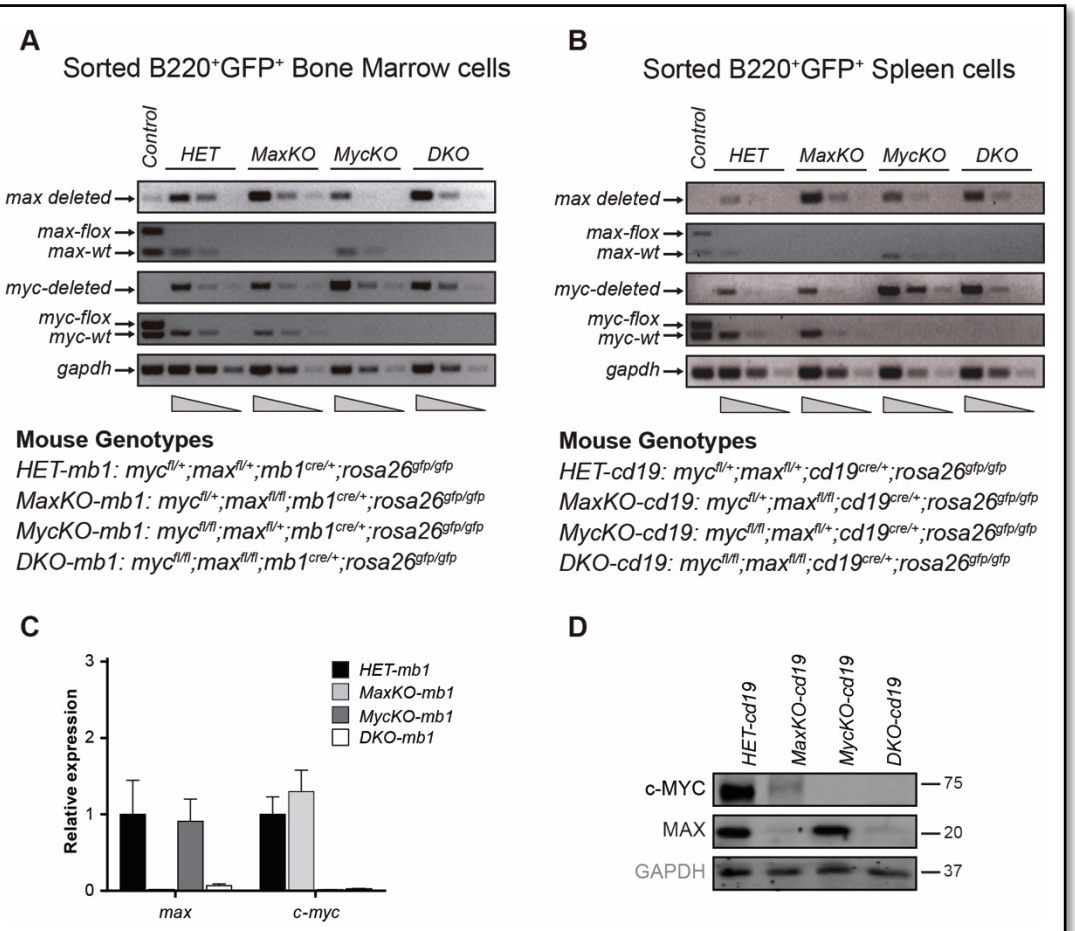

Figure R2. Efficient deletion of *c-myc* and *max* in B lymphocytes. Genomic PCR analysis of *max* and *c-myc* deleted, flox and wt alleles of B220$^+$ GFP$^+$ B lymphocytes sorted from (A) the BM of *HET-mb1* (heterozygous control), *MaxKO-mb1*, *MycKO-mb1* and *DKO-mb1* mice, or (B) the spleen of *HET-cd19* (heterozygous control), *MaxKO-cd19*, *MycKO-cd19* and *DKO-cd19* mice. (C) qPCR analysis of *max* and *c-myc* mRNA expression levels in B lymphocytes sorted from the BM of *HET-mb1*, *MaxKO-mb1*, *MycKO-mb1* and *DKO-mb1* mice, as in (A). (D) WB analysis of c-Myc and Max protein levels in sorted B lymphocytes from the spleen of *HET-cd19*, *MaxKO-cd19*, *MycKO-cd19* and *DKO-cd19* mice, as in (B). GAPDH was used as a loading control. Data is representative of at least three independent experiments.

To monitor and isolate deleted cells, we crossed offspring with the previously described *rosa26-egfp* reporter mouse (Mao et al., 2001), in which the enhanced green fluorescent protein (EGFP) was inserted after a floxed stop codon in the *rosa26* locus. We thus obtained *max*$^{fl(fl}$*;mb-1*$^{cre/+}$*;rosa26*$^{egfp/egfp}$ (hereafter *MaxKO-mb1*) and *max*$^{fl(fl}$*;cd19*$^{cre/+}$*;rosa26*$^{egfp/egfp}$ (hereafter *MaxKO-cd19*) mice, in which *max* deleted cells are quickly identified by EGFP expression (Figure R2 and (Alborán et al., 2004)).

Conditional double knockout (DKO) *c-myc*$^{fl/fl}$*;max*$^{fl/fl}$*;mb1*$^{cre/+}$*;rosa26*$^{egfp/egfp}$ (hereafter *DKO-mb1*) and *c-myc*$^{fl/fl}$*;max*$^{fl/fl}$*;cd19*$^{cre/+}$*;rosa26*$^{egfp/egfp}$ (hereafter *DKO-cd19*) mice were generated by breeding *MaxKO-mb1* and *MaxKO-cd19* mice with our previously reported *myc*$^{fl/fl}$*;mb1*$^{cre/+}$*;rosa26*$^{egfp/egfp}$ (hereafter *MycKO-mb1) (Vallespinos et al., 2011)* or *c-myc*$^{fl/fl}$*;cd19*$^{cre/+}$*;rosa26*$^{egfp/egfp}$ (hereafter *MycKO-cd19)* mice (Alboran et al., 2001; Alborán et al., 2004), respectively. In these mice, we also identified *c-myc* and *max* deleted B cells by EGFP the expression (Figure R2).

2. Max-knockout B lymphocytes differentiate into mature B cells

Previous results of our group showed that c-Myc-deficient B lymphocytes did not differentiate beyond the pre-B cell stage (Vallespinos et al., 2011). Deletion of *c-myc* at early developmental stages led to a defect in the transition from pro-/pre-B cells (when *mb-1* is expressed) to immature B cells, affecting the absolute numbers of mature B lymphocytes in the spleen of these mice (Figure R3A).

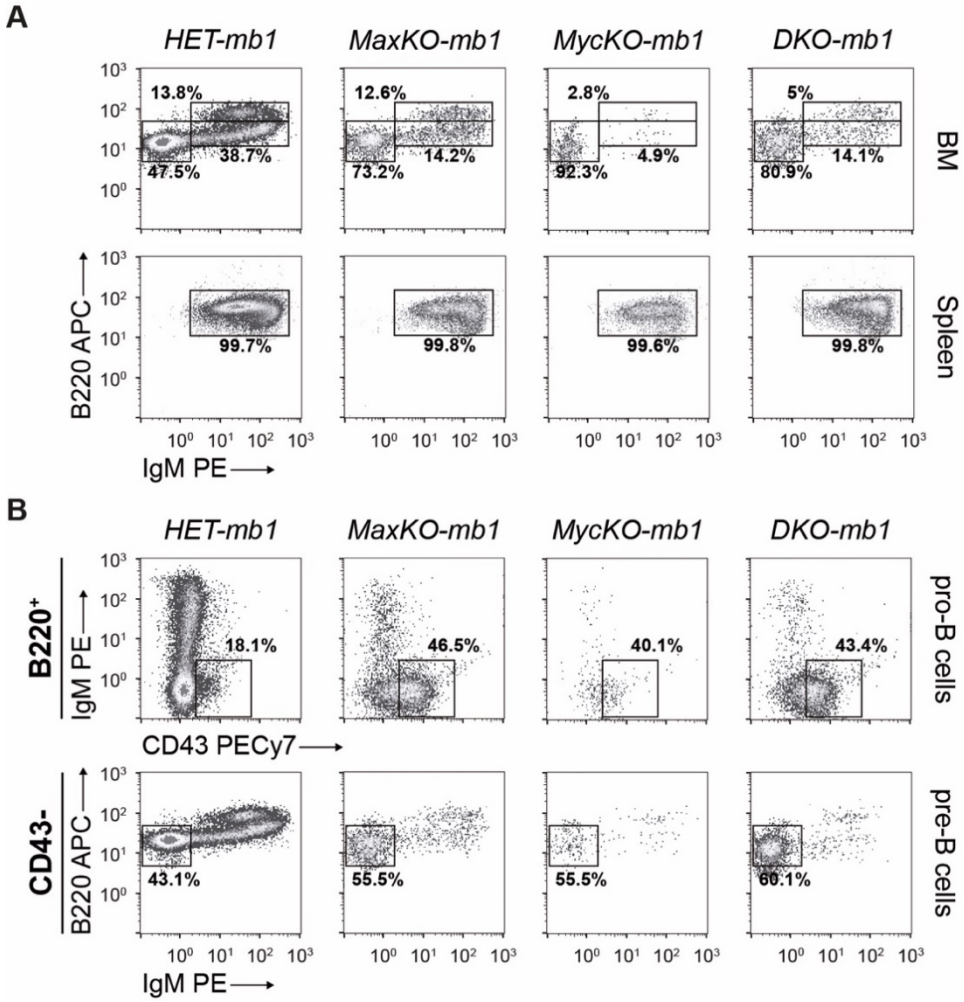

Figure R3. Flow cytometry analysis of B lymphocytes. GFP$^+$ B cells in the BM and spleen of *HET-mb1*, *MaxKO-mb1*, *MycKO-mb1* and *DKO-mb1* mice. (A) Single-cell suspensions were stained with antibodies to B220 and IgM, to identify pre-/pro-B cells (B220$^+$ IgM$^-$), immature (B220^{lo} IgM$^+$) and mature (B220^{hi} IgM$^+$) B lymphocytes in the BM, and the mature B cell population (B220$^+$ IgM$^+$) in the spleen. (B) BM B lymphocyte progenitors were analysed by staining of single-cell suspensions with antibodies against B220, IgM and CD43: pro-B cells (B220$^+$ IgM$^-$ CD43$^+$); pre-B cells (B220$^+$ IgM$^-$ CD43$^-$). Cells were gated on Ly6C and CD49b double-negative population to remove B220$^+$ non-B cells (plasmacytoid dendritic cells; pDCs), macrophages and NK cells present in the BM. Data is representative of at least three independent experiments.

To determine whether this phenotype was dependent on Max or c-Myc/Max, we analysed the B cell subpopulations in the BM and the spleen of *MaxKO-mb1*, *MycKO-mb1*, *DKO-mb1* and *c-myc$^{fl/+}$;max$^{fl/+}$;mb1$^{cre/+}$;rosa26$^{egfp/egfp}$* heterozygous

control mice (hereafter *HET-mb1*) by flow cytometry. These analyses were performed on GFP$^+$ B cells (deleted cells), as previously shown by PCR (Figure R2). We observed that MaxKO and DKO B cells differentiated from pro-B to mature stages, in contrast to the developmental block observed in MycKO B cells ((Vallespinos et al., 2011) and Figure R3A). However, analysis of the absolute numbers of B cells in the BM and spleen of these mice revealed a significant reduction in *MaxKO-mb1* (BM 2 x 10^5; spleen 1.8 x 10^6) and *DKO-mb1* (BM 0.5 x 10^4; spleen 0.6 x 10^6), compared to controls (BM 0.7 x 10^6; spleen 4.5 x 10^6) (Figure R4).

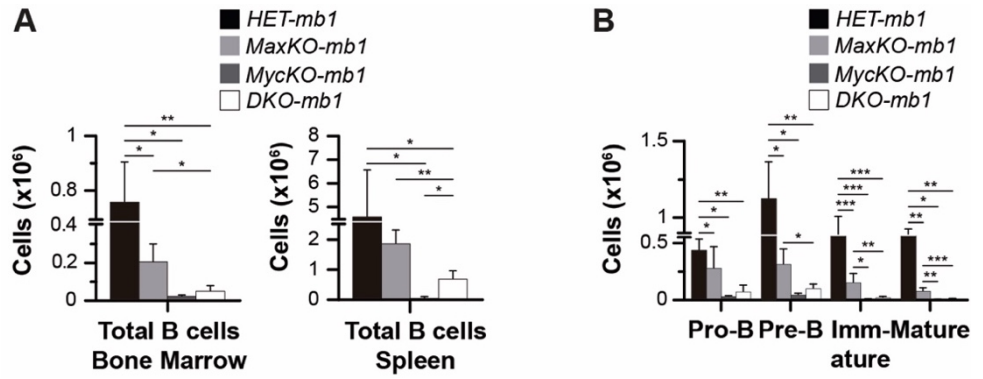

Figure R4. Absolute cell counts of B cells in BM and spleen. (A) Absolute numbers of B cells in the BM and spleen of *MaxKO-mb1* (n=6), *MycKO-mb1* (n=3), *DKO-mb1* (n=5) and control (n=4) mice. (B) Absolute numbers of B cell subpopulations in the BM of these mice, identified as described in Figure R3. Data is representative of at least three independent experiments; *p < 0.05, **p < 0.01, ***p < 0.001.

In *mb1-cre* mice, Cre recombinase is constitutively expressed from pro-B and thus, deletion can occur from that developmental stage. Consequently, immature and mature B lymphocytes in the BM of KO mice can result from wt cells that escape Cre-mediated deletion. To rule out this possibility, we carried out differentiation assays *in vitro* using sorted B220$^+$ IgM$^-$ GFP$^+$ BM B cells from *MaxKO-mb1* and *HET-mb1* control mice. Unlike c-Myc KO B cells (Vallespinos et al., 2011), cultured BM B cell progenitors from *MaxKO-mb1* were able to generate IgM$^+$ B cells, but in a less efficient way than control B cells (Figure R5). Despite these observations, the absolute numbers of B cells in the BM and spleen of mutant mice were dramatically decreased compared with

controls. This could be due to a defect in cell proliferation, an increase in cell apoptosis, or a combination of both.

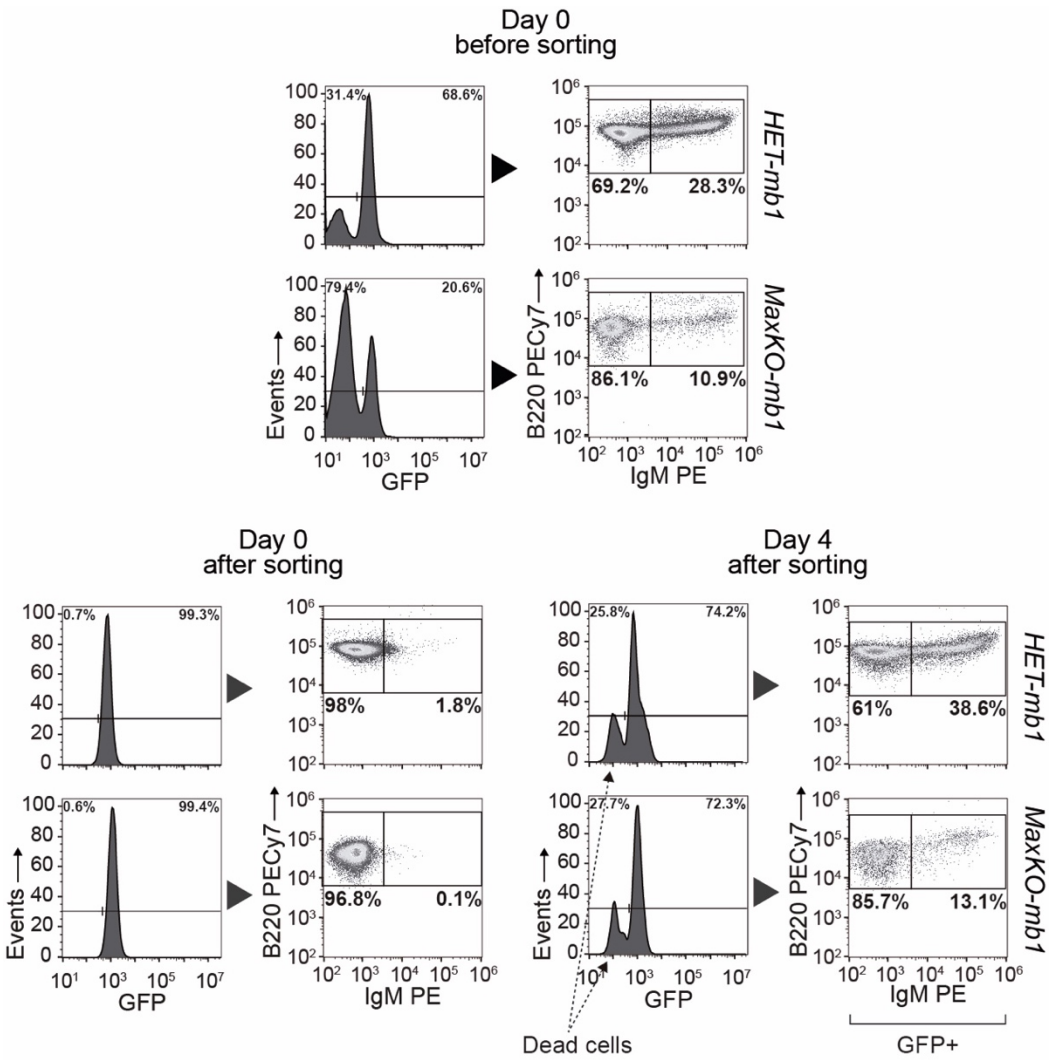

Figure R5. Max-deficient BM B lymphocytes differentiate *in vitro* into IgM$^+$ B cells. Isolated B220$^+$ IgM$^-$ GFP$^+$ BM B cells from *MaxKO-mb1* and *HET-mb1* mice were cultured in the presence of IL-7, SCF and Flt3-L cytokines for 4 days. Cells were then analysed by flow cytometry using antibodies against B220 and IgM markers. Data is representative of at least three independent experiments.

To test the proliferative status of pro-/pre-B, immature and mature B cells from the BM of *MaxKO-mb1*, *MycKO-mb1*, *DKO-mb1* and *HET-mb1* mice, we monitored *in vivo* EdU incorporation by flow cytometry. The proliferation burst of early B lymphocytes takes place mainly at the pro- to pre-B cell stage, when B lymphocytes undergo V(D)J recombination (Jung et al., 2006). EdU incorporation of sorted GFP^+ B lymphocytes mutant mice revealed a reduction in the percentage of cells in S phase at the pro-/pre-B cell stage, and a decrease in EdU fluorescence intensity in deficient versus control cells (S phase mean fluorescence intensity (MFI): 19.886 HET vs. 5.172 MaxKO, 4.017 MycKO and 4.416) (Figure R6A). We noticed that MaxKO and DKO B lymphocytes have some capacity to proliferate when compared with MycKO B cells. By Annexin-V staining, we did not observe apparent differences in the apoptotic status of B cells between the different genotypes except for MycKO mature B lymphocytes. MycKO B cells were more resistant to apoptosis than control cells, as previously reported (Figure R6B and (Alborán et al., 2004)).

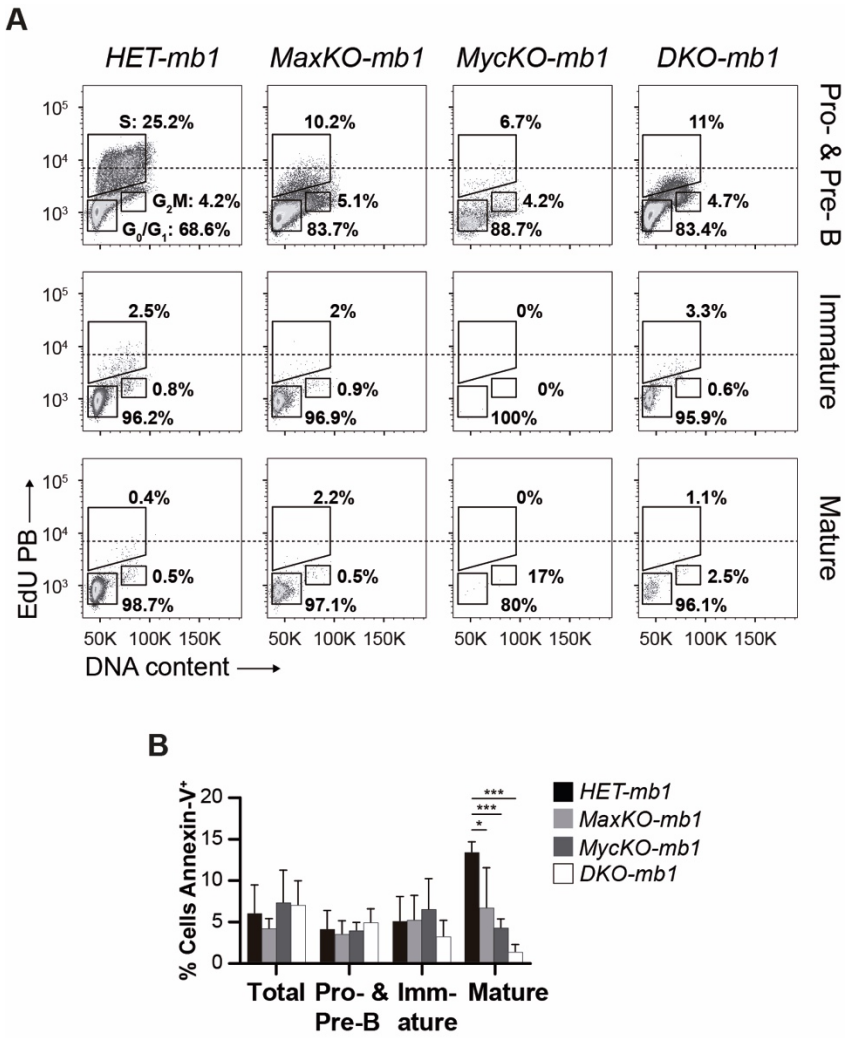

Figure R6. MaxKO and DKO B cells proliferate *in vivo*. (A) Cell cycle analysis of sorted GFP$^+$ pro-/pre-B (B220$^+$ IgM$^-$), immature (B220^{lo} IgM$^+$) and mature (B220^{hi} IgM$^+$) B lymphocytes from the BM of *MaxKO-mb1*, *MycKO-mb1*, *DKO-mb1* and *HET-mb1* mice. Mice were injected i.p. with 200 µg of EdU and analysed 4h later. Sorted B cells were stained with propidium iodide for DNA content. Dotted line is shown for EdU MFI comparations. (B) Percentage of GFP$^+$ Annexin-V$^+$ cells in the BM of *MaxKO-mb1* (n=3), *MycKO-mb1* (n=3), *DKO-mb1* (n=3) and control (n=4) mice. Single-cell suspensions were Ab- and Annexin-V-stained and gated as in Figure R3. Data is representative of at least three independent experiments; *p < 0.05, ***p < 0.001.

3. c-Myc/Max interplay in B cell function

c-Myc has been reported to play a major role in terminal B cell differentiation and function (Calado et al., 2012; Fernandez et al., 2013). Terminal differentiation involves the generation of antibody-secreting cells (ASC) and memory B cells that can undergo a change of the constant region of an antibody, in a process called Ig class switch recombination (CSR). Previous data from our laboratory showed that both processes were severely affected in c-Myc-deficient B lymphocytes ((Fernandez et al., 2013) and Figure R7). For these studies, we used *cd19-cre* mice (Rickert et al., 1995) to delete *c-myc*, *max* or both at late stages of B cell differentiation.

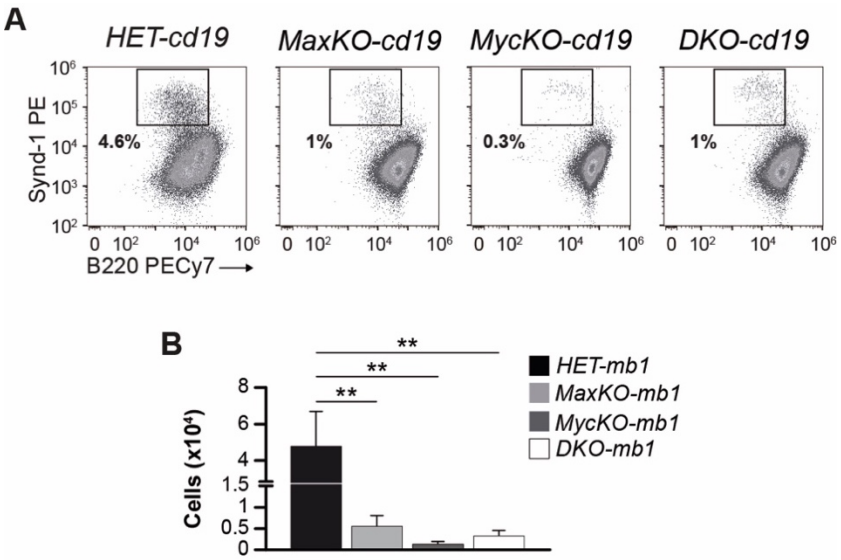

Figure R7. Generation of plasmablasts *in vitro.* (A) Flow cytometry analysis of sorted B220^{lo} Synd-1^{+} splenocytes from *MaxKO-cd19* (n=8), *MycKO-cd19* (n=4), *DKO-cd19* (n=5) and control (n=6) mice, after *in vitro* activation with LPS plus IL-4 for 72h. (B) Absolute numbers of B220^{lo} Synd-1^{+} from (A). Data is representative of at least three independent experiments; **p < 0.01.

To determine whether Max was necessary for the generation of terminally differentiated B cells, we purified B220^{+} GFP^{+} B cells from the spleen of *MaxKO-cd19*, *MycKO-cd19*, *DKO-cd19* and *HET-cd19* mice, and activated them with LPS and IL-4. Under these experimental conditions, normal B cells generate B220^{lo} Synd-1^{+}

plasmablasts (ASC) and IgG1$^+$ cells. In contrast to c-Myc-deficient B cells (1.1 x 10^3), we observed that MaxKO (5.5 x 10^3) and DKO (3.2 x 10^3) splenocytes were able to generate B220^{lo} Synd-1$^+$ cells, but to a lesser extent than control cells (4.8 x 10^4) (Figure R7).

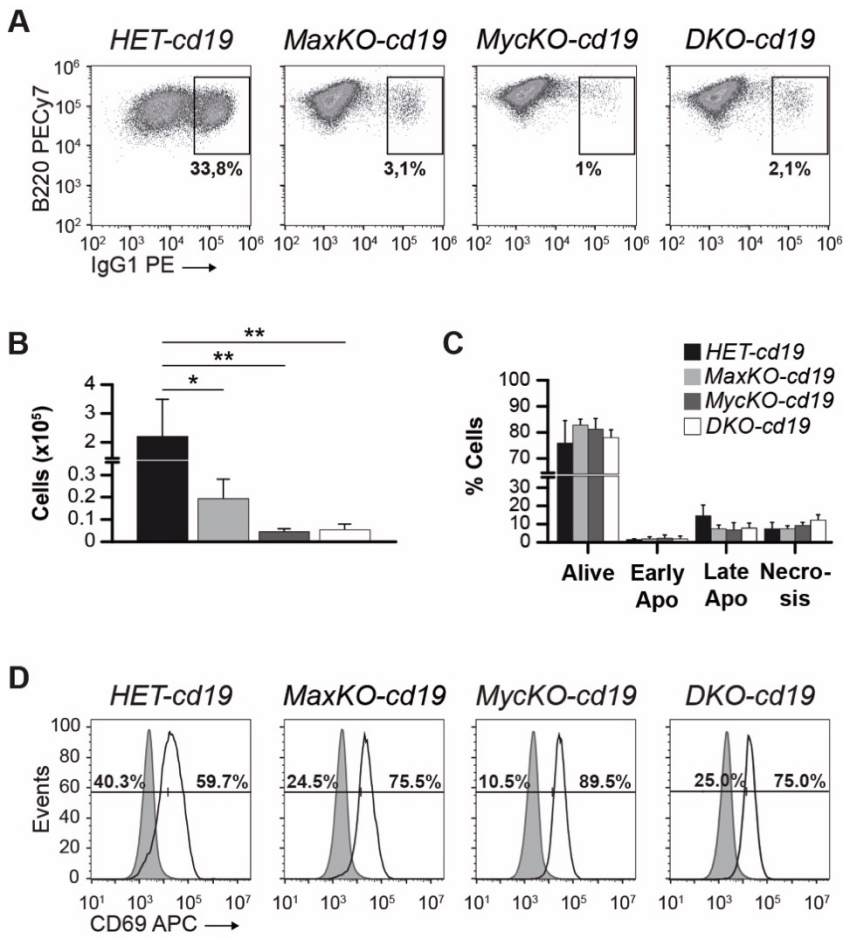

Figure R8. Class Switch Recombination in MaxKO and DKO B cells. Sorted B220$^+$ GFP$^+$ spleen cells from *MaxKO-cd19* (n=8), *MycKO-cd19* (n=4), *DKO-cd19* (n=5) and control (n=6) mice were activated with LPS plus IL-4, and analysed by flow cytometry 72h later to identify (A) CSR to IgG1 isotype of B cells. (B) Absolute numbers of B220+ GFP$^+$ IgG1$^+$ cells from (A). (C) Relative numbers of live, early apoptotic, late apoptotic and necrotic cells from cultures in (A). Cells were stained with Annexin-V and 7-AAD to monitor apoptosis. (D) CD69 surface expression in purified B220$^+$ GFP$^+$ mature B lymphocytes after 72 h in response to LPS plus IL-4. The solid grey peak represents CD69 expression levels in non-activated mature B cells, after sorting. Data is representative of at least three independent experiments; *p < 0.05, **p < 0.01.

To see whether these sorted B220+ GFP+ splenocytes could undergo CSR, we stimulated the cells with LPS plus IL-4, which mimics a T cell-dependent response in vitro, and promotes CSR to IgG1 and IgE isotypes (Chaudhuri and Alt, 2004). Flow cytometry analyses of stimulated cells, showed that MaxKO B lymphocytes generated significantly less IgG1+ cells (19.3 x 103) than control cells (22.1 x 104). DKO B lymphocytes were also capable of generating IgG1+ cells (5.4 x 103), but had a more dramatic defect in CSR, similar to the previously reported MycKO B cells (4.5 x 10^3) (Figure R8A and R8B)

To see whether these cells were capable of sensing mitogenic stimuli, we analysed the expression of the activation marker CD69, observing normal surface levels in all the mutants when compared to control cells (Figure R8D). The levels of apoptosis in the cells of these cultures were similar for all the genotypes (Figure R8C). Therefore, we concluded that both Max and c-Myc are required for generation of normal numbers of ASC and a robust CSR.

4. Max-deficient B lymphocytes do not generate germinal centers (GCs) upon immunization

Upon T-dependent stimulation, GCs are generated in secondary lymphoid organs. These structures contain highly proliferative B cells that undergo CSR and SHM to achieve functional diversification. Subsequently, these cells are selected to differentiate into plasma and/or memory B cells. The generation of GCs is one of the hallmarks of a T cell-dependent immune response, and c-Myc has been previously shown to be required for their generation ((Calado et al., 2012; Fernandez et al., 2013) and Figure R11).

To test GC formation during a T cell-dependent response in *MaxKO-cd19* mice, we immunized *MaxKO-cd19*, *MycKO-cd19*, *DKO-cd19* and *HET-cd19* mice with the antigen TNP-KLH. GC B lymphocytes are characterized by the expression B220 and high surface levels of GL-7 (Han et al., 1997). After 12 days of immunization, flow cytometry analysis of this marker revealed a decrease in the $B220^+$ $GL\text{-}7^+$ GFP^+ B cell

population in the spleen of immunized *MaxKO-cd19*, *MycKO-cd19* and *DKO-cd19* mice compared with controls (Figure R11A and R11B left panel). However, wt and non-immunized mice treated with PBS did not generate GCs (Figure R11B, right panel).

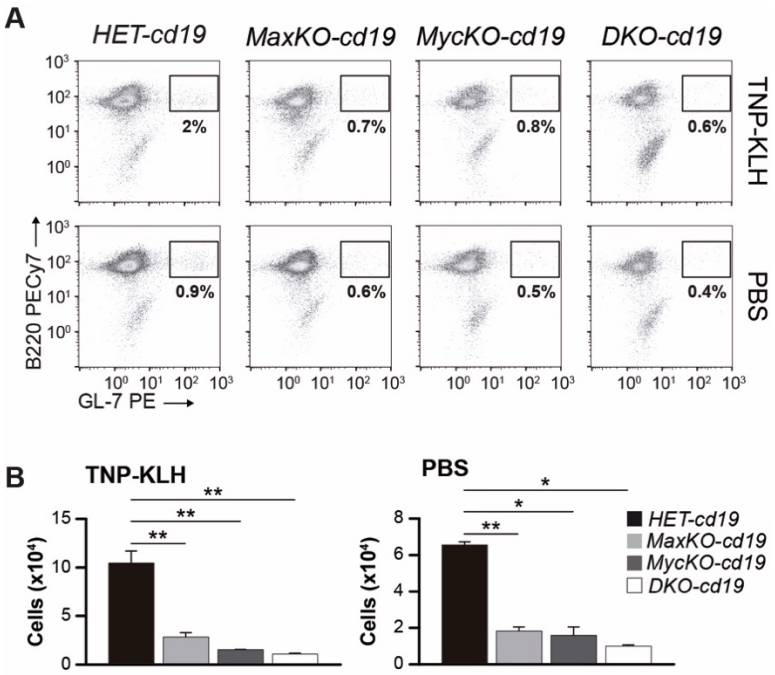

Figure R11. MaxKO and DKO B cells do not generate GC after immunization. (A) Flow cytometry analysis of GC B cells in the spleen of *MaxKO-cd19*, *MycKO-cd19*, *DKO-cd19* and *HET-cd19* control mice immunized with TNP-KLH. PBS-treated mice of the same genotypes were used as a control. (B) Absolute numbers of GC B cells from (A), (n=3). Data is representative of three independent experiments; *p < 0.05, **p < 0.01.

GC B lymphocytes can be also identified by PNA, which recognizes their surface proteoglycans (Coico et al., 1983). We performed immunofluorescence staining on spleen sections from immunized *MaxKO-cd19*, *MycKO-cd19*, *DKO-cd19* and control mice. We observed the presence of GCs in all immunized mice, whereas they were not detectable in PBS-treated mice (Figure R12A and Figure R13A). However, the number of GCs per mouse in spleen sections from mutant mice was lower than in control mice (Figure R12B, right panel). We examined the expression of

GFP in these PNA^+ spleen regions from *MaxKO-cd19*, *MycKO-cd19* and *DKO-cd19* mice, observing that these GCs contained mostly GFP^- (non-deleted) cells, as shown by the lack of PNA^+/GFP^+ colocalization (Figure R12). Thus, we conclude that c-Myc and Max are necessary for GC generation in these mice. The GCs observed in homozygous mice were likely generated by wt B cells that escaped Cre-mediated deletion (GFP^-).

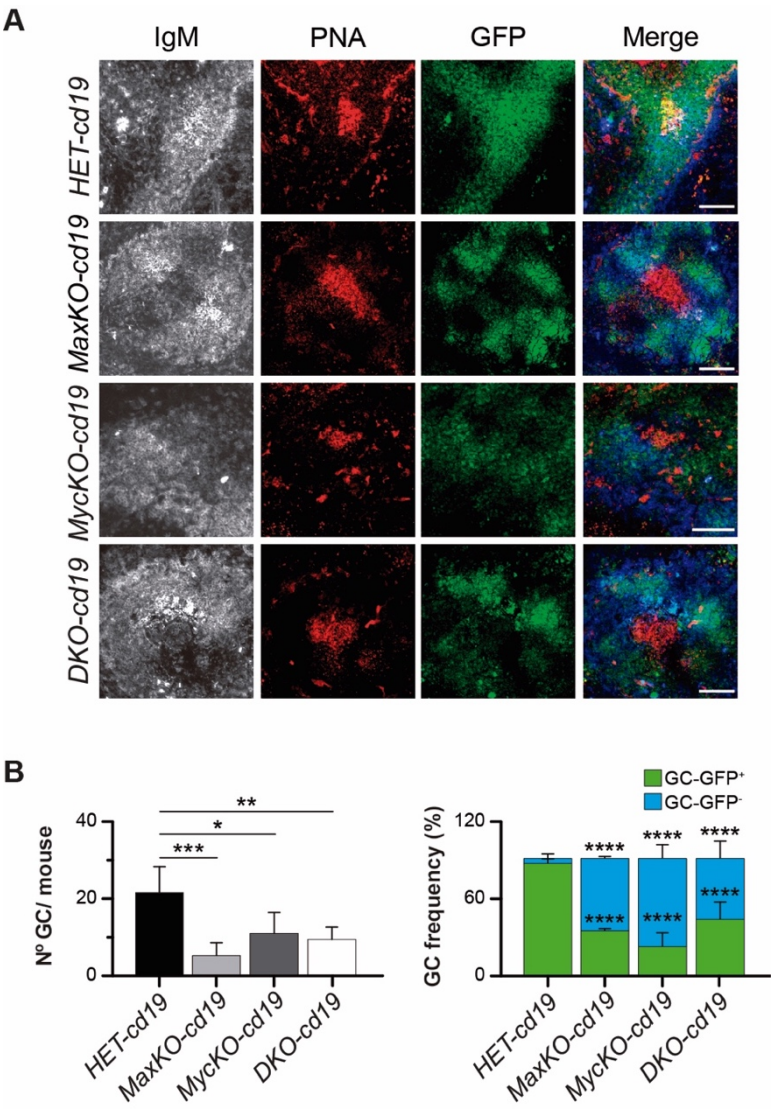

Figure R12. MaxKO and DKO B cells do not generate GCs after T cell-dependent stimulation. (A) Immunofluorescence analysis of GC formation in the spleen of *MaxKO-cd19*, *MycKO-cd19*, *DKO-cd19* and *HET-cd19* control mice, immunized with TNP-KLH. Spleen cryosections were stained with antibodies against IgM (grey/blue), PNA (red) and GFP (green) to identify GC B cells; scale bar, 80 μm. (B) Left, Number of GCs per mouse in spleen cryosections from (A): *MaxKO-cd19* (n=3; n=186 follicles analysed per mouse), *MycKO-cd19* (n=3; n=178 follicles analysed per mouse), *DKO-cd19* (n=3; n=191 follicles analysed per mouse), *HET-cd19* (n=3; n=203 follicles analysed per mouse). Right, Frequency of GFP^+ (deleted cells) or GFP^- (non-deleted cells) GC cells (PNA^+) in TNP-KLH immunized mice: *MaxKO-cd19* (n=13 GCs), *MycKO-cd19* (n=21 GCs), *DKO-cd19* (n=27 GCs) and heterozygous control (n=62 GCs); *p < 0.05, **p < 0.01, ***p < 0.001, ****p < 0.

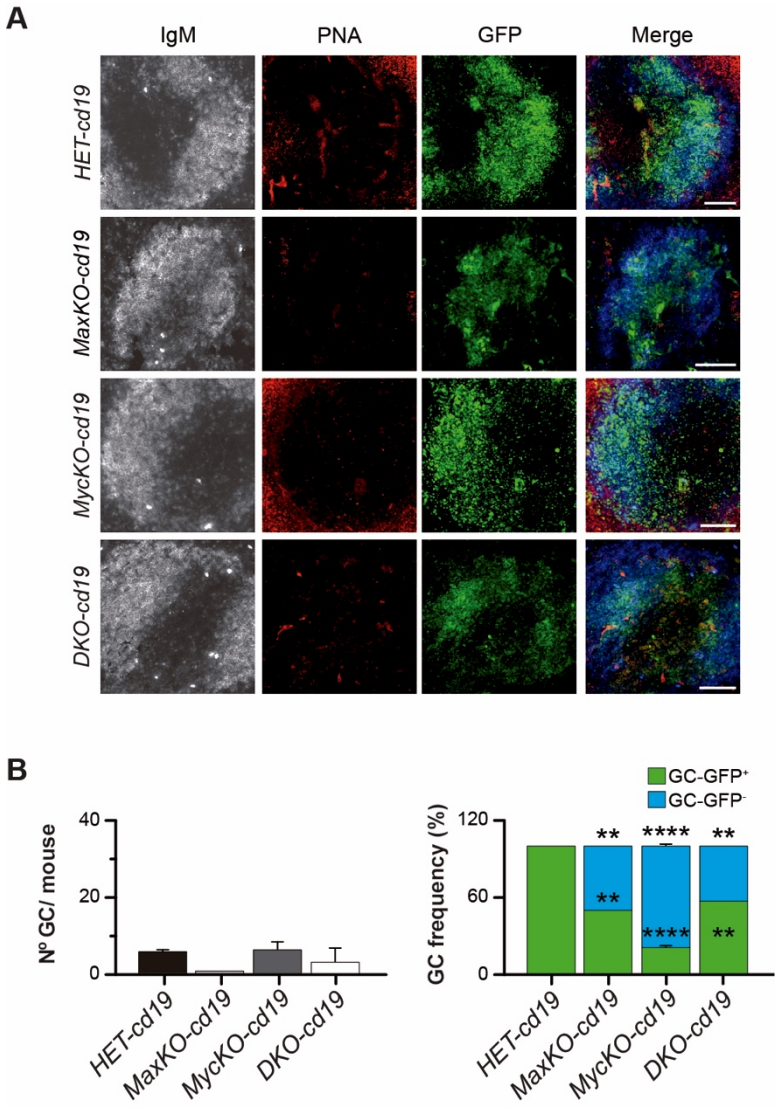

Figure R13. Analysis of GC formation upon PBS treatment. (A) Immunofluorescence analysis of GC formation in the spleen of *MaxKO-cd19*, *MycKO-cd19*, *DKO-cd19* and *HET-cd19* control mice, treated with PBS. Spleen cryosections were stained with antibodies against IgM (grey/blue), PNA (red) and GFP (green) to identify GC B cells; scale bar, 80 μm. (B) Left, Number of GCs per mouse in spleen cryosections from (A): *MaxKO-cd19* (n=2; n=84 follicles analysed per mouse), *MycKO-cd19* (n=2; n=163 follicles analysed per mouse), *DKO-cd19* (n=2; n=157 follicles analysed per mouse), *HET-cd19* (n=2; n=182 follicles analysed per mouse). Right, Frequency of GFP^+ (deleted cells) or GFP^- (non-deleted cells) GC cells (PNA^+) in PBS-treated mice: *MaxKO-cd19* (n=2 GCs), *MycKO-cd19* (n=14 GCs), *DKO-cd19* (n=7 GCs) and heterozygous control (n=13 GCs); $^{**}p < 0.01$, $^{****}p < 0.0001$.

5. MaxKO and DKO mature B lymphocytes are capable to undergo 2-3 cell divisions before ceasing proliferation

c-Myc has been widely described to be essential for control of cell proliferation, mainly through the regulation of G_1/S transition in the cell cycle (Bretones et al., 2015). c-Myc-deficient B cells do not proliferate upon activation *in vitro* (Alboran et al., 2001; Fernandez et al., 2013). To analyse the ability of MaxKO and DKO mature B cells to proliferate *in vitro*, we sorted B220$^+$ GFP$^+$ splenocytes from *MaxKO-cd19*, *MycKO-cd19*, *DKO-cd19* and *HET-cd19* mice, and activated them with LPS plus IL-4 for 72h. After stimulation, we observed a slight increase in the absolute numbers of MaxKO (1.48 x 10^5) and DKO (1.55 x 10^5) B cells, which was very similar between both conditions. As previously reported, no increase in B cell numbers was detected in MycKO cultures (0.85 x 10^5) (Figure R9A and (Fernandez et al., 2013)). Of note, the reduced size of B cells previously observed in MycKO B lymphocytes (Alboran et al., 2001) was slightly compensated in MaxKO and DKO B cells when compared to control cells (Figure R9B and R9C).

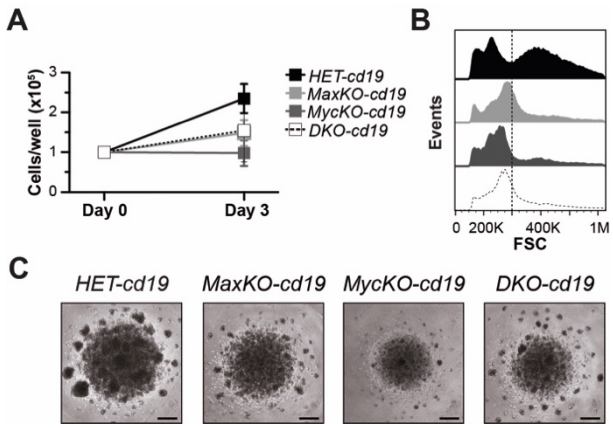

Figure R9. Stimulation cultures of mature B lymphocytes. (A) Number of cells in the cultures of B220$^+$ GFP$^+$ sorted B cells from the spleen of *MaxKO-cd19*, *MycKO-cd19*, *DKO-cd19* and *HET-cd19* mice, activated with LPS plus IL-4 for 72h (n=5). (B) Forward scatter (FSC) histograms of activated B lymphocytes from (A). (C) Photographs of B cell blast formed in the cultures from (A); Scale bar: 500 µm; 4x magnification. Data is representative of at least three independent experiments.

To monitor cell division, we analysed staining by a cell tracking dye by flow cytometry. Accordingly to our previous observations, MaxKO and DKO mature B lymphocytes retain some capacity to proliferate after activation with LPS plus IL-4. These cells were capable of undergoing 2-4 cell divisions in *in vitro* cultures. In contrast, c-Myc-deficient B lymphocytes did not divide (Figure R10A and (Fernandez et al., 2013)).

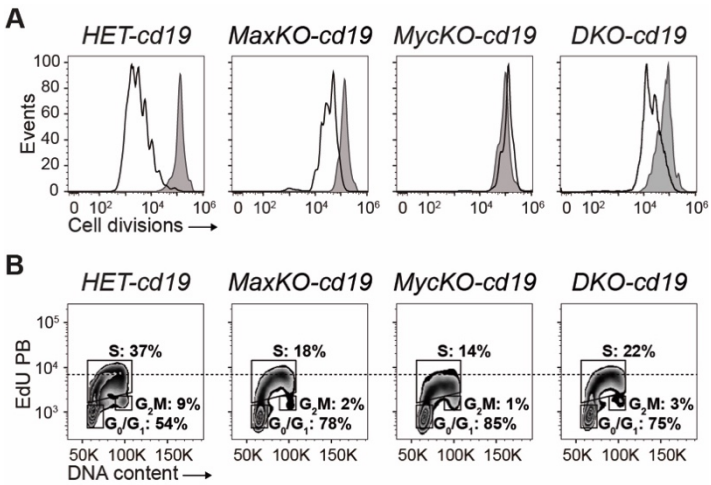

Figure R10. Proliferation in MaxKO and DKO B lymphocytes. (A) Number of cell divisions in activated mature B lymphocytes. Cells were B220$^+$ GFP$^+$ isolated from the spleen of *MaxKO-cd19* (n=5), *MycKO-cd19* (n=3), *DKO-cd19* (n=3) and control (n=5) mice. Before being activated *in vitro* with LPS plus IL-4, cells were stained with a cell tracer. After 72 h of culture, cells were analysed by flow cytometry to determine proliferation by dye dilution. (B) Cell cycle analysis by flow cytometry of sorted B220$^+$ GFP$^+$ B lymphocytes. Cells were activated *in vitro* as in (A), and EdU was added 4h before harvesting. Then, cells were stained with propidium iodide to measure DNA content. Dotted line is shown for EdU MFI comparations. Data is representative of at least three independent experiments.

To better understand the proliferative defect observed in mutant mice, we analysed the cell cycle *in vitro* by EdU incorporation and propidium iodide staining. MaxKO and DKO mature B lymphocytes showed a similar S phase EdU fluorescence intensity (MaxKO: 6,512; DKO: 6,420), higher than MycKO cells (MycKO MFI: 5,860), but lower than control cells (HET MFI: 7,871) (Figure R10B). The percentage of B cells in S and G_2/M phases was reduced in MaxKO, MycKO and DKO cells in contrast with

control cells, showing that c-Myc and Max are both needed for normal proliferation (Figure R10B).

6. Max regulation of DNA replication

Due to the observed differences in cell cycle and EdU incorporation in c-Myc-, Max- and c-Myc/Max-deficient B lymphocytes, we investigated whether these two transcription factors were implied in the regulation of DNA replication. To this aim, we performed stretched DNA fiber assays in sorted $B220^{+}$ GFP^{+} B lymphocytes, activated with LPS plus IL-4 for 48 h.

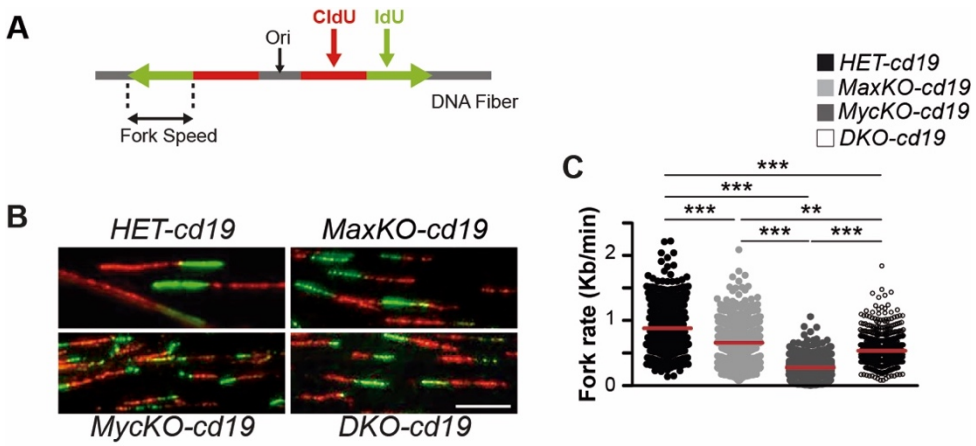

Figure R14. DNA replication analysis. (A) Schematic representation of replicating DNA fibers after CldU/IdU pulses. Since cells were first labelled with CldU (red) followed by IdU (green), the direction of fork movement can be determined in red-green tracks to analyse different replication patterns. (B) Representative images of stretched DNA fibers from sorted $B220^{+}GFP^{+}$ spleen B cells of *MaxKO-cd19*, *MycKO-cd19*, *DKO-cd19* and *HET-cd19* control mice, activated with LPS plus IL-4 for 48 h; scale bar, 10 μm. (C) Fork rate (Kb/min) of DNA fibers from mature B lymphocytes isolated and activated as in (B). Fork rate was determined by measuring the length of the labelled tracks in μm using ImageJ software, and converting it into Kb, then dividing this value by the labelling time. Data are pooled from three replicate experiments; horizontal red bars represent median values. 150-250 tracks were measured per condition (Quinet et al., 2017); $^{**}p < 0.01$, $^{***}p < 0.001$.

Fork speed (also known as fork rate) is defined as the velocity of replisomes moving away from replication origins upon their activation in S phase, and is a reflection of the number of activated origins and availability of replisome machinery and dNTPs (Técher et al., 2013). We noticed that the fork speed of c-Myc-deficient B cells was reduced compared to control cells (median 0.28 Kb/min vs. 0.88 Kb/min). We did not observe such a decrease in fork speed of MaxKO and DKO B cells (0.66 Kb/min and 0.54 Kb/min, respectively) (Figure R14). To characterize this phenotype in more detail, we decided to further investigate the replication machinery of our cells.

We did not observe any significant differences in the amount of Mcm3, Mcm4 and Mcm6 proteins, which are components of the MCM helicase complex essential for DNA replication initiation (Forsburg, 2008). Similarly, no apparent differences were observed among our three mutants and the heterozygous control in the amount of Cdc45 or Psf2, one of the subunits of the GINS complex (Aparicio et al., 2009; Takayama et al., 2003) (Figure R15).

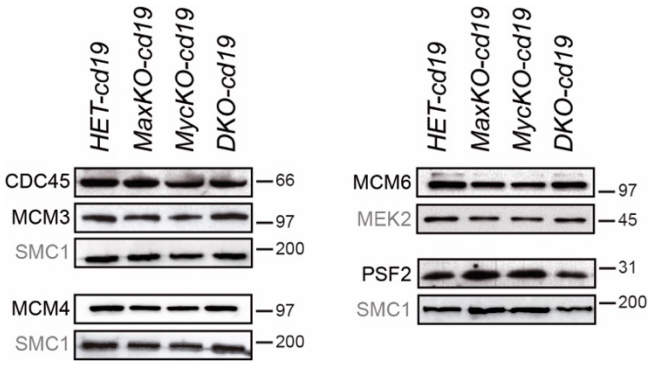

Figure R15. Western blot analysis of representative proteins of the DNA replication machinery. B220^{+} GFP^{+} cells were sorted from the spleen of *MaxKO-cd19*, *MycKO-cd19*, *DKO-cd19* and *HET-cd19* control mice, and activated *in vitro* with LPS plus IL-4 for 72h. MEK2 and SMC1 were used as loading controls. Blots are representative of three independent experiments.

Unexpectedly, we found that the levels of Cdc7 were dramatically reduced in *MycKO* B lymphocytes (Figure R16A). Cdc7 is the catalytic component of the DDK, responsible for MCM phosphorylation, and regulation of the initiation of DNA replication. Moreover, DDK-mediated Mcm2 subunit phosphorylation at Ser40 (Lei et al., 1997) was not observed in c-Myc-deficient B lymphocytes, and this also affected the total levels of Mcm2 protein (Figure R16B). These results show that the Cdc7 deficiency observed in MycKO B lymphocytes could account for the critical reduction in DNA replication observed in this genotype.

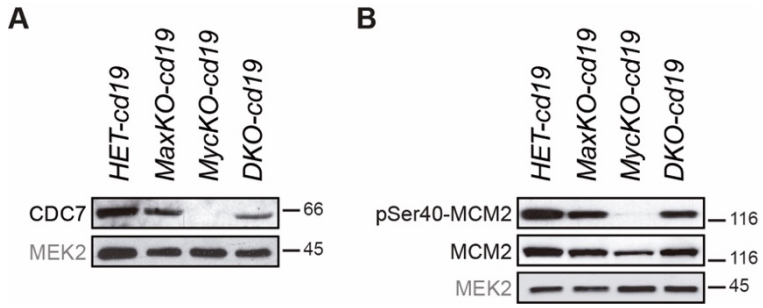

Figure R16. Immunoblot analysis of (A) CDC7 and (B) phosphorylated and total MCM2 helicase subunit in sorted mature B cells from *MaxKO-cd19*, *MycKO-cd19*, *DKO-cd19* and *HET-cd19* control mice. Cells were activated *in vitro* with LPS plus IL-4 for 72 h before western blot; MEK2 was used as loading control. Blots are representative of three independent experiments.

7. Gene expression profile of MaxKO, MycKO and DKO B lymphocytes

To analyse the transcriptional program of MycKO, MaxKO and DKO B lymphocytes, we performed a transcriptome-wide analysis of the mRNAs expressed in sorted $B220^{+}$ GFP^{+} splenocytes from *MaxKO-cd19*, *MycKO-cd19*, *DKO-cd19* and *HET-cd19*, activated with LPS plus IL-4 for 72h. RNA-Seq data identified 2,604, 3,313 and 2,559 differentially expressed genes (DEGs; $p < 0.01$) in B cells from *MaxKO-cd19*, *MycKO-cd19* and *DKO-cd19* mice, respectively, when individually compared

with the heterozygous control (Figure R17A). Hierarchical clustering analysis of all DEGs for the three mutant conditions showed that MaxKO and DKO B lymphocytes clustered closer to each other than to c-Myc-deficient B cells (Figure R17B).

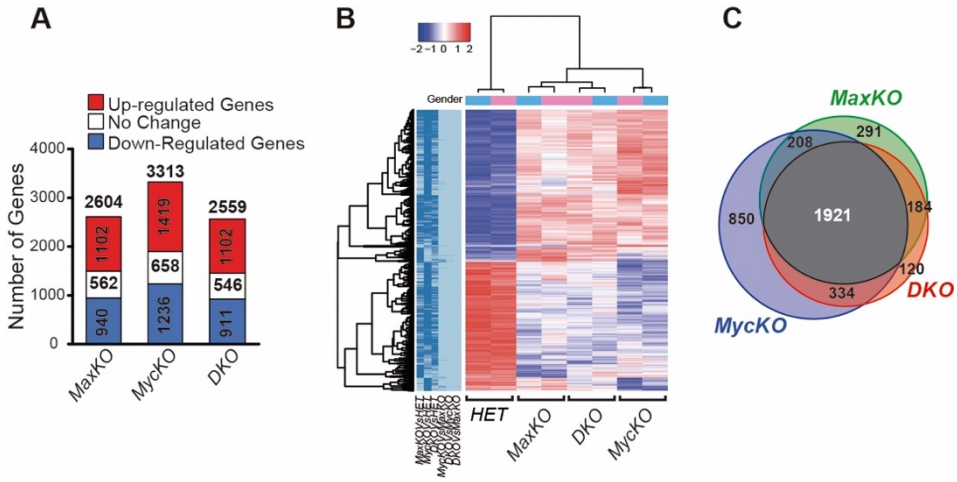

Figure R17.Gene expression analysis. (A) Bar plot of DEGs (adj. p-value < 0.01; FC > 1.5 in red (up-regulated genes), 1.5 < FC > -1.5 in white (unchanged genes), FC < -1.5 in blue (down-regulated genes). Mature splenic B cells were $B220^{+}$ GFP^{+} sorted from *MaxKO-cd19*, *MycKO-cd19*, *DKO-cd19* and *HET-cd19* control mice, and activated with LPS plus IL-4 for 72 h before RNA-Seq analysis; two samples for each condition were tested. (B) Hierarchical clustering heatmap of DEGs in each condition from (A). Dark blue in left panel indicates significance for that contrast column. Gender colour code: pink for female and blue for male mice. Heatmap colour code is same as in panel (A) (-2 to 2: raw Z-score). (C) Venn diagram showing the number of common DEGs in all conditions. The number in each circle stands for the quantity of DEGs between the different comparisons versus the control. Numbers in the overlapping regions represent the mutual DEGs shared between the different comparisons, and numbers in non-overlapping regions refer to the genes only deregulated in each experimental condition.

To further identify genes whose expression regulation was specific to one of our three experimental conditions, as well as those genes whose expression was common between some of them, we constructed Venn diagrams. This analysis showed that there were 1,921 genes deregulated in the three mutant conditions (Figure R17C), among which there were 1,445 overlapping DEGs with a fold expression change (FC) > 1.5 and < -1.5 (biological relevance cut-off): 797 up-, and 648 down-regulated (Figure R18).

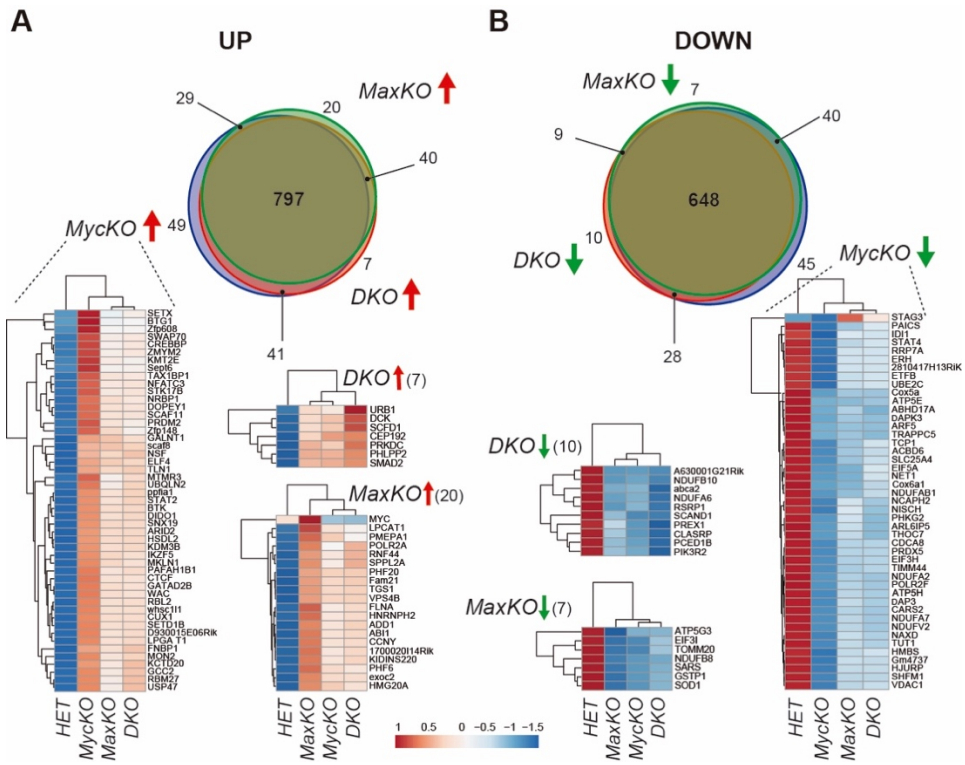

Figure R18. Heatmap analysis of deregulated genes. Venn diagram of up- (left panel) and down-regulated (right panel) DEGs for the three experimental conditions (MaxKO, MycKO and DKO versus control). FC > 1.5 and < -1.5; adj. p-value < 0.01. Heatmaps of unique DEGs to each condition. Dark blue in left panel indicates significance for that contrast column. Gender colour code: pink for female and blue for male mice. Heatmap colour code: red (up-regulated genes), white (unchanged genes), blue (down-regulated genes) (-1.5 to 1: raw Z-score)..

Following the Venn overlapping sections for the three experimental conditions, we performed an enrichment analysis to identify gene ontology (GO) categories (False Discovery Rate (FDR) < 0.05) that were over- or under-represented among DEGs. With this aim, we carried out functional classification analyses using DAVID Bioinformatics Resources (Huang et al., 2009), based on biological processes (BP) and molecular functions (MF) (Figure R20), as well as on KEGG (Kyoto Encyclopedia of Genes and Genomes) pathway annotations (Ogata et al., 2000) (Figure R19). We observed that up-regulated genes in the three experimental conditions were enriched in functional categories such as regulation of actin cytoskeleton, MAPK and NF-κB signalling, B cell

receptor and thyroid hormone signalling, among others (Figure R18A). Immune-related and transcriptional processes were also over-represented among up-regulated DEGs by GO analysis (Figure R19A and Figure R20A). For down-regulated genes, there was also a significant enrichment in diverse pathways, with ribosome and metabolic pathways the most over-represented (Figure R19B and R20B). All these DEGs were more affected in c-Myc-deficient B lymphocytes than in MaxKO or DKO B cells, which may explain the similar phenotypic behaviour observed between them (Figure R19, lower panel).

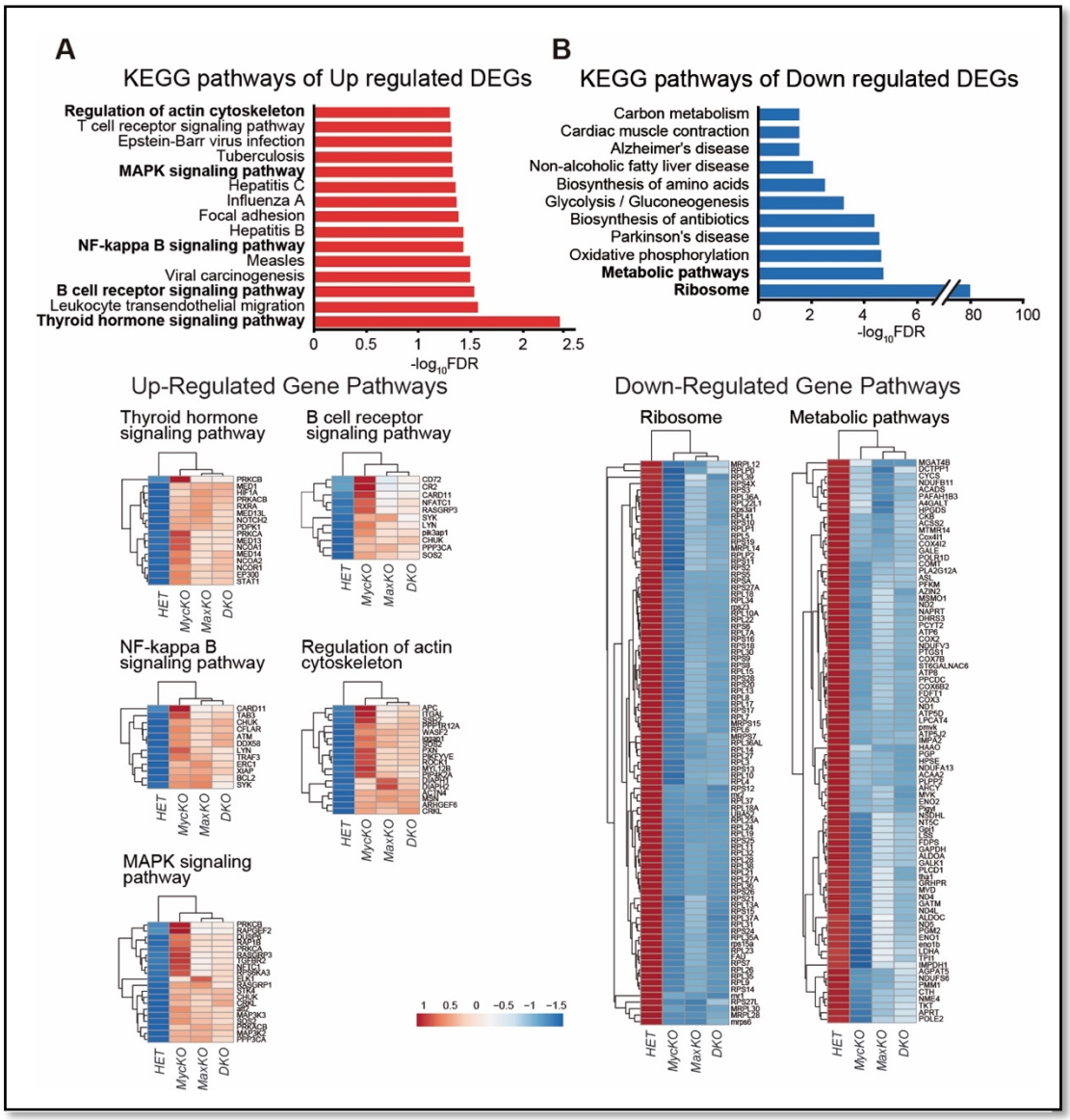

Figure R19. KEGG pathway analysis of deregulated genes. (A) Bar plot of KEGG pathway enrichment analysis (FDR < 0.05) (upper panels) and heatmaps (lower panels) resulting for the transcriptomic comparison of up-regulated genes common to our three experimental conditions (MaxKO, MycKO and DKO). FC > 1.5 and < -1.5; adj. p-value < 0.01. (B) KEGG pathways and heatmaps of down-regulated genes, as in (A). Relevant pathways are indicated in bold letters. Heatmap colour code: red (up-regulated genes), white (unchanged genes), blue (down-regulated genes) (-1.5 to 1: raw Z-score).

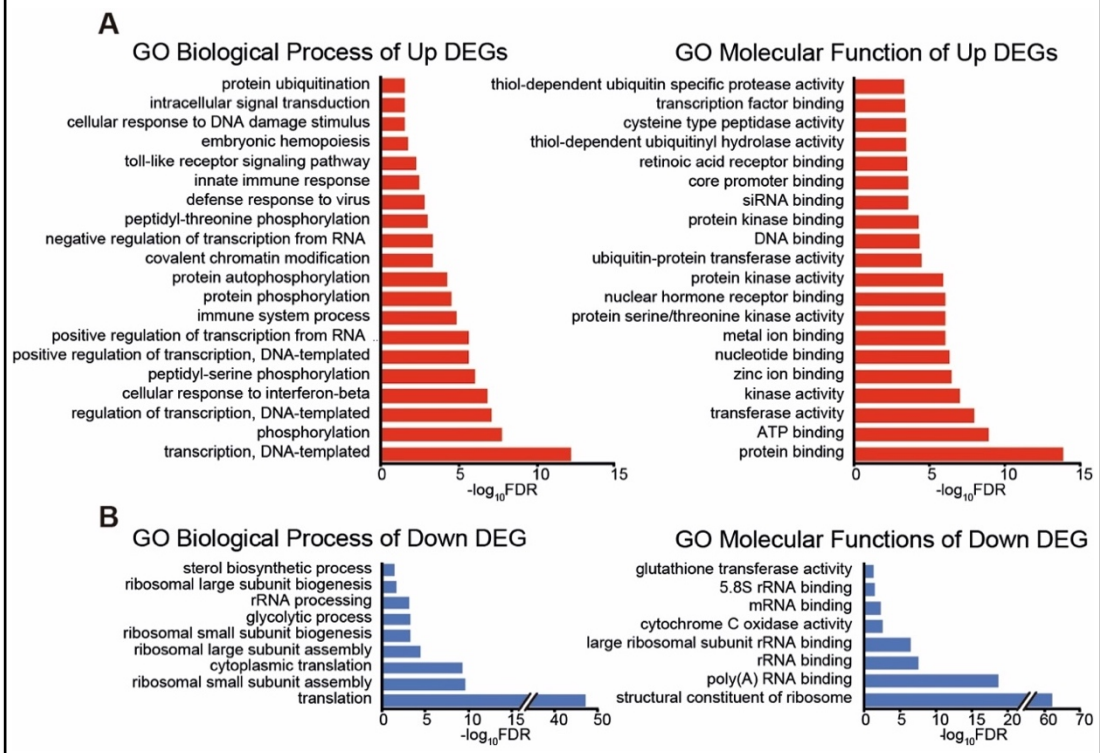

Figure R20. Gene Ontology analysis of deregulated genes. Bar plot representing the distribution of GO Biological Processes (left) and Molecular Functions (right) of (A) over-represented (red) or (B) under-represented (blue) DEGs (FC > 1.5 and < -1.5; adj. p-value < 0.01) common to our three experimental conditions (MaxKO, MycKO and DKO), determined by DAVID tools (FDR < 0.05).

Among all DEGs, we found 45 down- (Figure R21, left panel) and 49 upregulated (Figure R21, right panel) genes that were altered only in mature B cells from *MycKO-cd19* mice. These genes theoretically correspond to genes that are repressed or induced genes by c-Myc alone, respectively. Down-regulated genes were involved in a variety of molecular pathways (Figure R21, left panel), whereas up-

regulated genes were related to transcription regulation and chromatin modification processes, as well as histone methyltransferase activity (H3-K4 specific) (Figure R21, right panel). For *MaxKO-cd19* and *DKO-cd19* mice, enrichment analysis resulted in no statistically differences among up- and down-regulated genes only altered in those conditions, by enrichment analysis.

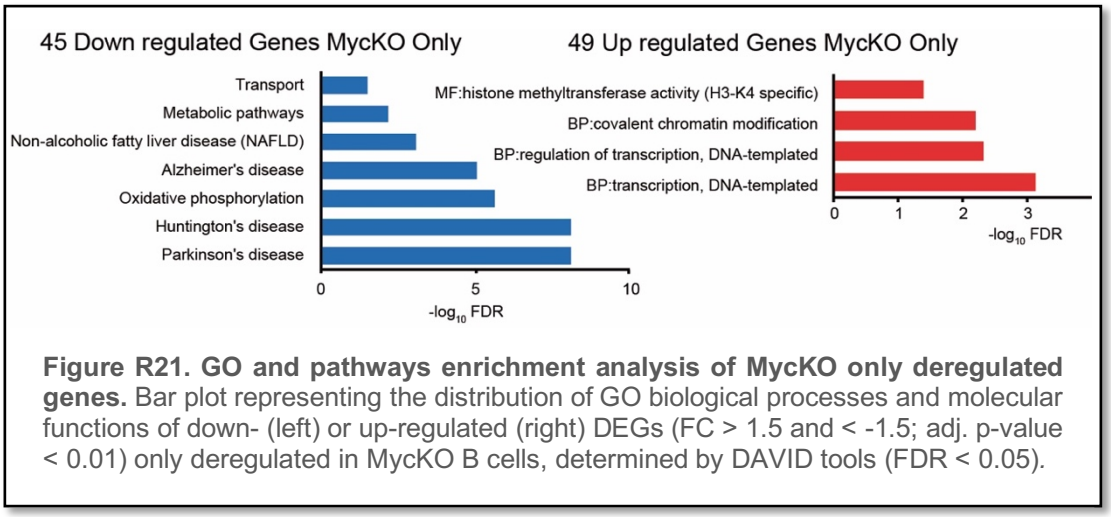

Figure R21. GO and pathways enrichment analysis of MycKO only deregulated genes. Bar plot representing the distribution of GO biological processes and molecular functions of down- (left) or up-regulated (right) DEGs (FC > 1.5 and < -1.5; adj. p-value < 0.01) only deregulated in MycKO B cells, determined by DAVID tools (FDR < 0.05).

RNA-Seq data was validated by qPCR analysis of randomly-chosen up- and down-regulated DEGs (Figure R21A), and by comparison with the previously reported gene expression profile of *MycKO-cd19* mice ((Fernandez et al., 2013) and Figure R21B). Strikingly, we found no differences in *cdc7* expression by qPCR analysis (Figure R21A), or RNA-Seq (Annex Table1), despite the dramatic reduction of this protein observed by western blot in MycKO mature B lymphocytes (Figure R16).

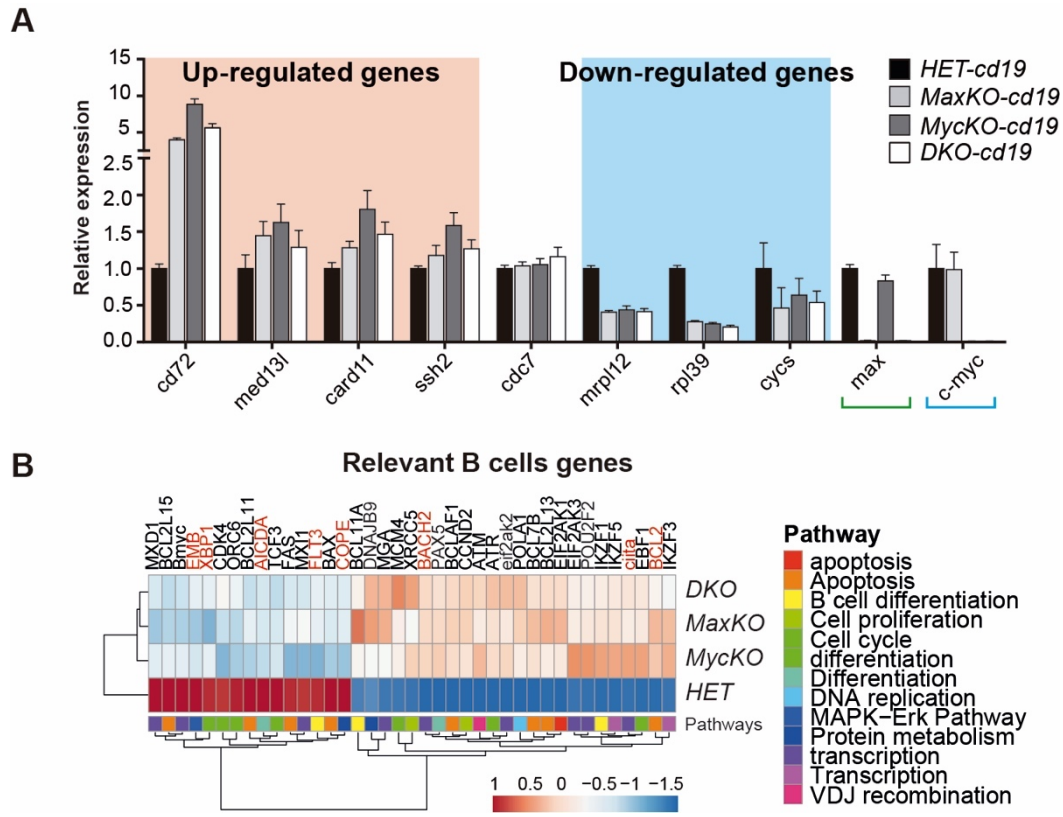

Figure R22. Real-time PCR analysis and pathway analysis of relevant B cell genes. (A) qPCR analysis of randomly-chosen up- and down-regulated DEGs (FC > 1.5 and < -1.5; adj. p-value < 0.01) for our three experimental conditions (*MaxKO*, *MycKO* and *DKO).* RNA templates were pooled from sorted B220^{+} GFP^{+} splenic B lymphocytes of *MaxKO-cd19*, *MycKO-cd19*, *DKO-cd19* and *HET-cd19* control mice (n=4). Prior to RNA extraction, mature B cells were activated *in vitro* with LPS plus IL-4, for 72 h. qPCR specific primers are described in Materials and Methods. *actin* was used as a housekeeping gene for normalization. (B) Heatmap of DEGs (FC > 1.5 and < -1.5; adj. p-value < 0.01) involved in B lymphocyte differentiation. Red highlighted genes were previously tested by qPCR on *MycKO-cd19* mice (Fernandez et al., 2013). The rainbow legend refers to main pathways classification.

We also performed a comparative analysis of our RNA-Seq results (Figure R19 and Figure R20) with previously reported *c-myc* expression data in primary B (Nie et al., 2012) and T (Chou et al., 2014) lymphocytes (Figure R23). As expected, we obtained an opposite functional pattern when MycKO mature B lymphocytes activated with LPS plus IL-4 were compared with LPS-activated primary B lymphocytes (Figure

R23A). A similar pattern of pathway expression was seen between our mature B lymphocytes lacking c-Myc and c-Myc-deficient T lymphocytes (Figure R23B).

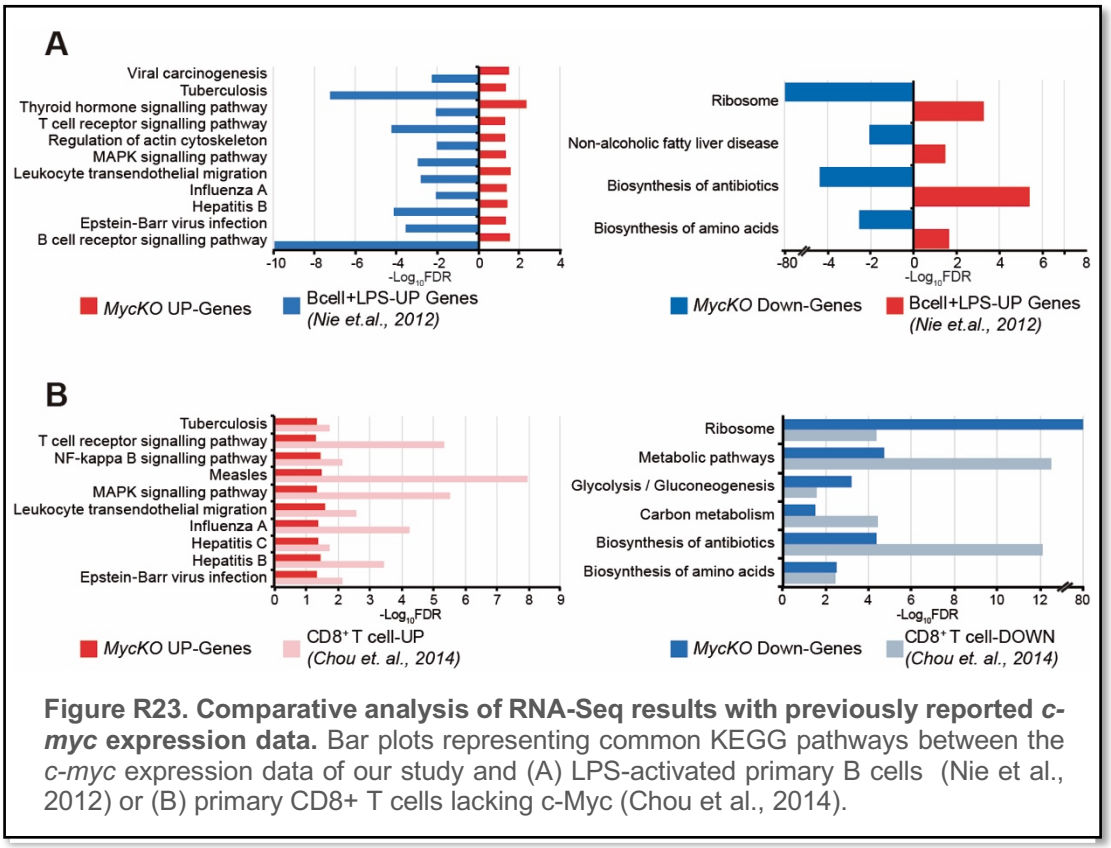

Figure R23. Comparative analysis of RNA-Seq results with previously reported *c-myc* expression data. Bar plots representing common KEGG pathways between the *c-myc* expression data of our study and (A) LPS-activated primary B cells (Nie et al., 2012) or (B) primary CD8+ T cells lacking c-Myc (Chou et al., 2014).

DISCUSSION

DISCUSSION

The Myc family of transcription factors regulate numerous biological functions through the binding with its mandatory partner Max. However, recent studies have raised the possibility that Myc performs some cell functions in a Max-independent manner. In this thesis, we have addressed the functional contribution of each factor to B lymphocyte differentiation and function. For this, we have generated unique *in vivo* models in which we specifically deleted *max*, *c-myc* and *c-myc/max* at early and mature B cell stages.

First, we bred $max^{fl/fl}$ mice with $mb\text{-}1^{cre/+}$ mice (Hobeika et al., 2006), in which Cre recombinase expression is controlled by the promoter of the *Ig-*α chain of the BCR (*mb-1* gene). Conditional inactivation of *max* from the pro-B cell subpopulation using *mb1-cre* bearing mice allowed us to define the requirement of this gene at early developmental stages. *In vivo*, we observed that, unlike c-Myc-deficient B lymphocytes, MaxKO and DKO B cells could progress through the B cell differentiation program, albeit less efficiently than *wt* B lymphocytes ((Vallespinos et al., 2011) and Figure R3A). Our *in vitro* results (Figure R5) show that B cell progenitors ($B220^+$ IgM^- GFP^+) from *MaxKO-mb1* mice were able to differentiate into mature B cells, ruling out the possibility of cells that had escaped Cre-mediated deletion. Accordingly, MycKO B cells do not differentiate *in vitro* (Vallespinos et al., 2011).Thus, mature B cells in the spleen of *MaxKO-mb1* mice were likely the result of cells that had differentiated from pro-B cells. Despite their capacity to differentiate, the absolute numbers of MaxKO and DKO B cells were significantly reduced in the BM and spleen of these mice (Figure R4). This result can be explained either by a defect in cell proliferation, an increased apoptosis or a combination of both. We observed that differentiating and mature B cells retain some capacity to proliferate when compared to MycKO B lymphocytes, without significant differences in apoptosis (Figure R6). Therefore, the limited proliferation capacity of Max and DKO B cells may explain the reduced absolute numbers in the BM and the spleen of *MaxKO-mb1* and *DKO-mb1* mice.

To study c-Myc/Max interplay in mature B lymphocytes, *max*$^{fl/fl}$ mice were bred with *cd19-cre* mice (Rickert et al., 1995) to generate *MaxKO-cd19, MycKO-cd19, DKO-cd19* and control mice. These mice are less efficient in Cre-mediated recombination in the BM than *mb-1*$^{cre/+}$ mice, leading to larger numbers of differentiating non-deleted B cells capable of populating the spleen, and subsequently undergo Cre deletion as mature B lymphocytes. Thus, this model provides a higher absolute number of deleted mature B cells in the spleen for the analysis. We used this model to test specific B cell functions in mature lymphocytes. Activation of sorted mature B cells with LPS plus IL-4 *in vitro*, mimics a T cell-dependent antigen *in vitro*. Our results show that, in spite of the ability of MaxKO and DKO B cells to generate ASC and to perform CSR to the IgG1 isotype, both c-Myc and Max were required in order to produce optimal numbers of these mature B lymphocytes (Figure R7 and R8).

The role of c-Myc in regulating G_1/S transition has been widely studied (Bretones et al., 2015). Previous results of our group have shown that primary B lymphocytes are not able to proliferate upon *in vitro* stimulation (Alboran et al., 2001; Fernandez et al., 2013). Unexpectedly, we observed that the absolute numbers of MaxKO and DKO B lymphocytes increased in culture when cells were activated with LPS plus IL-4 (Figure R9). A more detailed analysis of the cell cycle by Edu incorporation and propidium iodide staining showed a reduction in the percentage of cells in S and G_2/M phases in MaxKO, MycKO and DKO mature B cells when compared to controls (Figure R10). A less dramatic decrease was observed in pro- and pre-B cell stages *in vivo* using *mb1-cre* mice (Figure R6). As *mb1-cre* expression starts at the pro- and pre-B stages, it is possible that the difference in proliferation between developing (*mb1-cre*) and mature B cells (*cd19-cre*) was due to the presence of a mixed population of deleted and non-deleted cells at those early stages in *mb1-cre* mice.

Altogether, this data supports the general idea that c-Myc needs Max for its normal proliferative function; a lack of Myc leads to a strong inhibitory phenotype. We hypothesized that the presence of Max in Myc deprived B cells (MycKO cells), would

allow the occupation of Myc binding sites by Max alone or by interacting with other proteins of the Myc/Max/Mxd-Mga network, antagonizing Myc function.

We also analysed the immune response *in vivo* of *MaxKO-cd19*, *MycKO-cd19* and *DKO-cd19* mice to a T cell-dependent antigen such as TNP-KLH, by studying the formation of GCs. The formation of these structures is a hallmark of a robust immune response, being crucial for the final maturation and specialization of B lymphocytes. The generation of GC in our three mutant mice was greatly compromised when compared to controls (Figure R11 and R12). The limited capacity of these cells to proliferate upon *in vitro* stimulation (Figure R10) accounts for the dramatic reduction observed in the number of cells that differentiated to ASC or perform CSR (Figure R7 and R8). Thus, this decreased capacity to proliferate may explain the defect of these cells to generate GCs *in vivo*.

Some of the main effects of Myc in physiological and pathological scenarios can be explained by its ability to regulate DNA replication at transcriptional and not-transcriptional levels (Dominguez-Sola and Gautier, 2014). Here we show that DNA fork speed was dramatically reduced in c-Myc-deficient B cells upon *in vitro* activation (Figure R14). Moreover, no significant differences were observed in proteins of the pre-RC of these cells (Figure R15). However, we found a dramatic reduction in the levels of Cdc7 in MycKO B lymphocytes (Figure R16). This protein is the catalytic subunit of the DDK kinase, responsible for MCM helicase phosphorylation and activation during G_1/S transition (Heller et al., 2011; Weinreich and Stillman, 1999), which may explain the reduction in fork speed observed in this genotype, due to a decrease in origin firing and the decreased proliferation observed in these cells. Interestingly, the absence of Max in the DKO genomic context can partially rescue this replication phenotype. Using the GTRD database, we found an E-box located in a *cdc7* promoter proximal site (at 328 nt from the transcriptional start site) (Yevshin et al., 2017)). This finding prompted us to deeply analyse the possibility of a direct regulation of c-Myc over Cdc7. However, RNA-Seq and qPCR analysis did not show differences in *cdc7* expression between MycKO B lymphocytes and heterozygous control B cells (Figure R22). We speculate

that c-Myc may be regulating Cdc7 at a post-transcriptional level, by affecting the *cdc7* mRNA translation process and/or Cdc7 folding or stability.

In order to determine the transcriptional profile that underlies the phenotypic effects observed in mature B lymphocytes from *MaxKO-cd19*, *MycKOcd19* and *DKO-cd19* mice, we carried out RNA-Seq analyses of these cells after *in vitro* activation. Among all DEGs, 1,921 were simultaneously deregulated in the three mutant conditions. The gene expression profiles of MaxKO and DKO B cells clustered closer than MycKO B cells, by hierarchical clustering analysis (Figure R17). This fact provides an explanation for how DKO B lymphocytes are able to partially rescue some of the defects observed in the MycKO conditions. DKO B lymphocytes showed a phenotype more similar to MaxKO B cells in biological processes such as cell differentiation (Figure R3), proliferation (Figure R6 and Figure R10) and DNA replication (Figure R14-R16). In addition, since no significant differences were observed in *n-* and *l-myc* expression among our three mutants and control cells (Annex Table1), we ruled out the possibility of a functional compensation among the different Myc family members.

Of the 1,921 simultaneously deregulated genes, 1,445 genes were altered (up- or down-regulated) in the three experimental conditions, suggesting a high degree of overlap between the c-Myc and Max regulatory networks (Figure R18). In fact, these data indicate that those genes downregulated in MaxKO, MycKO and DKO mature activated B lymphocytes, were likely activated by the c-Myc/Max heterodimer. Accordingly, the genes upregulated in the three experimental conditions are likely those repressed by the c-Myc/Max complex in normal conditions.

The majority of upregulated DEGs in the three mutant conditions showed an enrichment in immune-related and transcriptional processes. Common down-regulated DEGs, however, were involved in metabolic and ribosome pathways (Figure R20). c-Myc has been previously described to regulate the expression of growth-related genes in B lymphocyte differentiation upon mitogenic stimulation, increasing cell size and protein synthesis (Iritani and Eisenman, 1999). Our results show that cell size of B lymphocytes is not absolutely dependent on Max, as DKO as well as MaxKO B cells

had some capacity to restore it when compared to MycKO B cells upon *in vitro* activation (Figure R9). The defect in protein synthesis might be a contributing factor to this phenotype.

GO data suggested that the absence of c-Myc, Max or both results in the up-regulation of genes involved in signalling pathways, which in the end are responsible for modulation of the effector signal of mutant B cells. We observed that these cells were able to sense mitogenic stimuli, as we observed an increase in CD69 surface expression, though they were not able to respond properly (Figure R8D). A possible explanation could be that the absence of c-Myc and Max prevents the induction of a negative feedback loop of these transcription factors to regulate the response, as seen in immature B cells (Benhamou et al., 2016). We hypothesize that the presence of Max only in the MycKO model acts as an inhibitor by occupying c-Myc-binding sites on E-boxes. In addition, the observed defects in ribosome components and function may prevent B lymphocytes from executing their biological functions.

The RNA-seq analysis was validated by comparison with previously described *c-myc* expression data. Despite the differences in experimental settings and stimulus, we found stunning similarities in the up- and down-regulated pathways between our data and c-Myc-deficient T cells (Chou et al., 2014), with the MAPK and NF-κB signalling pathways the most over-represented, and metabolic and ribosome pathways down-regulated. Moreover, LPS-activated primary B cells (Nie et al., 2012) showed the opposite pattern of pathway expression when compared to our LPS plus IL-4 activated c-Myc-deficient B lymphocytes (Figure R23). Altogether, these results suggest a similar functional pattern in B and T lymphocytes.

Previous results from our group and others have shown that c-Myc is necessary for relevant biological functions in these cells, such as cell proliferation and apoptosis. More importantly, c-Myc is required not only for normal B cell differentiation, but also for a competent and robust immune response (Alboran et al., 2001; Alborán et al., 2004; Calado et al., 2012; Fernandez et al., 2013; Vallespinos et al., 2011). Here our data suggest that c-Myc must act together with Max to perform its normal function, but none of these transcription factors are strictly needed for the initiation of some cellular

processes in primary B lymphocytes. In the absence of c-Myc, Max likely plays an inhibitory role over c-Myc-regulated functions, either alone or by binding to other proteins of the Myc/Max/Mxd-Mga network. We unexpectedly found a reduction of c-Myc levels in MaxKO mature B cells by WB (Figure R1D), despite normal levels of *c-myc* RNA (Figure R22). This observation needs to be studied in more detail in future experiments; Max is likely influencing c-Myc regulation at an mRNA translation and/or at protein stability level. This effect became evident in the DKO mouse model, where the absence of both c-Myc and Max did not completely hinder certain biological functions, such as cell proliferation or apoptosis, when compared to MaxKO B cells. We speculate that it is likely a Max-dependent mechanism that regulates c-Myc levels in primary B lymphocytes, which would explain the similar phenotype observed between *MaxKO-cd19* and *DKO-cd19* mice. In light of this data, we cannot conclude Max-independent functions of Myc in developing and mature B lymphocytes.

Overall, our work has shown that c-Myc is needed for normal regulation of its target genes, having the most severe phenotype of all the mutant conditions, as previously described in other studies (Fernandez et al., 2013; Vallespinos et al., 2011). In fact, this work support an antagonistic role of Max in Myc functions, either by occupying E-boxes or dimerizing with Mxd or Mga proteins (Conacci-Sorrell et al., 2014; Link and Hurlin, 2015). In addition, in this study we have observed a similar pattern of pathway regulation between c-Myc and Max, reinforcing the idea that c-Myc needs Max to regulate certain target genes that can afterwards amplify the transcriptional signal (Sabo and Amati, 2014). We propose that c-Myc/Max heterodimers might be the main effectors of c-Myc function in B lymphocyte differentiation, despite the fact that some relevant biological function can still be initiated in the absence of it. Thus, the first stages of these processes are likely to be independent of c-Myc/Max heterodimers, but both factors are required to maintain, amplify or fine-tune these functions.

The generation of c-Myc/max double KO mutants in a conditional setting provided us the possibility to analyse the contribution of c-Myc and Max to B lymphocyte differentiation and function. Moreover, due to the central role of Max in the

Myc/Max/Mxd-Mga network, these DKO mice, together with the MycKO and MaxKO models, offer a good scenario for further study of the c-Myc/Max relationship in other tissues. These mouse models also provide a powerful tool to study Max interplay with other related proteins, apart from c-Myc.

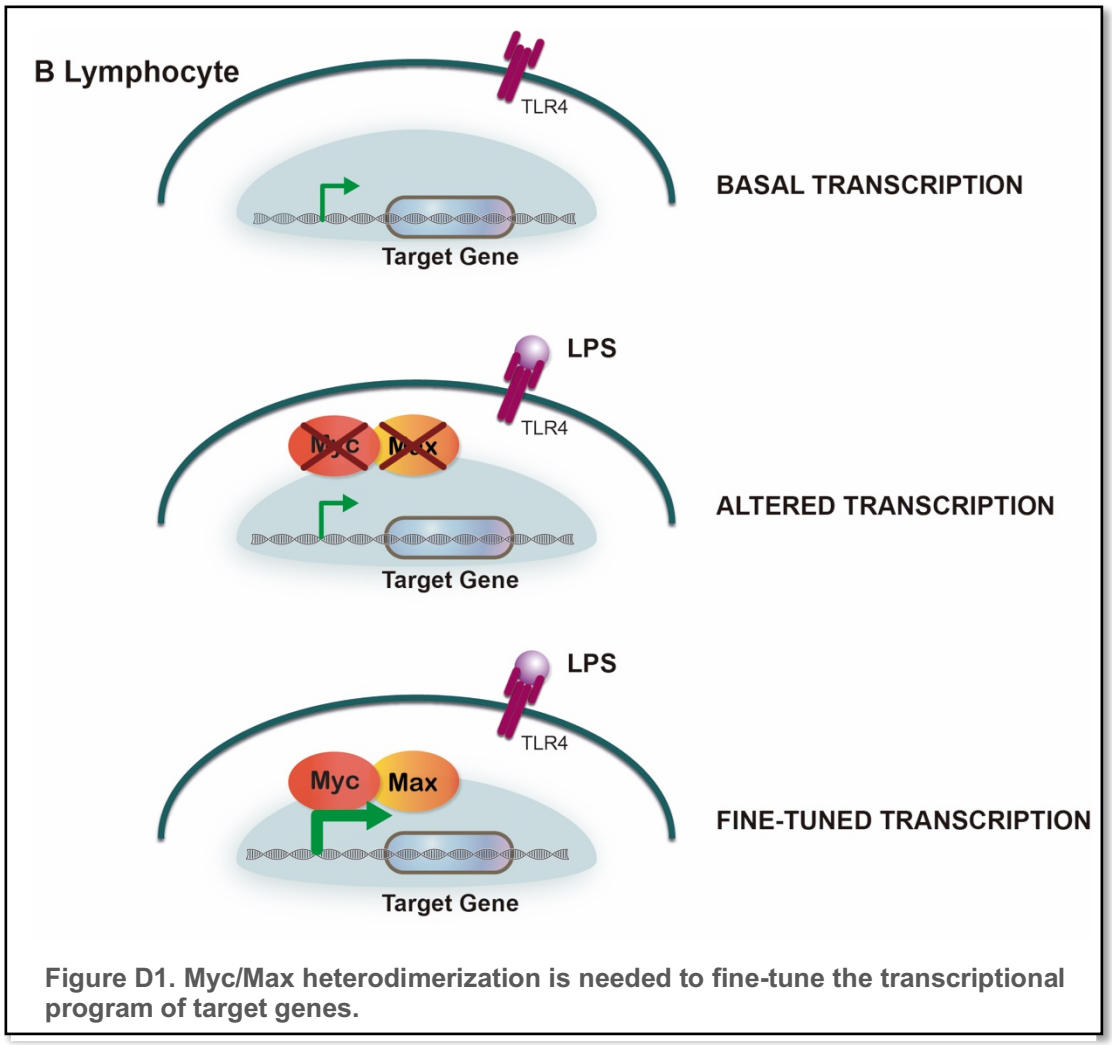

Figure D1. Myc/Max heterodimerization is needed to fine-tune the transcriptional program of target genes.

CONCLUSIONS

CONCLUSIONS

1. B cell progenitors can differentiate into immature and mature B lymphocytes in the absence of Max and c-Myc/Max, in *MaxKO-mb1* and *DKO-mb1* mice, respectively.

2. Max-deficient and DKO mature B lymphocytes generate antibody secreting cells and undergo class switch recombination to IgG1 *in vitro*.

3. Max and c-Myc are necessary for the formation of germinal centers and a robust T cell-dependent immune response.

4. B cell apoptosis is normal in developing and mature B lymphocytes in the absence of either Max or c-Myc/Max.

5. Upon activation, MaxKO and DKO mature B cells can undergo a few cell divisions before ceasing proliferation *in vitro*.

6. DNA replication is impaired in c-Myc-deficient B lymphocytes, and this phenotype correlates with the absence of Cdc7.

7. A c-Myc-dependent post-transcriptional mechanism controls Cdc7 in primary B cells.

8. MaxKO, MycKO and DKO mature B cells show upregulation of gene expression of members of multiple B cell-related signaling pathways.

9. Max has an inhibitory effect in the absence of c-Myc in primary B lymphocytes.

10. A Max-dependent mechanism controls c-Myc levels in primary B lymphocytes.

CONCLUSIONES

1. Los progenitores de linfocitos B pueden diferenciarse a células B inmaduras y maduras en ausencia de Max y de c-Myc/Max, en ratones *MaxKO-mb1* y *DKO-mb1*, respectivamente.

2. Los linfocitos B maduros deficientes en Max y c-Myc/Max generan células secretoras de anticuerpos y llevan a cabo el cambio de clase de las inmunoglobulinas hacia IgG1 *in vitro*.

3. Max y c-Myc son necesarios para la formación de centros germinales y la generación de una respuesta inmunológica robusta dependiente de células T.

4. El proceso de apoptosis celular en los linfocitos B es normal en ausencia de Max y de c-Myc/Max, tanto en células B en desarrollo como en células B maduras.

5. Tras la activación, los linfocitos B maduros MaxKO y DKO pueden llevar a cabo 2-3 divisiones celulares antes de dejar de proliferar *in vitro*.

6. Los linfocitos B deficientes en c-Myc tienen impedido el proceso de replicación del ADN, y este fenotipo se correlaciona con la ausencias de Cdc7.

7. Los niveles de Cdc7 en linfocitos B primarios están controlados por un mecanismo post-transcripcional dependiente de c-Myc.

8. Los linfocitos B maduros MaxKO, MycKO y DKO muestras un aumento en la expresión génica de múltiples miembros de vías de señalización relacionadas con las células B.

9. Max tiene una efecto inhibitorio en ausencia de c-Myc en los linfocitos B primarios.

10. Los niveles de c-Myc en linfocitos B primarios están controlados por un mecanismo dependiente de Max.

BIBLIOGRAPHY

BIBLIOGRAPHY

Aladjem, M.I., and Redon, C.E. (2017). Order from Clutter: Selective Interactions at Mammalian Replication Origins. Nat. Rev. Genet. *18*, 101–116.

Alboran, I.M. de, O'Hagan, R.C., Gärtner, F., Malynn, B., Davidson, L., Rickert, R., Rajewsky, K., DePinho, R.A., and Alt, F.W. (2001). Analysis of C-MYC Function in Normal Cells via Conditional Gene-Targeted Mutation. Immunity *14*, 45–55.

Alborán, I.M. de, Baena, E., and Martinez-A, C. (2004). c-Myc-deficient B Lymphocytes are Resistant to Spontaneous and Induced Cell Death. Cell Death Differ. *11*, 61–68.

Alvarez, S., Díaz, M., Flach, J., Rodriguez-Acebes, S., López-Contreras, A.J., Martínez, D., Cañamero, M., Fernández-Capetillo, O., Isern, J., Passegué, E., et al. (2015). Replication Stress Caused by Low MCM Expression Limits Fetal Erythropoiesis and Hematopoietic Stem Cell Functionality. Nat. Commun. *6*.

Amati, B., Dalton, S., Brooks, M.W., Littlewood, T.D., Evan, G.I., and Land, H. (1992). Transcriptional Activation by the Human c-Myc Oncoprotein in Yeast requires Interaction with Max. Nature *359*, 423–426.

Amati, B., Brooks, M.W., Littlewood, T.D., Evan, G.I., and Land, H. (1993a). Oncogenic Activity of the c-Myc Protein Requires Dimerization with Max. Cell *72*, 233–245.

Amati, B., Littlewood, T.D., Evan, G.I., and Land, H. (1993b). The c-Myc Protein Induces Cell Cycle Progression and Apoptosis through Dimerization with Max. EMBO J. *12*, 5083–5087.

Aparicio, T., Ibarra, A., and Méndez, J. (2006). Cdc45-MCM-GINS, a New Power Player for DNA Replication. Cell Div. *1*, 18.

Aparicio, T., Guillou, E., Coloma, J., Montoya, G., and Méndez, J. (2009). The Human GINS Complex Associates with Cdc45 and MCM and is Essential for DNA Replication. Nucleic Acids Res. *37*, 2087–2095.

Ayer, D.E., and Eisenman, R.N. (1993). A switch from Myc:Max to Mad:Max heterocomplexes accompanies monocyte/macrophage differentiation. Genes Dev. *7*, 2110–2119.

Ayer, D.E., Kretzner, L., and Eisenman, R.N. (1993). Mad: A Heterodimeric Partner for Max that Antagonizes Myc Transcriptional Activity. Cell *72*, 211–222.

Benhamou, D., Labi, V., Novak, R., Dai, I., Shafir-Alon, S., Weiss, A., Gaujoux, R., Arnold, R., Shen-Orr, S.S., Rajewsky, K., et al. (2016). A c-Myc/miR17-92/Pten Axis Controls PI3K-Mediated Positive and Negative Selection in B Cell Development and Reconstitutes CD19 Deficiency. Cell Rep. *16*, 419–431.

Blackwell, T., Kretzner, L., Blackwood, E., Eisenman, R., and Weintraub, H. (1990). Sequence-specific DNA Binding by the c-Myc Protein. Science *250*, 1149–1151.

Blackwood, E., and Eisenman, R. (1991). Max: A Helix-Loop-Helix Zipper Protein that Forms a Sequence-specific DNA-binding Complex with Myc. Science *251*, 1211–1217.

Blackwood, E.M., Lüscher, B., and Eisenman, R.N. (1991). Myc and Max Associate in vivo. Genes Dev. *6*, 71–80.

Borlado, L.R., and Méndez, J. (2008). CDC6: from DNA Replication to Cell Cycle Checkpoints and Oncogenesis. Carcinogenesis *29*, 237–243.

Bretones, G., Delgado, M.D., and León, J. (2015). Myc and Cell Cycle Control. Biochim. Biophys. Acta BBA - Gene Regul. Mech. *1849*, 506–516.

Búa, S., Sotiropoulou, P., Sgarlata, C., Borlado, L.R., Eguren, M., Domínguez, O., Ortega, S., Malumbres, M., Blanpain, C., and Méndez, J. (2015). Deregulated

Expression of Cdc6 in the Skin Facilitates Papilloma Formation and Affects the Hair Growth Cycle. Cell Cycle *14*, 3897–3907.

Busslinger, M. (2004). Transcriptional Control of Early B Cell Development. Annu. Rev. Immunol. *22*, 55–79.

Calado, D.P., Sasaki, Y., Godinho, S.A., Pellerin, A., Köchert, K., Sleckman, B.P., de Alborán, I.M., Janz, M., Rodig, S., and Rajewsky, K. (2012). The Cell-Cycle Regulator c-Myc is Essential for the Formation and Maintenance of Germinal Centers. Nat. Immunol. *13*, 1092–1100.

Chaudhuri, J., and Alt, F.W. (2004). Class-Switch Recombination: Interplay of Transcription, DNA Deamination and DNA Repair. Nat. Rev. Immunol. *4*, 541–552.

Chen, H., Liu, H., and Qing, G. (2018). Targeting Oncogenic Myc as a Strategy for Cancer Treatment. Signal Transduct. Target. Ther. *3*, 1–7.

Chou, C., Pinto, A.K., Curtis, J.D., Persaud, S.P., Cella, M., Lin, C.-C., Edelson, B.T., Allen, P.M., Colonna, M., Pearce, E.L., et al. (2014). c-Myc-induced transcription factor AP4 is required for host protection mediated by CD8+ T cells. Nat. Immunol. *15*, 884–893.

Chung, J.B., Silverman, M., and Monroe, J.G. (2003). Transitional B Cells: Step by Step Towards Immune Competence. Trends Immunol. *24*, 342–348.

Coico, R.F., Bhogal, B.S., and Thorbecke, G.J. (1983). Relationship of Germinal Centers in Lymphoid Tissue to Immunologic Memory. VI. Transfer of B Cell Memory with Lymph Node Cells Fractionated According to their Receptors for Peanut Agglutinin. J. Immunol. Baltim. Md 1950 *131*, 2254–2257.

Cole, M.D. (1986). The myc Oncogene: Its Role in Transformation and Differentiation. Annu Rev Genet *20*, 361–384.

Comino-Méndez, I., Gracia-Aznárez, F.J., Schiavi, F., Landa, I., Leandro-García, L.J., Letón, R., Honrado, E., Ramos-Medina, R., Caronia, D., Pita, G., et al. (2011). Exome Sequencing Identifies MAX Mutations as a Cause of Hereditary Pheochromocytoma. Nat. Genet. *43*, 663–667.

Conacci-Sorrell, M., McFerrin, L., and Eisenman, R.N. (2014). An Overview of MYC and Its Interactome. Cold Spring Harb. Perspect. Med. *4*.

Cowling, V.H., and Cole, M.D. (2007). The Myc Transactivation Domain Promotes Global Phosphorylation of the RNA Polymerase II Carboxy-Terminal Domain Independently of Direct DNA Binding. Mol. Cell. Biol. *27*, 2059–2073.

Dang, C.V. (2012). MYC on the Path to Cancer. Cell *149*, 22–35.

Davis, A.C., Wims, M., Spotts, G.D., Hann, S.R., and Bradley, A. (1993). A Null c-myc Mutation Causes Lethality before 10.5 Days of Gestation in Homozygotes and Reduced Fertility in Heterozygous Female Mice. Genes Dev. *7*, 671–682.

DePinho, R.A., Schreiber-Agus, N., and Alt, F.W. (1991). myc Family Oncogenes in the Development of Normal and Neoplastic Cells. In Adv Cancer Res, pp. 1–46.

Desbarats, L., Gaubatz, S., and Eilers, M. (1996). Discrimination between Different E-box-binding Proteins at an Endogenous Target Gene of c-myc. Genes Dev. *10*, 447–460.

Dominguez-Sola, D., and Gautier, J. (2014). MYC and the Control of DNA Replication. Cold Spring Harb. Perspect. Med. *4*.

Dominguez-Sola, D., Ying, C.Y., Grandori, C., Ruggiero, L., Chen, B., Li, M., Galloway, D.A., Gu, W., Gautier, J., and Dalla-Favera, R. (2007). Non-transcriptional Control of DNA Replication by c-Myc. Nature *448*, 445–451.

Fernandez, D., Ortiz, M., Rodriguez, L., Garcia, A., Martinez, D., and Moreno de Alboran, I. (2013). The Proto-Oncogene c-myc Regulates Antibody Secretion and Ig Class Switch Recombination. J. Immunol. *190*, 6135–6144.

Fernandez, P.C., Frank, S.R., Wang, L., Schroeder, M., Liu, S., Greene, J., Cocito, A., and Amati, B. (2003). Genomic Targets of the Human c-Myc Protein. Genes Dev. *17*, 1115–1129.

Forsburg, S.L. (2008). The MCM Helicase: Linking Checkpoints to the Replication Fork. Biochem. Soc. Trans. *36*, 114–119.

Gallant, P., and Steiger, D. (2009). Myc's Secret Life without Max. Cell Cycle *8*, 3848–3853.

Gatto, D., and Brink, R. (2010). The Germinal Center Reaction. J. Allergy Clin. Immunol. *126*, 898–907.

Gelmann, E.P., Psallidopoulos, M.C., Papas, T.S., and Dalla-Favera, R. (1983). Identification of Reciprocal Translocation Sites within the c-myc Oncogene and Immunoglobulin mu Locus in a Burkitt Lymphoma. Nature *306*, 799–803.

Grandori, C., Cowley, S., P. James, L., and N. Eisenman, R. (2000). The MYC/MAX/MAD Network and the Transcriptional Control of Cell Behavior.

Han, S., Zheng, B., Takahashi, Y., and Kelsoe, G. (1997). Distinctive Characteristics of Germinal Center B Cells. Semin. Immunol. *9*, 255–260.

Hardy, R.R., and Hayakawa, K. (2001). B Cell Development Pathways. Annu. Rev. Immunol. *19*, 595–621.

Heller, R.C., Kang, S., Lam, W.M., Chen, S., Chan, C.S., and Bell, S.P. (2011). Eukaryotic Origin-Dependent DNA Replication in vitro Reveals Sequential Action of DDK and S-CDK Kinases. Cell *146*, 80–91.

Hishida, T., Nozaki, Y., Nakachi, Y., Mizuno, Y., Okazaki, Y., Ema, M., Takahashi, S., Nishimoto, M., and Okuda, A. (2011). Indefinite Self-Renewal of ESCs through Myc/Max Transcriptional Complex-Independent Mechanisms. Cell Stem Cell *9*, 37–49.

Hobeika, E., Thiemann, S., Storch, B., Jumaa, H., Nielsen, P.J., Pelanda, R., and Reth, M. (2006). Testing Gene Function Early in the B Cell Lineage in mb1-cre Mice. Proc. Natl. Acad. Sci. U. S. A. *103*, 13789–13794.

Honjo, T., Kinoshita, K., and Muramatsu, M. (2002). Molecular Mechanism of Class Switch Recombination: Linkage with Somatic Hypermutation. Annu. Rev. Immunol. *20*, 165–196.

Hopewell, R., and Ziff, E.B. (1995). The Nerve Growth Factor-responsive PC12 Cell Line Does Not Express the Myc Dimerization Partner Max. Mol. Cell. Biol. *15*, 3470–3478.

Huang, D.W., Sherman, B.T., and Lempicki, R.A. (2009). Systematic and Integrative Analysis of Large Gene Lists Using DAVID Bioinformatics Resources. Nat. Protoc. *4*, 44–57.

Hurlin, P., Steingrímsson, E., Copeland, N., A. Jenkins, N., and N. Eisenman, R. (2000). Mga, a Dual-Specificity Transcription Factor that Interacts with Max and Contains a T-domain DNA-binding Motif. EMBO J. *18*, 7019–7028.

Hurlin, P.J., Quéva, C., Koskinen, P.J., Steingrímsson, E., Ayer, D.E., Copeland, N.G., Jenkins, N.A., and Eisenman, R.N. (1995). Mad3 and Mad4: Novel Max-interacting Transcriptional Repressors that Suppress c-myc Dependent Transformation and are Expressed During Neural and Epidermal Differentiation. EMBO J. *14*, 5646–5659.

Hurlin, P.J., Quéva, C., and Eisenman, R.N. (1997). Mnt, a Novel Max-interacting Protein is Coexpressed with Myc in Proliferating Cells and Mediates Repression at Myc Binding Sites. Genes Dev. *11*, 44–58.

Iritani, B.M., and Eisenman, R.N. (1999). c-Myc Enhances Protein Synthesis and Cell Size during B Lymphocyte Development. Proc. Natl. Acad. Sci. U. S. A. *96*, 13180–13185.

Jung, D., Giallourakis, C., Mostoslavsky, R., and Alt, F.W. (2006). Mechanism and Control of V(D)J Recombination at the Immunoglobulin Heavy Chain Locus. Annu. Rev. Immunol. *24*, 541–570.

Kato, G.J., Lee, W.M., Chen, L.L., and Dang, C.V. (1992). Max: functional domains and interaction with c-Myc. Genes Dev. *6*, 81–92.

Kondo, M., Weissman, I.L., and Akashi, K. (1997). Identification of Clonogenic Common Lymphoid Progenitors in Mouse Bone Marrow. Cell *91*, 661–672.

Kress, T.R., Sabò, A., and Amati, B. (2015). MYC: Connecting Selective TranscriptionalControl to Global RNA Production. Nat. Rev. Cancer *15*, 593–607.

Kretzner, L., Blackwood, E.M., and Eisenman, R.N. (1992). Myc and Max Proteins Possess Distinct Transcriptional Activities. Nature *359*, 426–429.

Kurosaki, T., Kometani, K., and Ise, W. (2015). Memory B Cells. Nat. Rev. Immunol. *15*, 149–159.

Kwan, K.Y., Shen, J., and Corey, D.P. (2015). C-MYC Transcriptionally Amplifies SOX2 Target Genes to Regulate Self-Renewal in Multipotent Otic Progenitor Cells. Stem Cell Rep. *4*, 47–60.

Laherty, C.D., Yang, W.-M., Sun, J.-M., Davie, J.R., Seto, E., and Eisenman, R.N. (1997). Histone Deacetylases Associated with the mSin3 Corepressor Mediate Mad Transcriptional Repression. Cell *89*, 349–356.

Laiosa, C.V., Stadtfeld, M., and Graf, T. (2006). Determinants of Lymphoid-Myeloid Lineage Diversification. Annu. Rev. Immunol. *24*, 705–738.

Lei, M., Kawasaki, Y., Young, M.R., Kihara, M., Sugino, A., and Tye, B.K. (1997). Mcm2 is a Target of Regulation by Cdc7–Dbf4 during the Initiation of DNA Synthesis. Genes Dev. *11*, 3365–3374.

Li, B., and Dewey, C.N. (2011). RSEM: Accurate Transcript Quantification from RNA-Seq Data with or without a Reference Genome. BMC Bioinformatics *12*, 323.

Li, Z., Van Calcar, S., Qu, C., Cavenee, W.K., Zhang, M.Q., and Ren, B. (2003). A Global Transcriptional Regulatory Role for c-Myc in Burkitt's Lymphoma Cells. Proc. Natl. Acad. Sci. U. S. A. *100*, 8164–8169.

Lindeman, G.J., Harris, A.W., Bath, M.L., Eisenman, R.N., and Adams, J.M. (1995). Overexpressed max is Not Oncogenic and Attenuates myc-induced Lymphoproliferation and Lymphomagenesis in Transgenic Mice. Oncogene *10*, 1013–1017.

Link, J.M., and Hurlin, P.J. (2015). The activities of MYC, MNT and the MAX-interactome in lymphocyte proliferation and oncogenesis. Biochim. Biophys. Acta *1849*, 554–562.

Lüscher, B. (2001). Function and Regulation of the Transcription Factors of the Myc/Max/Mad Network. Gene *277*, 1–14.

Manis, J.P., Tian, M., and Alt, F.W. (2002). Mechanism and Control of Class-Switch Recombination. Trends Immunol. *23*, 31–39.

Mao, X., Fujiwara, Y., Chapdelaine, A., Yang, H., and Orkin, S.H. (2001). Activation of EGFP Expression by Cre-mediated Excision in a New ROSA26 Reporter Mouse Strain. Blood *97*, 324–326.

McMahon, S.B., Wood, M.A., and Cole, M.D. (2000). The Essential Cofactor TRRAP Recruits the Histone Acetyltransferase hGCN5 to c-Myc. Mol. Cell. Biol. *20*, 556–562.

Meyer, N., and Penn, L.Z. (2008). Reflecting on 25 Years With MYC. Nat. Rev. Cancer *8*, 976–990.

Mourón, S., Rodriguez-Acebes, S., Martínez-Jiménez, M.I., García-Gómez, S., Chocrón, S., Blanco, L., and Méndez, J. (2013). Repriming of DNA synthesis at stalled replication forks by human PrimPol. Nat. Struct. Mol. Biol. *20*, 1383–1389.

Nie, Z., Hu, G., Wei, G., Cui, K., Yamane, A., Resch, W., Wang, R., Green, D.R., Tessarollo, L., Casellas, R., et al. (2012). c-Myc Is a Universal Amplifier of Expressed Genes in Lymphocytes and Embryonic Stem Cells. Cell *151*, 68–79.

Nutt, S.L., and Kee, B.L. (2007). The Transcriptional Regulation of B Cell Lineage Commitment. Immunity *26*, 715–725.

Ogata, H., Goto, S., Sato, K., Fujibuchi, W., Bono, H., and Kanehisa, M. (2000). KEGG: Kyoto Encyclopedia of Genes and Genomes. Nucleic Acids Res. *28*, 27–30.

Okada, M., Miller, T.C., Wen, L., and Shi, Y.-B. (2017). A Balance of Mad and Myc Expression Dictates Larval Cell Apoptosis and Adult Stem Cell Development during Xenopus Intestinal Metamorphosis. Cell Death Dis. *8*, e2787.

Orian, A., van Steensel, B., Delrow, J., Bussemaker, H.J., Li, L., Sawado, T., Williams, E., Loo, L.W.M., Cowley, S.M., Yost, C., et al. (2003). Genomic Binding by the Drosophila Myc, Max, Mad/Mnt Transcription Factor Network. Genes Dev. *17*, 1101–1114.

Pang, S.H.M., Carotta, S., and Nutt, S.L. (2014). Transcriptional Control of Pre-B Cell Development and Leukemia Prevention. In Curr Top Microbiol Immunol, W. Ellmeier, and I. Taniuchi, eds. pp. 189–213.

Pillai, S., and Cariappa, A. (2009). The Follicular versus Marginal Zone B Lymphocyte Cell Fate Decision. Nat. Rev. Immunol. *9*, 767–777.

Prendergast, G.C., Lawe, D., and Ziff, E.B. (1991). Association of Myn, the Murine Homolog of Max, with c-Myc Stimulates Methylation-sensitive DNA Binding and Ras Cotransformation. Cell *65*, 395–407.

Quinet, A., Carvajal-Maldonado, D., Lemacon, D., and Vindigni, A. (2017). DNA Fiber Analysis: Mind the Gap! In Methods in Enzymology, (Elsevier), pp. 55–82.

Remeseiro, S., Cuadrado, A., Gómez-López, G., Pisano, D.G., and Losada, A. (2012). A Unique Role of Cohesin-SA1 in Gene Regulation and Development. EMBO J. *31*, 2090–2102.

Ribon, V., Leff, T., and Saltiel, A.R. (1994). c-Myc Does Not Require Max for Transcriptional Activity in PC-12 Cells. Mol. Cell. Neurosci. *5*, 277–282.

Rickert, R.C., Rajewsky, K., and Roes, J. (1995). Impairment of T-cell-dependent B-cell Responses and B-l cell Development in CD19-deficient Mice. Nature *376*, 352–355.

Ritchie, M.E., Phipson, B., Wu, D., Hu, Y., Law, C.W., Shi, W., and Smyth, G.K. (2015). limma Powers Differential Expression Analyses for RNA-sequencing and Microarray Studies. Nucleic Acids Res. *43*, e47.

Robinson, M.D., McCarthy, D.J., and Smyth, G.K. (2010). edgeR: a Bioconductor Package for Differential Expression Analysis of Digital Gene Expression Data. Bioinformatics *26*, 139–140.

Romero, O.A., Torres-Diz, M., Pros, E., Savola, S., Gomez, A., Moran, S., Saez, C., Iwakawa, R., Villanueva, A., Montuenga, L.M., et al. (2014). MAX Inactivation in Small Cell Lung Cancer Disrupts MYC–SWI/SNF Programs and Is Synthetic Lethal with BRG1. Cancer Discov. *4*, 292–303.

Sabo, A., and Amati, B. (2014). Genome Recognition by MYC. Cold Spring Harb. Perspect. Med. *4*, a014191–a014191.

Sanderson, R.D., Lalor, P., and Bernfield, M. (1989). B Lymphocytes Express and Lose Syndecan at Specific Stages of Differentiation. Mol. Biol. Cell *1*, 27–35.

Schmitz, R., Ceribelli, M., Pittaluga, S., Wright, G., and Staudt, L.M. (2014). Oncogenic Mechanisms in Burkitt Lymphoma. Cold Spring Harb. Perspect. Med. *4*, a014282–a014282.

Shapiro-Shelef, M., and Calame, K. (2005). Regulation of Plasma-Cell Development. Nat. Rev. Immunol. *5*, 230–242.

Sheiness, D., Fanshier, L., and Bishop, J.M. (1978). Identification of Nucleotide Sequences Which May Encode the Oncogenic Capacity of Avian Retrovirus MC29. J Virol *28*, 600–610.

Shen-Li, H., O'Hagan, R.C., Hou, H., Horner, J.W., Lee, H.-W., and DePinho, R.A. (2000). Essential Role for Max in Early Embryonic Growth and Development. Genes Dev. *14*, 17–22.

Siddiqui, K., On, K.F., and Diffley, J.F.X. (2013). Regulating DNA Replication in Eukarya. Cold Spring Harb. Perspect. Biol. *5*.

Soucek, L., Helmer-Citterich, M., Sacco, A., Jucker, R., Cesareni, G., and Nasi, S. (1998). Design and Properties of a Myc Derivative that Efficiently Homodimerizes. Oncogene *17*, 2463–2472.

Soucek, L., Jucker, R., Panacchia, L., Ricordy, R., Tatò, F., and Nasi, S. (2002). Omomyc, a Potential Myc Dominant Negative, Enhances Myc-induced Apoptosis. Cancer Res. *62*, 3507–3510.

Soucek, L., Whitfield, J., Martins, C.P., Finch, A.J., Murphy, D.J., Sodir, N.M., Karnezis, A.N., Swigart, L.B., Nasi, S., and Evan, G.I. (2008). Modelling Myc Inhibition as a Cancer Therapy. Nature *455*, 679–683.

Spencer, C.A., and Groudine, M. (1991). Control of c-myc Regulation in Normal and Neoplastic Cells. Adv Cancer Res *56*, 1–48.

Steiger, D., Furrer, M., Schwinkendorf, D., and Gallant, P. (2008). Max-independent Functions of Myc in Drosophila melanogaster. Nat. Genet. *40*, 1084–1091.

Takayama, Y., Kamimura, Y., Okawa, M., Muramatsu, S., Sugino, A., and Araki, H. (2003). GINS, a Novel Multiprotein Complex Required for Chromosomal DNA Replication in Budding Yeast. Genes Dev. *17*, 1153–1165.

Técher, H., Koundrioukoff, S., Azar, D., Wilhelm, T., Carignon, S., Brison, O., Debatisse, M., and Le Tallec, B. (2013). Replication Dynamics: Biases and Robustness of DNA Fiber Analysis. J. Mol. Biol. *425*, 4845–4855.

Thomas, K.R., and Capecchi, M.R. (1987). Site-directed Mutagenesis by Gene Targeting in Mouse Embryo-derived Stem Cells. Cell *51*, 503–512.

Vallespinos, M., Fernandez, D., Rodriguez, L., Alvaro-Blanco, J., Baena, E., Ortiz, M., Dukovska, D., Martinez, D., Rojas, A., Campanero, M.R., et al. (2011). B Lymphocyte Commitment Program Is Driven by the Proto-Oncogene c-myc. J. Immunol. *186*, 6726–6736.

Valovka, T., Schönfeld, M., Raffeiner, P., Breuker, K., Dunzendorfer-Matt, T., Hartl, M., and Bister, K. (2013). Transcriptional Control of DNA Replication Licensing by Myc. Sci. Rep. *3*.

Vaqué, J.P., Fernández-García, B., García-Sanz, P., Ferrandiz, N., Bretones, G., Calvo, F., Crespo, P., Marín, M.C., and León, J. (2008). c-Myc Inhibits Ras-

Mediated Differentiation of Pheochromocytoma Cells by Blocking c-Jun Up-Regulation. Mol. Cancer Res. *6*, 325–339.

Walter, W., Sánchez-Cabo, F., and Ricote, M. (2015). GOplot: an R Package for Visually Combining Expression Data with Functional Analysis. Bioinformatics *31*, 2912–2914.

Weinreich, M., and Stillman, B. (1999). Cdc7p-Dbf4p Kinase Binds to Chromatin during S Phase and is Regulated by both the APC and the RAD53 Checkpoint Pathway. EMBO J. *18*, 5334–5346.

Wert, M., Kennedy, S., Palfrey, H.C., and Hay, N. (2001). Myc Drives Apoptosis in PC12 Cells in the Absence of Max. Oncogene *20*, 3746–3750.

Whitfield, J.R., Beaulieu, M.-E., and Soucek, L. (2017). Strategies to Inhibit Myc and Their Clinical Applicability. Front. Cell Dev. Biol. *5*.

Wiese, K.E., and Eilers, M. (2011). Pluripotency without Max. Cell Stem Cell *9*, 4–6.

Yevshin, I., Sharipov, R., Valeev, T., Kel, A., and Kolpakov, F. (2017). GTRD: A Database of Transcription Factor Binding Sites Identified by ChIP-seq Experiments. Nucleic Acids Res. *45*, D61–D67.

Zervos, A.S., Gyuris, J., and Brent, R. (1993). Mxi1, a Protein that Specifically Interacts with Max to Bind Myc-Max Recognition Sites. Cell *72*, 223–232.

ANNEX

ANNEX

Annex 1. Table of common deregulated genes

	MaxKO vs HET		MycKO vs HET		DKO vs HET	
Gene Symbol	**logFC**	**adj.P.Val**	**logFC**	**adj.P.Val**	**logFC**	**adj.P.Val**
0610009E02Rik	-4,70	0,002	-2,17	0,005	-1,94	0,009
0610030E20Rik	0,72	0,002	0,88	0,000	0,69	0,002
1110032F04Rik	1,35	0,001	1,39	0,001	1,54	0,001
1110037F02Rik	0,55	0,001	0,55	0,001	0,51	0,002
1700020I14Rik	0,72	0,001	0,52	0,004	0,58	0,003
1700025G04Rik	-1,85	0,001	-2,29	0,000	-1,89	0,001
1810006J02Rik	4,12	0,008	5,80	0,001	5,50	0,002
2010107E04Rik	-0,71	0,002	-0,59	0,004	-0,62	0,004
2410006H16Rik	-0,82	0,004	-0,87	0,002	-0,99	0,002
2610002M06Rik	0,70	0,002	0,63	0,003	0,62	0,004
2700060E02Rik	-0,67	0,001	-0,65	0,001	-0,54	0,003
2700094K13Rik	-0,57	0,001	-0,58	0,001	-0,47	0,003
2810417H13Rik	-0,45	0,008	-0,73	0,001	-0,44	0,009
2900097C17Rik	1,48	0,001	1,41	0,001	1,50	0,001
4930523C07Rik	0,88	0,001	1,41	0,000	0,81	0,001
4931406P16Rik	0,75	0,004	0,82	0,002	0,81	0,003
4932438A13Rik	0,75	0,004	1,23	0,000	0,85	0,002
5730488B01Rik	2,23	0,003	2,28	0,002	2,31	0,003
8030462N17Rik	1,18	0,002	1,26	0,001	1,16	0,002
9030617O03Rik	-1,08	0,006	-1,16	0,004	-1,18	0,004
9330151L19Rik	-1,14	0,001	-2,20	0,000	-1,61	0,000
9930021J03Rik	0,75	0,007	0,85	0,003	0,76	0,007
9930111J21Rik1	2,65	0,004	2,89	0,002	2,63	0,004
9930111J21Rik2	2,01	0,000	2,44	0,000	2,15	0,000
A230050P20Rik	-0,61	0,005	-0,81	0,001	-0,63	0,004
A430078G23Rik	1,30	0,004	1,47	0,002	1,32	0,004
A4GALT	-2,36	0,000	-1,15	0,004	-1,47	0,002
A630001G21Rik	-0,60	0,002	-0,58	0,001	-0,62	0,001
AA467197	-1,72	0,003	-1,76	0,002	-2,61	0,001
AAAS	-0,56	0,002	-0,50	0,002	-0,44	0,005
AAK1	0,77	0,001	0,93	0,000	0,78	0,001
ABCA1	5,14	0,001	3,29	0,005	4,79	0,001
abca2	-0,47	0,006	-0,45	0,006	-0,60	0,002
Abcb1b	-1,81	0,002	-1,33	0,004	-1,31	0,005
ABCB7	0,67	0,002	0,85	0,000	0,74	0,001
ABCB9	-1,33	0,006	-1,14	0,009	-1,30	0,006
ABCC5	0,86	0,003	0,71	0,007	0,82	0,004
ABHD17A	-0,53	0,002	-0,61	0,001	-0,60	0,001
ABHD2	1,41	0,000	1,57	0,000	1,37	0,000
ABHD4	-1,20	0,003	-1,06	0,005	-1,14	0,004
ABHD8	-0,81	0,005	-0,72	0,007	-0,80	0,005
ABI1	0,62	0,001	0,46	0,003	0,50	0,003
ABI3	-0,82	0,001	-0,66	0,003	-0,89	0,001
ABLIM1	0,82	0,000	0,93	0,000	0,79	0,000
ACAA2	-0,80	0,002	-0,78	0,002	-0,84	0,002
ACADS	-0,82	0,001	-0,64	0,003	-0,71	0,002
ACAP2	0,80	0,001	0,84	0,000	0,78	0,001
ACBD6	-0,55	0,003	-0,71	0,001	-0,50	0,004
ACHE	-1,94	0,001	-2,39	0,001	-2,01	0,001
ACKR2	-1,30	0,003	-1,26	0,003	-1,16	0,005

	MaxKO vs HET		MycKO vs HET		DKO vs HET	
Gene Symbol	**logFC**	**adj.P.Val**	**logFC**	**adj.P.Val**	**logFC**	**adj.P.Val**
ACO2	0,37	0,006	0,37	0,005	0,46	0,002
ACSS2	-2,67	0,001	-2,20	0,001	-1,96	0,001
ACTN4	0,66	0,001	0,64	0,000	0,65	0,001
ACTR2	0,70	0,000	0,63	0,000	0,59	0,001
ACTR3B	-1,64	0,001	-1,76	0,001	-1,78	0,001
ACVR1B	0,84	0,003	0,97	0,001	0,75	0,005
ADAM10	0,95	0,000	1,14	0,000	0,98	0,000
ADAM15	-1,33	0,001	-1,53	0,000	-1,53	0,001
ADAM33	-1,98	0,008	-4,36	0,001	-2,64	0,004
ADAMTS10	-0,75	0,003	-0,93	0,001	-1,04	0,001
ADAR	0,69	0,002	0,88	0,000	0,85	0,001
ADD1	0,64	0,001	0,49	0,004	0,54	0,003
ADD3	1,33	0,000	1,47	0,000	1,25	0,000
ADGRL1	-1,16	0,004	-1,32	0,002	-1,33	0,002
ADNP	1,49	0,000	1,72	0,000	1,39	0,000
AES	-0,67	0,003	-0,75	0,002	-0,95	0,001
AFF1	0,85	0,004	1,15	0,001	0,91	0,003
AFF4	0,85	0,006	1,20	0,001	0,95	0,003
AFTPH	0,82	0,000	0,82	0,000	0,76	0,000
AGO01	0,78	0,001	0,90	0,000	0,76	0,001
AGO02	0,62	0,002	0,84	0,000	0,74	0,001
AGPAT5	-0,93	0,002	-1,01	0,001	-0,71	0,007
AHCY	-1,02	0,007	-1,17	0,004	-1,35	0,003
AI506816	-1,23	0,002	-1,47	0,001	-0,81	0,008
AICDA	-1,65	0,000	-1,89	0,000	-1,70	0,000
AIDA	0,88	0,000	0,74	0,000	0,75	0,001
AIM1	1,30	0,000	1,00	0,000	0,97	0,000
AIM1L	-1,04	0,006	-1,78	0,001	-1,55	0,001
AK2	-0,56	0,002	-1,05	0,000	-0,76	0,001
AKAP10	0,89	0,001	1,05	0,000	0,94	0,001
AKAP11	1,19	0,000	1,10	0,000	1,14	0,000
AKAP13	1,06	0,001	1,28	0,000	1,15	0,001
AKAP9	0,54	0,008	0,53	0,008	0,57	0,007
AKNA	0,76	0,002	0,97	0,000	0,80	0,001
ALDH2	-0,51	0,005	-0,76	0,001	-0,68	0,001
ALDH3A2	0,83	0,001	0,87	0,000	0,78	0,001
ALDOA	-1,15	0,001	-1,80	0,000	-1,25	0,001
ALDOC	-0,90	0,008	-3,09	0,000	-1,73	0,001
ALG10B	1,29	0,000	1,38	0,000	1,41	0,000
ALMS1	0,92	0,003	0,95	0,002	0,89	0,003
AMFR	0,45	0,004	0,44	0,004	0,41	0,007
AMPD2	-0,68	0,002	-0,76	0,001	-0,55	0,006
ANAPC1	0,61	0,001	0,53	0,001	0,65	0,000
ANAPC5	-0,37	0,005	-0,49	0,001	-0,36	0,006
ANKFY1	0,87	0,000	1,04	0,000	0,93	0,000
ANKHD1	0,67	0,001	0,77	0,000	0,69	0,001
ANKIB1	1,26	0,000	1,22	0,000	1,19	0,000
ANKRD12	0,71	0,003	0,82	0,001	0,59	0,008
ANKRD13A	0,52	0,003	0,54	0,002	0,40	0,008
ANKRD17	0,61	0,002	0,72	0,000	0,69	0,001
ANKRD44	1,48	0,000	1,52	0,000	1,39	0,000
ANKRD52	1,09	0,001	1,01	0,001	1,07	0,001
ANO6	0,64	0,002	0,84	0,000	0,59	0,003
ANXA2	-2,19	0,005	-1,97	0,006	-1,99	0,007
AP1G1	0,40	0,006	0,49	0,002	0,42	0,005
AP2B1	0,85	0,000	0,88	0,000	0,89	0,000
APC	0,68	0,004	1,12	0,000	0,80	0,002

	MaxKO vs HET		MycKO vs HET		DKO vs HET	
Gene Symbol	**logFC**	**adj.P.Val**	**logFC**	**adj.P.Val**	**logFC**	**adj.P.Val**
API5	0,48	0,007	0,50	0,005	0,53	0,005
apitd1	-0,98	0,000	-0,54	0,005	-0,72	0,002
APOBEC1	-1,39	0,000	-1,63	0,000	-1,46	0,000
APOLD1	-3,05	0,003	-3,80	0,002	-3,23	0,003
APRT	-0,74	0,001	-1,00	0,000	-0,61	0,003
AQR	0,46	0,004	0,60	0,001	0,59	0,001
ARAP2	1,39	0,000	1,68	0,000	1,45	0,000
AREL1	0,73	0,001	0,73	0,000	0,74	0,001
ARF5	-0,56	0,002	-0,61	0,001	-0,58	0,002
ARF6	0,61	0,001	0,60	0,001	0,55	0,002
ARFGEF1	0,89	0,000	1,09	0,000	0,94	0,000
ARFGEF2	0,60	0,001	0,73	0,000	0,71	0,000
ARHGAP17	0,70	0,002	0,94	0,000	0,71	0,001
ARHGAP26	1,77	0,000	1,89	0,000	1,60	0,000
ARHGAP30	0,50	0,002	0,54	0,001	0,55	0,002
ARHGAP5	1,43	0,007	1,51	0,005	1,35	0,010
ARHGAP8	-2,04	0,002	-1,38	0,007	-1,44	0,007
ARHGEF18	1,29	0,002	1,17	0,003	1,02	0,007
ARHGEF25	-2,36	0,006	-3,20	0,003	-3,15	0,003
ARHGEF6	0,84	0,000	0,87	0,000	0,87	0,000
ARID1B	0,98	0,000	1,03	0,000	0,85	0,000
ARID2	0,57	0,006	0,67	0,002	0,57	0,005
ARID5A	-0,71	0,003	-1,61	0,000	-1,06	0,000
ARID5B	1,24	0,000	0,76	0,003	1,15	0,000
ARIH1	0,51	0,002	0,55	0,001	0,47	0,003
ARL5C	-1,95	0,000	-1,47	0,000	-1,89	0,000
ARL6IP4	-0,86	0,002	-0,92	0,001	-0,85	0,002
ARL6IP5	-0,48	0,009	-0,64	0,002	-0,57	0,004
ARMC8	1,02	0,001	1,05	0,001	1,00	0,001
ARNT	0,66	0,005	0,76	0,002	0,70	0,004
ARRDC2	-1,38	0,002	-1,08	0,005	-1,41	0,002
ASCC3	1,18	0,001	1,53	0,000	1,30	0,001
ASL	-0,66	0,002	-0,85	0,001	-0,68	0,002
ASXL2	0,73	0,001	0,77	0,000	0,77	0,001
ATAD2	0,64	0,010	0,72	0,005	0,73	0,005
ATAD2B	1,76	0,004	1,93	0,002	1,82	0,004
ATE1	0,74	0,003	0,79	0,002	0,67	0,005
atf2	0,66	0,002	0,75	0,001	0,65	0,002
ATF5	-0,67	0,003	-0,86	0,001	-0,60	0,004
ATF7	1,01	0,002	1,06	0,001	1,00	0,003
ATF7IP	1,05	0,008	1,30	0,002	1,04	0,008
ATL3	1,07	0,000	0,83	0,000	0,97	0,000
ATM	2,40	0,000	2,70	0,000	2,61	0,000
ATOX1	-0,78	0,006	-0,88	0,003	-0,90	0,003
ATP11A	-0,82	0,001	-2,28	0,000	-0,95	0,000
ATP11C	1,30	0,000	1,46	0,000	1,24	0,000
ATP1B3	-0,70	0,007	-0,80	0,003	-0,79	0,004
ATP2A3	0,97	0,001	1,00	0,001	0,90	0,002
ATP2B1	0,86	0,009	1,20	0,001	0,90	0,007
ATP5D	-0,91	0,000	-0,94	0,000	-0,93	0,000
ATP5E	-0,58	0,006	-0,62	0,004	-0,56	0,008
ATP5F1	-0,39	0,006	-0,56	0,001	-0,39	0,006
ATP5G3	-0,64	0,002	-0,47	0,005	-0,47	0,007
ATP5H	-0,46	0,005	-0,62	0,001	-0,48	0,004
ATP5J	-0,59	0,004	-0,62	0,002	-0,61	0,003
ATP5J2	-0,73	0,001	-0,77	0,000	-0,71	0,001
ATP6	-0,96	0,002	-1,30	0,000	-1,13	0,001
ATP6V1A	0,72	0,000	0,65	0,000	0,68	0,001

	MaxKO vs HET		MycKO vs HET		DKO vs HET	
Gene Symbol	**logFC**	**adj.P.Val**	**logFC**	**adj.P.Val**	**logFC**	**adj.P.Val**
ATP7A	1,96	0,001	2,30	0,000	2,11	0,001
ATP7B	-1,32	0,009	-3,35	0,001	-2,32	0,002
ATP8	-1,02	0,002	-1,25	0,001	-1,09	0,002
ATP8A1	1,67	0,000	2,10	0,000	1,78	0,000
ATPIF1	-0,88	0,000	-0,69	0,001	-0,81	0,001
ATR	0,63	0,005	0,64	0,004	0,69	0,003
ATRN	0,98	0,003	0,95	0,003	1,03	0,002
atxn7	0,96	0,000	1,06	0,000	0,90	0,001
ATXN7L3B	0,72	0,001	0,77	0,001	0,71	0,001
AUP1	-0,79	0,000	-0,70	0,000	-0,73	0,000
AURKA	-0,74	0,001	-0,66	0,001	-0,53	0,004
AVL9	0,80	0,001	1,06	0,000	0,88	0,001
AVPI1	-1,86	0,002	-2,21	0,001	-2,07	0,002
AW112010	1,28	0,001	1,78	0,000	1,39	0,001
AXIN1	0,48	0,005	0,52	0,003	0,48	0,005
AZI2	0,61	0,003	0,72	0,001	0,69	0,002
AZIN1	0,53	0,001	0,36	0,007	0,47	0,002
AZIN2	-1,69	0,001	-2,71	0,000	-2,70	0,000
B230219D22Rik	0,71	0,004	0,76	0,002	0,69	0,004
B3GNT2	0,80	0,005	1,49	0,000	0,94	0,002
B3GNT5	1,04	0,000	0,90	0,001	0,91	0,001
BACH2	1,64	0,001	1,65	0,001	1,65	0,001
BAG1	-0,53	0,002	-0,52	0,001	-0,55	0,001
BAHD1	0,49	0,007	0,51	0,005	0,59	0,003
BANK1	1,59	0,000	1,34	0,000	1,19	0,001
BATF	-1,05	0,009	-1,33	0,002	-1,23	0,005
BAX	-0,68	0,001	-0,82	0,000	-0,65	0,002
BAZ1A	0,62	0,007	0,93	0,001	0,75	0,003
bbx	0,95	0,001	0,95	0,001	1,00	0,001
BC005561	1,26	0,004	1,49	0,001	1,30	0,003
BCAR3	0,95	0,000	1,38	0,000	1,01	0,000
BCL2	1,17	0,000	1,13	0,000	0,92	0,000
BCL2L11	-0,87	0,003	-1,17	0,001	-1,11	0,001
BCL2L13	0,56	0,002	0,44	0,005	0,50	0,003
BCOR	1,29	0,003	1,57	0,001	1,40	0,002
BDP1	0,87	0,002	1,19	0,000	1,03	0,001
BHLHB9	0,83	0,005	0,89	0,003	0,87	0,004
BICD2	0,78	0,006	0,70	0,008	0,72	0,008
BIRC5	-0,59	0,004	-0,94	0,000	-0,72	0,002
BIRC6	0,83	0,000	1,09	0,000	0,90	0,000
BMI1	1,14	0,000	1,22	0,000	1,15	0,000
BNIP3L	-1,40	0,002	-2,22	0,000	-2,02	0,001
Bod1l	0,69	0,001	0,86	0,000	0,72	0,001
bola2	-0,72	0,002	-1,11	0,000	-0,84	0,001
BORA	-0,65	0,003	-0,90	0,001	-0,59	0,004
BPTF	0,74	0,000	0,89	0,000	0,74	0,000
BRI3BP	-0,92	0,000	-1,31	0,000	-0,93	0,000
BRPF3	0,50	0,009	0,76	0,001	0,62	0,003
BRWD1	1,19	0,001	1,51	0,000	1,15	0,001
BSG	-1,01	0,001	-1,26	0,000	-1,06	0,001
BSPRY	-1,82	0,001	-1,98	0,001	-1,48	0,002
BTAF1	0,62	0,002	0,73	0,001	0,74	0,001
BTBD7	1,38	0,001	1,61	0,000	1,46	0,001
BTBD9	0,70	0,006	0,81	0,002	0,68	0,006
BTF3	-0,76	0,000	-0,85	0,000	-0,74	0,001
BTG1	0,51	0,009	1,07	0,000	0,53	0,008
BTK	0,54	0,005	0,67	0,001	0,56	0,004

	MaxKO vs HET		MycKO vs HET		DKO vs HET	
Gene Symbol	**logFC**	**adj.P.Val**	**logFC**	**adj.P.Val**	**logFC**	**adj.P.Val**
bzrap1	-2,17	0,002	-1,93	0,003	-2,16	0,002
BZW2	-1,10	0,001	-1,02	0,001	-0,73	0,003
C1QBP	-0,88	0,000	-0,95	0,000	-0,57	0,003
C2CD3	0,91	0,000	0,88	0,000	0,86	0,000
C330007P06Rik	0,72	0,002	0,84	0,001	0,74	0,002
CACNA1B	-1,29	0,004	-2,34	0,001	-1,44	0,003
CACNB1	-2,16	0,002	-1,58	0,003	-1,76	0,003
CAMK1D	1,37	0,000	1,07	0,001	1,18	0,001
CAMSAP2	0,74	0,005	1,17	0,000	0,81	0,003
CAPRIN1	0,47	0,004	0,38	0,009	0,51	0,003
CARD11	0,69	0,007	1,19	0,000	0,76	0,005
CARD6	0,87	0,001	1,01	0,000	0,75	0,002
CARMIL2	-0,77	0,002	-1,18	0,000	-0,68	0,003
CARS2	-0,55	0,009	-0,73	0,002	-0,57	0,008
CASP7	0,77	0,004	0,76	0,004	0,66	0,009
CAST	0,93	0,000	1,00	0,000	0,95	0,000
CBFA2T3	-1,09	0,000	-0,85	0,001	-0,95	0,001
CBLB	1,90	0,001	2,41	0,000	1,91	0,001
CBX5	0,45	0,005	0,56	0,001	0,50	0,003
CCDC107	-0,78	0,004	-0,71	0,005	-0,80	0,004
CCDC134	-0,63	0,008	-0,95	0,001	-0,88	0,002
ccdc15	2,03	0,004	2,20	0,002	2,12	0,003
CCDC40	-2,65	0,002	-3,24	0,001	-3,31	0,001
CCDC50	0,77	0,002	1,43	0,000	0,92	0,001
CCDC58	-1,08	0,001	-1,62	0,000	-1,13	0,001
CCDC82	1,03	0,005	1,21	0,002	0,98	0,006
CCDC88A	1,23	0,001	1,53	0,000	1,37	0,001
CCDC88B	-1,16	0,001	-1,67	0,000	-1,52	0,000
CCND2	1,46	0,000	1,38	0,000	1,47	0,000
CCNG2	-1,94	0,000	-1,17	0,002	-1,83	0,000
CCNL2	-0,63	0,005	-0,83	0,001	-0,80	0,002
CCNY	0,63	0,001	0,47	0,003	0,50	0,002
CCP110	0,84	0,001	0,82	0,001	0,95	0,001
CCR4	-2,68	0,001	-1,80	0,001	-1,97	0,001
CCSER2	0,63	0,003	0,85	0,000	0,69	0,002
CCT5	-0,72	0,001	-0,72	0,000	-0,57	0,002
CD164	0,56	0,002	0,58	0,001	0,50	0,003
CD180	1,36	0,001	2,30	0,000	1,65	0,000
CD2AP	0,77	0,001	0,84	0,000	0,78	0,001
CD38	1,25	0,002	0,90	0,007	0,94	0,007
CD68	-1,58	0,001	-1,68	0,001	-0,91	0,010
CD72	0,88	0,003	1,88	0,000	1,15	0,001
CD81	-0,72	0,001	-0,64	0,001	-0,62	0,002
CD84	1,06	0,004	1,16	0,002	1,01	0,005
cdc25b	-1,23	0,000	-1,02	0,000	-0,94	0,000
CDC34	-0,72	0,001	-0,67	0,001	-0,49	0,004
CDC73	0,50	0,009	0,64	0,002	0,63	0,003
CDCA8	-0,58	0,002	-0,79	0,000	-0,58	0,002
CDK12	0,86	0,007	0,97	0,003	0,95	0,005
CDK13	0,86	0,000	1,02	0,000	0,82	0,000
CDK18	-2,74	0,002	-1,75	0,007	-2,07	0,005
CDK19	0,85	0,004	1,57	0,000	0,80	0,005
CDK2AP1	-0,56	0,003	-0,43	0,008	-0,44	0,008
CDK5RAP2	0,88	0,000	0,96	0,000	0,82	0,001
CDK5RAP3	-0,65	0,002	-0,83	0,001	-0,60	0,003
CDK6	0,85	0,005	1,25	0,000	1,19	0,001
CDKN1A	-1,94	0,001	-1,49	0,002	-1,41	0,002
CEACAM1	0,86	0,001	1,09	0,000	0,81	0,002

	MaxKO vs HET		MycKO vs HET		DKO vs HET	
Gene Symbol	**logFC**	**adj.P.Val**	**logFC**	**adj.P.Val**	**logFC**	**adj.P.Val**
CELF2	1,11	0,000	1,13	0,000	1,08	0,000
Cep112it	0,74	0,003	0,81	0,001	0,81	0,002
CEP128	0,93	0,001	0,79	0,001	0,74	0,003
CEP170	0,79	0,002	0,67	0,003	0,59	0,007
CEP170B	-0,85	0,001	-0,82	0,001	-0,95	0,001
CEP192	0,52	0,004	0,59	0,002	0,62	0,002
CEP290	1,23	0,008	1,41	0,003	1,32	0,005
cep350	0,84	0,001	1,18	0,000	0,95	0,001
CERCAM	-1,36	0,002	-1,84	0,001	-1,48	0,002
CERS6	1,17	0,002	1,00	0,004	1,29	0,001
CFAP97	0,68	0,004	0,72	0,002	0,62	0,006
CFLAR	0,73	0,002	0,85	0,001	0,76	0,001
CHD9	1,31	0,001	1,64	0,000	1,43	0,001
CHM	0,95	0,001	1,18	0,000	0,90	0,001
chrnb1	-1,30	0,002	-1,21	0,003	-1,23	0,003
CHST10	-0,95	0,002	-1,01	0,001	-0,83	0,003
CHST15	1,45	0,001	2,27	0,000	1,69	0,000
CHST3	1,36	0,000	1,72	0,000	1,39	0,000
CHUK	0,61	0,002	0,68	0,001	0,65	0,002
ciita	1,40	0,000	1,72	0,000	1,48	0,000
CISD1	-1,01	0,000	-1,01	0,000	-0,91	0,000
CKAP5	0,39	0,008	0,43	0,005	0,42	0,006
CKB	-2,63	0,001	-2,15	0,002	-1,84	0,004
CKS2	-0,64	0,004	-1,12	0,000	-0,72	0,002
CLASP1	0,71	0,002	0,71	0,001	0,68	0,002
CLASRP	-0,48	0,005	-0,57	0,002	-0,68	0,001
CLCN6	-0,57	0,007	-0,63	0,004	-0,61	0,005
Cldn13	-2,89	0,002	-3,96	0,001	-3,56	0,002
CLDN4	-2,48	0,005	-5,93	0,001	-2,90	0,003
CLK3	-1,16	0,000	-1,23	0,000	-1,30	0,000
CLN6	-0,66	0,007	-0,62	0,008	-0,62	0,009
CLTC	0,87	0,000	0,90	0,000	0,85	0,000
CMPK2	1,84	0,002	1,96	0,001	1,94	0,002
CMTM6	0,80	0,001	0,81	0,000	0,72	0,001
CMTR1	0,69	0,001	0,65	0,001	0,76	0,001
CNOT1	0,65	0,001	0,70	0,000	0,72	0,000
CNOT6	0,50	0,004	0,54	0,002	0,53	0,003
CNTLN	1,02	0,002	0,86	0,003	0,97	0,002
CNTNAP1	-0,98	0,007	-1,37	0,002	-1,07	0,005
COA5	0,78	0,000	0,73	0,000	0,70	0,001
COBLL1	1,64	0,001	2,19	0,000	1,81	0,001
COG5	1,52	0,000	1,44	0,000	1,51	0,000
COL11A2	-1,35	0,001	-1,60	0,000	-1,66	0,000
COL18A1	-3,96	0,003	-3,09	0,004	-3,72	0,004
COL4A3BP	0,92	0,000	0,86	0,000	0,79	0,001
COL7A1	-2,06	0,007	-1,98	0,008	-2,38	0,005
COMT	-0,67	0,004	-0,80	0,002	-0,62	0,006
COPA	0,58	0,002	0,57	0,001	0,56	0,002
COPB1	0,36	0,009	0,36	0,008	0,43	0,004
COPB2	0,54	0,002	0,52	0,002	0,59	0,001
COPE	-0,74	0,001	-0,99	0,000	-0,75	0,001
COPG2	0,73	0,002	0,56	0,008	0,64	0,005
COPZ2	-2,75	0,005	-2,73	0,005	-2,60	0,006
CORO2A	0,92	0,000	1,13	0,000	0,83	0,000
COX1	-1,19	0,000	-1,24	0,000	-1,30	0,000
COX2	-1,15	0,000	-1,55	0,000	-1,35	0,000
COX3	-0,93	0,001	-1,12	0,000	-1,05	0,001

	MaxKO vs HET		MycKO vs HET		DKO vs HET	
Gene Symbol	**logFC**	**adj.P.Val**	**logFC**	**adj.P.Val**	**logFC**	**adj.P.Val**
Cox4l1	-0,94	0,000	-0,89	0,000	-0,84	0,000
COX4l2	-3,31	0,004	-2,82	0,006	-2,58	0,008
Cox5a	-0,56	0,003	-0,67	0,001	-0,56	0,003
Cox5b	-0,50	0,005	-0,51	0,004	-0,45	0,008
Cox6a1	-0,56	0,004	-0,60	0,002	-0,48	0,007
Cox6b1	-0,51	0,003	-0,54	0,002	-0,49	0,004
COX6B2	-1,35	0,009	-1,71	0,003	-1,57	0,005
COX7A2L	-0,57	0,001	-0,72	0,000	-0,71	0,000
COX7B	-0,60	0,003	-0,69	0,001	-0,68	0,002
COX7C	-0,62	0,001	-0,67	0,001	-0,59	0,001
COX8A	-0,50	0,002	-0,41	0,005	-0,45	0,004
CPEB4	0,78	0,002	0,91	0,001	0,80	0,002
CR1L	0,65	0,002	0,95	0,000	0,80	0,001
CR2	1,20	0,008	2,32	0,000	1,33	0,005
CRADD	-1,35	0,003	-2,49	0,000	-1,93	0,001
CREBBP	0,54	0,003	0,87	0,000	0,59	0,002
CREBRF	1,11	0,003	1,32	0,001	1,01	0,004
CRKL	1,11	0,001	1,18	0,000	1,21	0,000
CROCC	-0,94	0,003	-1,04	0,002	-1,08	0,002
CSF1	-2,68	0,000	-3,18	0,000	-2,66	0,000
CSGALNACT2	1,01	0,006	1,51	0,001	1,21	0,002
CSNK2B	-0,46	0,004	-0,58	0,001	-0,47	0,004
CSTF2T	0,86	0,001	0,78	0,002	0,79	0,002
CTCF	0,58	0,001	0,76	0,000	0,58	0,001
CTDSPL2	0,66	0,003	0,78	0,001	0,74	0,002
CTH	-1,19	0,001	-1,67	0,000	-1,13	0,002
CTNNAL1	-0,98	0,001	-1,05	0,001	-0,76	0,003
CTNND1	1,21	0,006	1,51	0,001	1,39	0,003
CTSS	0,75	0,000	1,12	0,000	0,81	0,000
CUL7	-0,90	0,000	-0,84	0,000	-0,83	0,001
CUX1	0,56	0,003	0,70	0,001	0,56	0,003
CWC15	-0,44	0,008	-0,55	0,002	-0,49	0,005
CYB561A3	0,61	0,003	0,64	0,002	0,54	0,005
CYBB	1,60	0,000	1,93	0,000	1,76	0,000
CYCS	-0,79	0,003	-0,63	0,007	-0,64	0,008
CYFIP1	0,72	0,003	0,60	0,006	0,68	0,004
CYLD	0,79	0,000	0,72	0,000	0,73	0,000
Cyp4f16	-2,05	0,000	-1,60	0,001	-2,31	0,000
CYP51	-0,55	0,007	-0,92	0,001	-0,65	0,003
D230017M19Rik	-1,47	0,004	-1,10	0,009	-1,37	0,005
D330041H03Rik	-0,95	0,005	-0,86	0,006	-0,94	0,005
D430019H16Rik	-3,50	0,003	-3,04	0,003	-3,82	0,003
D5Ertd579e	0,66	0,005	0,98	0,001	0,63	0,007
D8Ertd738e	-0,65	0,001	-0,77	0,000	-0,59	0,002
D8Ertd82e	0,79	0,003	0,79	0,003	0,70	0,006
D930015E06Rik	0,55	0,006	0,72	0,001	0,59	0,004
DACT3	-1,67	0,002	-1,83	0,001	-1,44	0,004
DALRD3	-0,59	0,008	-0,77	0,002	-0,64	0,005
DAP3	-0,48	0,003	-0,66	0,001	-0,51	0,002
DAPK3	-0,55	0,010	-0,64	0,005	-0,58	0,008
DBI	-0,99	0,001	-1,02	0,000	-1,04	0,001
DBNL	0,58	0,003	0,51	0,004	0,51	0,005
DBP	-0,80	0,004	-1,87	0,000	-1,29	0,001
DBT	0,68	0,007	0,82	0,002	0,82	0,003
DCAF7	0,74	0,002	0,67	0,002	0,69	0,003
DCK	0,45	0,006	0,48	0,004	0,60	0,002
DCLK2	1,43	0,001	1,49	0,000	1,38	0,001
DCTPP1	-1,08	0,000	-0,77	0,001	-0,68	0,002

	MaxKO vs HET		MycKO vs HET		DKO vs HET	
Gene Symbol	**logFC**	**adj.P.Val**	**logFC**	**adj.P.Val**	**logFC**	**adj.P.Val**
DDAH2	-1,08	0,002	-0,97	0,002	-1,40	0,001
ddb2	-1,28	0,000	-0,96	0,001	-1,17	0,000
DDIT4	-1,74	0,002	-2,58	0,000	-2,19	0,001
ddr1	-2,07	0,006	-2,30	0,004	-2,19	0,005
DDT	-1,50	0,000	-2,11	0,000	-1,85	0,000
DDX3X	0,49	0,002	0,53	0,001	0,53	0,001
DDX5	0,67	0,000	0,62	0,000	0,59	0,000
DDX58	0,93	0,003	1,11	0,001	1,05	0,002
DDX6	0,90	0,000	0,90	0,000	0,83	0,001
DDX60	2,71	0,004	2,74	0,003	2,73	0,004
DEK	0,45	0,003	0,40	0,004	0,45	0,003
DENND1B	1,16	0,000	1,30	0,000	1,09	0,000
DENND5B	0,74	0,004	1,72	0,000	1,29	0,000
DHCR24	-0,56	0,008	-1,14	0,000	-0,61	0,006
DHRS3	-1,24	0,002	-1,79	0,000	-1,50	0,001
DHX15	0,51	0,002	0,49	0,002	0,52	0,002
DHX29	0,98	0,000	0,68	0,002	0,94	0,001
DHX40	0,70	0,007	0,63	0,010	0,88	0,002
DHX9	0,83	0,000	0,73	0,000	0,81	0,000
DIAPH1	0,98	0,000	0,79	0,000	0,82	0,000
DIAPH2	1,27	0,001	0,96	0,002	1,05	0,002
DIAPH3	0,73	0,001	0,52	0,006	0,74	0,001
DICER1	0,68	0,001	0,69	0,001	0,68	0,001
DIDO1	0,54	0,001	0,68	0,000	0,57	0,001
DIP2B	1,31	0,000	1,52	0,000	1,30	0,000
DIS3L2	0,84	0,002	0,61	0,010	0,72	0,005
DKKL1	-2,18	0,002	-1,61	0,003	-2,43	0,001
DLG1	0,65	0,002	0,70	0,001	0,66	0,002
DMWD	-1,38	0,002	-1,19	0,002	-1,40	0,002
DMXL1	1,56	0,000	2,32	0,000	1,83	0,000
DNAAF2	-1,54	0,001	-2,42	0,000	-1,72	0,001
DNAH8	1,89	0,001	1,56	0,001	1,38	0,003
DNAJC13	0,92	0,001	1,07	0,000	1,01	0,000
DNAJC14	0,80	0,000	0,86	0,000	0,77	0,001
Doc2g	-1,38	0,005	-1,52	0,003	-1,40	0,005
dock10	0,99	0,000	1,04	0,000	0,90	0,000
DOCK11	0,99	0,000	1,04	0,000	1,02	0,000
DOCK2	0,87	0,000	0,81	0,000	0,78	0,000
DOCK8	0,57	0,002	0,90	0,000	0,68	0,001
DOK1	-0,58	0,003	-0,68	0,001	-0,68	0,001
dok2	-1,81	0,001	-2,23	0,000	-2,30	0,001
DOPEY1	0,56	0,006	0,76	0,001	0,55	0,006
DOPEY2	0,83	0,008	1,08	0,002	0,84	0,008
DPY19L3	0,91	0,001	0,87	0,001	0,74	0,003
DPY19L4	0,75	0,003	0,82	0,002	0,67	0,006
DPYSL2	-0,68	0,008	-1,07	0,001	-1,00	0,002
DR1	0,41	0,008	0,53	0,002	0,42	0,008
DTX1	1,16	0,001	1,58	0,000	1,00	0,001
DTX3L	0,76	0,002	0,61	0,005	0,76	0,002
DUSP6	1,59	0,001	1,89	0,000	1,59	0,001
DVL1	-0,72	0,001	-0,93	0,000	-0,86	0,000
DYNC1H1	0,65	0,001	0,88	0,000	0,80	0,000
DYRK1A	0,77	0,003	1,10	0,000	0,78	0,003
DYRK4	-2,16	0,002	-3,84	0,000	-2,46	0,001
E430025E21Rik	0,86	0,000	0,80	0,000	0,79	0,001
EAF1	0,49	0,006	0,71	0,001	0,60	0,002
EBF1	1,30	0,000	1,55	0,000	1,31	0,000

	MaxKO vs HET		MycKO vs HET		DKO vs HET	
Gene Symbol	**logFC**	**adj.P.Val**	**logFC**	**adj.P.Val**	**logFC**	**adj.P.Val**
ECHDC2	-3,02	0,002	-2,40	0,003	-1,72	0,008
EDEM3	0,81	0,002	1,38	0,000	1,26	0,000
EEA1	0,97	0,002	1,13	0,001	0,99	0,002
EEF1A1	-0,36	0,003	-0,52	0,000	-0,31	0,006
EEF1B2	-1,14	0,000	-1,34	0,000	-1,10	0,000
EEF1D	-0,65	0,001	-0,76	0,000	-0,53	0,003
EEF1G	-0,88	0,000	-0,96	0,000	-0,82	0,000
EEF2	-0,44	0,005	-0,57	0,001	-0,45	0,005
EFCAB14	0,88	0,000	0,85	0,000	0,93	0,000
EFNA4	-4,31	0,002	-2,12	0,007	-2,73	0,004
EFR3A	0,73	0,001	0,77	0,001	0,62	0,002
EGFL7	-3,70	0,001	-2,59	0,001	-2,39	0,001
EGLN3	-3,28	0,001	-5,31	0,001	-3,90	0,001
EGR3	1,75	0,004	3,26	0,000	2,31	0,001
EHD4	0,58	0,003	1,08	0,000	0,82	0,001
EIF2AK1	0,51	0,003	0,43	0,006	0,46	0,005
eif2ak2	1,05	0,001	1,16	0,000	1,21	0,000
EIF2AK3	0,63	0,005	0,84	0,001	0,61	0,005
EIF3E	-0,46	0,005	-0,57	0,001	-0,41	0,009
EIF3F	-0,69	0,001	-0,71	0,001	-0,69	0,001
EIF3H	-0,51	0,001	-0,67	0,000	-0,50	0,001
EIF3I	-0,61	0,001	-0,56	0,001	-0,45	0,004
EIF3K	-0,78	0,001	-0,94	0,000	-0,74	0,001
EIF4E2	-0,66	0,001	-0,65	0,001	-0,57	0,003
EIF4EBP1	-1,15	0,001	-1,46	0,000	-0,95	0,002
EIF4EBP2	0,70	0,001	0,60	0,001	0,65	0,001
EIF4G2	0,62	0,000	0,65	0,000	0,65	0,000
EIF5A	-0,60	0,001	-0,66	0,000	-0,45	0,004
ELF1	0,85	0,001	0,94	0,000	0,87	0,001
ELF4	0,55	0,006	0,61	0,003	0,55	0,007
ELK1	1,09	0,000	0,80	0,002	0,84	0,002
EMB	-1,79	0,000	-1,39	0,001	-1,18	0,002
EMC8	-0,51	0,009	-0,58	0,004	-0,55	0,007
endog	-0,78	0,009	-1,27	0,001	-0,78	0,009
ENKD1	-1,10	0,001	-1,11	0,001	-1,05	0,002
ENO1	-1,08	0,006	-2,40	0,000	-1,36	0,002
eno1b	-1,00	0,008	-2,36	0,000	-1,29	0,002
ENO2	-0,77	0,005	-0,84	0,003	-0,90	0,003
ENOX2	1,01	0,002	1,03	0,002	0,86	0,006
ENPP4	1,46	0,005	1,98	0,001	1,53	0,004
EP300	0,68	0,001	0,81	0,000	0,71	0,001
EP400	0,57	0,001	0,72	0,000	0,70	0,000
EPC1	0,66	0,002	1,01	0,000	0,69	0,001
EPC2	1,04	0,003	1,17	0,001	1,00	0,004
EPG5	0,89	0,005	1,06	0,002	1,00	0,003
EPHA2	-2,91	0,000	-3,23	0,000	-2,71	0,000
EPHX1	2,00	0,002	2,34	0,001	2,08	0,002
EPS15	0,57	0,002	0,80	0,000	0,61	0,001
EPS8	1,20	0,003	1,83	0,000	1,52	0,001
ERAP1	1,00	0,000	0,84	0,000	1,09	0,000
ERBIN	1,00	0,000	1,14	0,000	0,95	0,000
ERC1	1,00	0,001	0,91	0,001	0,88	0,002
ERG	-2,80	0,007	-4,62	0,003	-4,06	0,004
ERGIC3	-0,50	0,003	-0,54	0,002	-0,45	0,005
ERH	-0,39	0,008	-0,62	0,001	-0,37	0,009
ERMP1	0,80	0,003	0,69	0,004	0,75	0,004
ERO1L	-1,68	0,002	-2,06	0,001	-1,58	0,003
ERO1LB	0,83	0,000	0,93	0,000	0,94	0,000

	MaxKO vs HET		MycKO vs HET		DKO vs HET	
Gene Symbol	**logFC**	**adj.P.Val**	**logFC**	**adj.P.Val**	**logFC**	**adj.P.Val**
ERP29	-0,71	0,001	-0,89	0,000	-0,70	0,001
ESCO1	0,59	0,005	0,74	0,001	0,62	0,004
ETFB	-0,50	0,005	-0,82	0,000	-0,48	0,006
ETNK1	0,72	0,000	0,81	0,000	0,79	0,000
EVA1B	-1,47	0,001	-1,67	0,000	-1,89	0,000
exoc2	0,72	0,001	0,59	0,002	0,58	0,002
EXOC3	0,57	0,002	0,51	0,003	0,55	0,003
Exoc3l	-1,46	0,006	-1,47	0,005	-1,70	0,004
EXOC3L4	-4,69	0,007	-5,21	0,005	-4,95	0,006
EXOC5	0,80	0,001	0,89	0,000	0,77	0,001
EXOC6	1,20	0,003	1,48	0,001	1,33	0,002
EZH1	0,69	0,004	0,73	0,002	0,64	0,006
F730311O21Rik	1,78	0,002	2,03	0,001	1,70	0,003
FABP5	-1,34	0,001	-2,41	0,000	-1,62	0,000
FADS2	-0,68	0,004	-1,15	0,000	-0,57	0,007
FADS3	-2,07	0,001	-1,24	0,004	-1,33	0,004
FAM120C	1,91	0,005	1,73	0,006	1,94	0,004
FAM122B	1,04	0,000	0,73	0,002	0,73	0,003
FAM13B	1,07	0,000	1,25	0,000	1,00	0,001
FAM162A	-1,47	0,003	-2,84	0,000	-1,96	0,001
FAM168A	0,65	0,004	0,77	0,001	0,64	0,004
FAM168B	0,51	0,002	0,52	0,001	0,51	0,002
FAM172A	1,19	0,000	1,00	0,000	1,08	0,000
fam173a	-0,66	0,005	-0,60	0,007	-0,75	0,003
FAM178A	0,93	0,000	0,97	0,000	1,00	0,000
FAM179B	0,81	0,001	1,02	0,000	0,93	0,000
FAM206A	0,73	0,001	0,59	0,002	0,70	0,001
fam208b	0,82	0,010	0,88	0,006	0,89	0,007
FAM20B	0,76	0,004	1,13	0,000	0,90	0,002
Fam21	0,64	0,002	0,55	0,004	0,57	0,004
FAM212B	-1,22	0,003	-1,38	0,001	-1,09	0,004
FAM213A	-0,88	0,002	-0,73	0,004	-0,98	0,001
FAM35A	1,30	0,006	1,44	0,003	1,25	0,008
FAM3C	0,93	0,003	1,77	0,000	1,09	0,001
FAM43A	1,48	0,000	1,53	0,000	1,34	0,001
FAM45A	0,74	0,005	0,86	0,002	0,78	0,004
FAM49A	1,74	0,000	1,79	0,000	1,45	0,001
FAM64A	-0,83	0,001	-1,15	0,000	-0,95	0,000
FAM65B	0,69	0,001	0,74	0,001	0,48	0,006
FAM71F2	-3,33	0,007	-4,39	0,004	-2,89	0,010
FAR1	0,48	0,003	0,56	0,001	0,53	0,002
FAU	-1,05	0,000	-1,30	0,000	-1,20	0,000
FBXL14	0,57	0,006	0,84	0,001	0,68	0,003
FBXL6	-0,54	0,007	-0,66	0,003	-0,61	0,005
FBXO33	0,89	0,001	0,92	0,000	0,63	0,004
FBXO44	-2,45	0,002	-2,13	0,002	-2,37	0,002
FBXW11	0,51	0,003	0,43	0,006	0,51	0,003
FCMR	2,16	0,005	4,02	0,000	2,98	0,001
FDFT1	-0,88	0,000	-1,11	0,000	-1,01	0,000
FDPS	-1,00	0,000	-1,61	0,000	-1,14	0,000
FEM1A	0,65	0,002	0,87	0,000	0,78	0,001
FGF11	-1,56	0,006	-1,95	0,003	-1,98	0,003
FGL2	1,28	0,003	1,60	0,001	1,11	0,007
FHL3	-0,83	0,001	-0,75	0,002	-0,93	0,001
FKBP1A	-0,68	0,002	-0,74	0,001	-0,56	0,005
FKBP2	-0,97	0,001	-0,65	0,003	-0,70	0,002
FLII	0,41	0,005	0,34	0,009	0,37	0,008

	MaxKO vs HET		MycKO vs HET		DKO vs HET	
Gene Symbol	**logFC**	**adj.P.Val**	**logFC**	**adj.P.Val**	**logFC**	**adj.P.Val**
FLNA	0,76	0,001	0,51	0,005	0,58	0,003
FLOT1	-0,72	0,001	-0,81	0,001	-0,90	0,001
FMR1	0,61	0,002	0,60	0,002	0,64	0,002
FNBP1	0,52	0,003	0,62	0,001	0,58	0,002
FNDC9	-1,59	0,001	-1,09	0,005	-1,19	0,004
FOCAD	-1,37	0,000	-1,40	0,000	-1,35	0,000
FOSL2	-2,31	0,004	-3,01	0,002	-2,28	0,004
FOXJ3	0,81	0,002	0,79	0,002	0,81	0,002
FOXK1	0,90	0,002	0,87	0,002	0,95	0,001
FOXN3	1,56	0,001	1,58	0,000	1,48	0,001
FOXP1	1,73	0,000	2,02	0,000	1,64	0,000
FOXP4	-0,71	0,002	-0,90	0,001	-0,82	0,001
FPGT	0,95	0,002	0,77	0,006	0,77	0,007
FRY	1,94	0,001	1,95	0,000	1,58	0,002
FRYL	0,69	0,001	1,01	0,000	0,75	0,001
FSCN1	-2,35	0,003	-2,49	0,002	-1,63	0,010
FTO	0,84	0,001	0,48	0,007	0,65	0,002
FUT8	0,75	0,008	1,13	0,001	0,86	0,004
FXYD5	-1,24	0,000	-1,46	0,000	-1,52	0,000
FYCO1	0,80	0,010	1,14	0,001	0,80	0,010
FZR1	-0,44	0,005	-0,53	0,002	-0,43	0,006
G3BP2	0,38	0,006	0,43	0,003	0,42	0,004
GABBR1	-0,88	0,001	-1,00	0,000	-1,21	0,000
GABPA	0,69	0,001	0,59	0,001	0,67	0,001
GABPB2	0,84	0,000	0,74	0,001	0,84	0,000
GADD45G	-0,94	0,003	-1,35	0,000	-1,24	0,001
GADD45GIP1	-0,93	0,001	-0,97	0,000	-0,78	0,002
GALE	-1,48	0,000	-1,45	0,000	-1,36	0,000
GALK1	-1,43	0,001	-2,39	0,000	-1,59	0,001
GALNT1	0,58	0,001	0,62	0,001	0,53	0,002
GAPDH	-1,17	0,000	-2,00	0,000	-1,34	0,000
GAS2L1	-1,47	0,005	-1,29	0,007	-1,22	0,010
GATAD2B	0,47	0,008	0,60	0,002	0,46	0,010
GATM	-0,99	0,010	-1,74	0,001	-1,25	0,004
GBF1	0,90	0,000	0,86	0,000	0,86	0,000
Gbp10	3,15	0,007	3,60	0,003	3,73	0,003
GBP3	0,58	0,002	0,43	0,007	0,57	0,002
GBP4	0,86	0,002	1,01	0,001	1,00	0,001
gbp6	2,39	0,002	2,41	0,001	2,31	0,002
Gbp9	1,19	0,001	1,30	0,001	1,24	0,001
GCAT	-1,96	0,000	-2,06	0,000	-1,33	0,000
GCC2	0,49	0,009	0,67	0,002	0,58	0,004
GCNT1	2,64	0,001	3,65	0,000	3,08	0,000
GCSAM	-4,68	0,007	-4,67	0,006	-5,85	0,003
GFER	-0,65	0,003	-0,76	0,001	-0,54	0,007
GFI1B	4,59	0,006	6,42	0,001	5,17	0,003
GFPT1	0,67	0,001	0,67	0,001	0,78	0,001
GGA2	0,75	0,002	0,78	0,002	0,71	0,003
GGN	-1,77	0,008	-2,01	0,004	-2,15	0,004
gk	0,73	0,008	0,93	0,002	0,79	0,006
GLG1	1,17	0,000	1,17	0,000	1,17	0,000
GLIS2	-2,86	0,002	-2,49	0,002	-2,64	0,002
GLRX3	-0,75	0,000	-0,75	0,000	-0,64	0,001
GLTSCR1L	1,36	0,000	1,20	0,000	1,20	0,001
GLTSCR2	-0,78	0,001	-0,75	0,001	-0,76	0,001
GLYR1	0,41	0,003	0,36	0,005	0,37	0,006
Gm10036	-1,10	0,002	-1,42	0,001	-1,28	0,001
Gm10073	-1,01	0,001	-1,05	0,000	-1,00	0,001

	MaxKO vs HET		MycKO vs HET		DKO vs HET	
Gene Symbol	**logFC**	**adj.P.Val**	**logFC**	**adj.P.Val**	**logFC**	**adj.P.Val**
Gm11808	-0,93	0,000	-0,87	0,000	-1,04	0,000
Gm12185	1,80	0,008	2,45	0,001	1,88	0,006
Gm16754	-1,61	0,007	-2,34	0,002	-1,87	0,004
Gm2000	-1,03	0,000	-1,18	0,000	-1,13	0,000
Gm20559	1,57	0,006	1,95	0,002	1,74	0,004
Gm37416	-1,06	0,001	-1,19	0,001	-0,95	0,002
Gm4070	1,37	0,001	1,46	0,001	1,10	0,003
Gm4737	-0,59	0,001	-0,92	0,000	-0,60	0,001
Gm5431	2,62	0,006	3,17	0,002	3,34	0,002
Gm5547	-1,73	0,006	-2,21	0,002	-2,11	0,003
Gm7292	1,43	0,000	1,31	0,000	1,39	0,000
Gm8186	-0,56	0,005	-0,53	0,006	-0,53	0,006
Gm8369	1,30	0,009	2,03	0,001	1,48	0,005
Gm9843	-0,62	0,003	-0,80	0,001	-0,69	0,002
GMFG	-0,94	0,000	-1,22	0,000	-1,23	0,000
GNA15	-1,65	0,000	-1,55	0,000	-1,88	0,000
GNAI2	0,55	0,001	0,47	0,001	0,35	0,005
gnai3	0,62	0,001	0,51	0,002	0,61	0,001
GNAS	-0,48	0,002	-0,37	0,005	-0,45	0,003
GNAZ	-2,57	0,001	-1,59	0,002	-1,62	0,002
GNPTAB	0,78	0,002	1,13	0,000	0,94	0,001
GNS	1,15	0,000	1,24	0,000	0,92	0,001
GORASP1	-1,25	0,003	-2,12	0,000	-1,41	0,002
gosr1	0,71	0,003	0,76	0,001	0,60	0,006
GPALPP1	0,73	0,004	0,63	0,007	0,67	0,006
GPATCH2L	1,15	0,003	1,22	0,002	1,16	0,003
GPATCH8	0,60	0,002	0,57	0,001	0,59	0,002
Gpi1	-1,07	0,000	-1,89	0,000	-1,27	0,000
GPR132	-0,63	0,001	-1,05	0,000	-0,86	0,000
GPR15	-1,26	0,009	-1,60	0,003	-1,29	0,008
GPR174	0,70	0,006	1,54	0,000	0,98	0,001
GPRASP1	1,17	0,010	1,63	0,001	1,47	0,003
GPRIN3	-1,21	0,002	-1,35	0,001	-1,34	0,001
GPX1	-0,46	0,006	-0,59	0,001	-0,46	0,006
GPX4	-1,54	0,000	-1,20	0,000	-1,52	0,000
GRAMD1A	-1,18	0,001	-0,97	0,001	-1,25	0,001
GRAMD2	-1,78	0,006	-2,53	0,002	-1,54	0,009
GRAP2	1,58	0,000	1,41	0,000	1,25	0,001
GRHPR	-0,75	0,002	-1,37	0,000	-0,97	0,001
GRIK5	-1,96	0,000	-1,98	0,000	-1,66	0,000
GRINA	-0,73	0,003	-0,58	0,006	-0,84	0,001
GRM6	-1,16	0,001	-0,57	0,010	-0,82	0,002
GSN	-1,06	0,001	-1,06	0,001	-1,30	0,001
GSTP1	-0,65	0,001	-0,57	0,001	-0,51	0,002
GstT1	-3,14	0,001	-3,58	0,000	-3,23	0,001
GstT2	-1,41	0,002	-3,43	0,000	-2,14	0,000
GstT3	-1,73	0,001	-2,71	0,000	-2,08	0,000
GstT4	-3,33	0,008	-2,90	0,010	-3,95	0,006
GTF3A	-0,70	0,001	-0,66	0,001	-0,56	0,002
GZMB	4,48	0,007	5,92	0,001	5,26	0,003
H2AFJ	-1,07	0,000	-1,23	0,000	-1,11	0,000
H2AFZ	-0,45	0,003	-0,52	0,001	-0,36	0,009
H2-Eb2	1,18	0,001	1,47	0,000	1,24	0,000
H2-M5	-3,37	0,000	-4,19	0,000	-3,51	0,000
H2-T22	0,52	0,004	0,58	0,002	0,54	0,004
H2-T23	0,47	0,009	0,75	0,001	0,61	0,003
HAAO	-1,30	0,002	-1,04	0,004	-1,33	0,002

	MaxKO vs HET		MycKO vs HET		DKO vs HET	
Gene Symbol	**logFC**	**adj.P.Val**	**logFC**	**adj.P.Val**	**logFC**	**adj.P.Val**
HACD3	0,60	0,003	0,69	0,001	0,66	0,002
HADHB	0,65	0,002	0,69	0,001	0,72	0,001
HAPLN4	-3,05	0,007	-3,46	0,005	-2,87	0,008
HBP1	0,78	0,005	0,65	0,010	0,72	0,007
HCFC1	1,00	0,000	0,96	0,000	1,11	0,000
HCK	2,87	0,001	3,62	0,000	2,84	0,001
HDAC7	-1,43	0,000	-1,63	0,000	-1,48	0,000
HDAC9	2,89	0,000	3,70	0,000	3,24	0,000
HDGFRP2	-0,71	0,001	-0,66	0,001	-0,72	0,001
HEATR5B	0,76	0,002	0,96	0,000	0,80	0,001
HECA	0,73	0,002	0,95	0,000	0,75	0,002
hectd1	0,86	0,000	0,99	0,000	0,86	0,000
HEG1	0,65	0,005	0,84	0,001	0,71	0,003
HELZ2	0,94	0,001	1,61	0,000	1,26	0,000
HERC1	0,75	0,000	0,84	0,000	0,72	0,001
HERC2	1,19	0,000	1,42	0,000	1,30	0,000
HERC4	0,53	0,006	0,87	0,000	0,66	0,002
HERC6	1,14	0,001	1,49	0,000	1,28	0,001
HERPUD2	1,02	0,003	1,18	0,001	0,98	0,003
HES6	-0,79	0,004	-0,83	0,003	-0,95	0,002
HEXB	0,65	0,002	1,00	0,000	0,54	0,005
HIF1A	1,08	0,000	0,95	0,000	1,03	0,000
HIF1AN	0,61	0,006	0,83	0,001	0,63	0,005
HIF3A	-1,91	0,002	-1,89	0,002	-1,95	0,002
HIGD1A	-1,00	0,004	-1,43	0,001	-1,24	0,002
HILPDA	-1,86	0,002	-2,66	0,001	-2,43	0,001
HINT1	-0,68	0,001	-0,82	0,000	-0,68	0,001
HIPK1	0,73	0,001	1,16	0,000	0,92	0,000
HIPK2	2,43	0,000	2,06	0,000	2,25	0,000
HIPK3	1,25	0,000	1,57	0,000	1,27	0,000
hivep1	0,64	0,001	0,62	0,001	0,63	0,002
HIVEP2	1,27	0,004	2,25	0,000	1,75	0,001
HJURP	-0,45	0,007	-0,65	0,001	-0,45	0,007
HLX	-1,81	0,000	-2,02	0,000	-1,77	0,000
HMBS	-0,44	0,005	-0,66	0,001	-0,43	0,006
HMG20A	0,64	0,002	0,55	0,003	0,50	0,006
HMG20B	-0,66	0,002	-0,56	0,002	-0,81	0,001
HMGCS1	-0,45	0,008	-0,87	0,000	-0,65	0,001
HNF1B	3,36	0,010	5,29	0,001	4,31	0,003
HNRNPH2	0,62	0,001	0,44	0,003	0,48	0,002
HNRNPUL1	0,50	0,009	0,48	0,009	0,49	0,010
HOOK2	-0,88	0,003	-1,16	0,001	-1,03	0,002
HOOK3	0,78	0,001	0,76	0,001	0,69	0,002
HP1BP3	0,49	0,002	0,42	0,004	0,41	0,005
HPGDS	-2,54	0,000	-1,40	0,000	-1,58	0,000
HPS3	0,86	0,004	0,75	0,007	0,72	0,010
HPSE	-1,48	0,001	-1,41	0,001	-1,66	0,001
HRAS	-0,82	0,002	-0,75	0,002	-0,64	0,006
HSD17B4	0,56	0,007	0,55	0,007	0,54	0,008
HSDL2	0,56	0,010	0,66	0,004	0,57	0,009
HTATSF1	0,45	0,008	0,75	0,000	0,62	0,002
HTR7	-1,05	0,006	-2,01	0,000	-1,34	0,002
HTRA2	-0,80	0,001	-0,79	0,001	-0,68	0,002
HTT	0,63	0,001	0,79	0,000	0,70	0,000
HUWE1	0,43	0,003	0,53	0,001	0,53	0,001
ICE1	0,51	0,003	0,52	0,002	0,58	0,002
IDI1	-0,39	0,009	-0,75	0,000	-0,42	0,007
IDS	1,07	0,000	1,19	0,000	0,94	0,001

	MaxKO vs HET		MycKO vs HET		DKO vs HET	
Gene Symbol	**logFC**	**adj.P.Val**	**logFC**	**adj.P.Val**	**logFC**	**adj.P.Val**
IER3	-2,35	0,007	-2,77	0,004	-2,53	0,006
IFFO2	-2,02	0,003	-1,60	0,005	-1,70	0,005
Ifi203	0,63	0,005	0,73	0,002	0,66	0,004
Ifi209	1,52	0,000	1,97	0,000	1,72	0,000
Ifi213	1,96	0,007	3,53	0,000	2,79	0,001
Ifi214	2,71	0,003	3,60	0,001	3,17	0,002
Ifi47	1,41	0,002	1,27	0,002	1,31	0,003
IFIH1	1,62	0,000	1,86	0,000	1,69	0,000
IFIT1	2,58	0,001	3,07	0,000	2,80	0,001
IGHA	-3,58	0,002	-2,33	0,004	-2,05	0,006
ighd	1,82	0,000	2,13	0,000	1,75	0,000
Ighe	-2,50	0,001	-1,76	0,004	-1,67	0,007
Ighg1	-0,77	0,001	-1,61	0,000	-0,74	0,001
Ighg2b	-2,40	0,001	-1,59	0,002	-1,86	0,001
Ighg2c	-4,03	0,001	-2,07	0,003	-1,85	0,005
igkc	-1,37	0,000	-0,78	0,001	-0,93	0,000
Igkv8-27	-1,20	0,000	-0,78	0,001	-0,72	0,002
IGSF8	-1,07	0,002	-0,79	0,007	-0,89	0,005
Igtp	1,30	0,002	1,47	0,001	1,28	0,002
IKZF1	0,78	0,004	0,95	0,001	0,74	0,006
IKZF5	0,58	0,005	0,69	0,002	0,56	0,007
IL10RB	0,96	0,006	1,52	0,000	1,17	0,002
IL1R2	-2,44	0,000	-4,96	0,000	-3,12	0,000
IL1RAP	1,12	0,004	1,38	0,001	1,11	0,004
IMPA2	-1,42	0,001	-1,63	0,000	-1,44	0,001
IMPDH1	-0,70	0,003	-1,28	0,000	-0,63	0,005
IMPDH2	-0,70	0,000	-1,00	0,000	-0,59	0,001
INO80	0,94	0,002	0,74	0,005	0,86	0,003
INO80D	0,82	0,000	1,04	0,000	0,85	0,000
INPP4A	0,74	0,007	1,04	0,001	0,73	0,008
INPP4B	2,81	0,007	3,69	0,001	3,22	0,004
INPP5F	0,85	0,001	1,27	0,000	0,80	0,001
INPPL1	-0,82	0,006	-0,70	0,010	-0,91	0,004
INTS2	0,70	0,001	0,73	0,001	0,85	0,000
INVS	0,96	0,001	1,06	0,001	0,78	0,004
IPO8	0,75	0,001	0,75	0,000	0,65	0,001
IPO9	0,37	0,009	0,42	0,004	0,42	0,006
iqgap1	0,89	0,000	1,03	0,000	0,85	0,000
IRAK2	1,13	0,007	2,02	0,000	1,30	0,003
IRAK3	0,87	0,001	0,59	0,005	0,63	0,004
IREB2	0,48	0,003	0,55	0,001	0,47	0,003
IRF1	1,12	0,000	1,22	0,000	0,97	0,001
IRF2BPL	0,71	0,003	0,98	0,000	0,54	0,010
IRF9	1,06	0,002	1,36	0,001	1,15	0,002
Irgm1	1,79	0,001	1,95	0,000	1,82	0,001
Irgm2	1,76	0,001	2,20	0,000	1,88	0,001
ISCU	-0,63	0,002	-0,71	0,001	-0,65	0,002
ISG15	0,97	0,007	1,19	0,002	1,34	0,002
ISOC1	0,73	0,004	0,78	0,002	0,97	0,001
ISYNA1	-0,62	0,006	-0,78	0,002	-0,60	0,007
ITCH	0,64	0,004	0,69	0,002	0,61	0,005
ITGA3	-2,50	0,003	-1,87	0,005	-2,37	0,003
ITGAL	0,70	0,003	1,06	0,000	0,80	0,001
ITK	3,00	0,006	3,78	0,001	3,19	0,005
ITPR1	1,38	0,000	1,54	0,000	1,39	0,000
ITSN2	0,76	0,000	0,86	0,000	0,77	0,000
JADE2	1,15	0,002	1,75	0,000	1,44	0,001

	MaxKO vs HET		MycKO vs HET		DKO vs HET	
Gene Symbol	**logFC**	**adj.P.Val**	**logFC**	**adj.P.Val**	**logFC**	**adj.P.Val**
JADE3	0,80	0,010	0,83	0,007	0,96	0,004
JAG2	-2,87	0,000	-3,47	0,000	-3,14	0,000
JAK1	0,96	0,000	0,93	0,000	0,90	0,000
JAK2	0,62	0,008	0,82	0,002	0,64	0,007
JDP2	-2,50	0,001	-2,44	0,000	-2,35	0,001
Jhy	1,85	0,004	2,67	0,000	1,54	0,010
JUNB	-0,83	0,002	-1,53	0,000	-1,06	0,001
KANK3	-1,51	0,009	-1,68	0,006	-1,48	0,010
KANSL1	0,71	0,002	0,96	0,000	0,71	0,002
KAT6A	1,53	0,000	1,67	0,000	1,50	0,000
KAT7	0,47	0,006	0,57	0,002	0,52	0,003
KCNA3	2,27	0,001	2,98	0,000	2,68	0,000
KCNAB3	-1,12	0,007	-2,70	0,000	-2,23	0,001
KCNK13	1,94	0,003	1,61	0,008	1,65	0,008
KCNN4	-1,07	0,002	-1,35	0,001	-0,93	0,004
KCTD20	0,48	0,008	0,61	0,002	0,56	0,004
KDM3B	0,54	0,001	0,66	0,000	0,56	0,001
KDM7A	1,03	0,002	0,77	0,006	0,85	0,004
KIDINS220	0,66	0,003	0,49	0,009	0,55	0,007
KIF16B	0,99	0,001	1,08	0,000	1,04	0,001
KIF1B	0,83	0,003	1,28	0,000	1,01	0,001
KIF5B	0,56	0,002	0,85	0,000	0,77	0,000
Kifc5b	-0,79	0,001	-0,84	0,001	-0,63	0,004
KLC1	-0,95	0,008	-1,28	0,002	-1,10	0,004
KLC3	-2,75	0,000	-3,17	0,000	-2,44	0,001
KLF3	1,20	0,001	0,79	0,004	1,02	0,001
KLF6	1,06	0,001	1,43	0,000	1,07	0,001
KLHL11	1,83	0,005	1,81	0,005	1,87	0,005
KLHL28	1,53	0,002	1,77	0,001	1,40	0,003
KLHL6	-0,90	0,002	-0,60	0,009	-1,02	0,001
KMT2A	0,79	0,001	1,41	0,000	1,02	0,000
KMT2C	1,06	0,000	1,50	0,000	1,17	0,000
KMT2E	0,49	0,002	0,79	0,000	0,45	0,003
KMT5C	-1,04	0,000	-1,22	0,000	-1,13	0,000
KNL1	0,75	0,003	0,81	0,001	0,83	0,002
KNSTRN	-0,48	0,005	-0,51	0,003	-0,48	0,004
KPNA4	0,55	0,003	0,83	0,000	0,63	0,002
KRTCAP2	-0,88	0,003	-0,80	0,003	-0,74	0,005
LAMC1	0,54	0,003	0,90	0,000	0,81	0,000
laptm4a	0,59	0,002	0,72	0,000	0,64	0,001
LARP4	0,49	0,003	0,41	0,007	0,57	0,002
LARP4B	0,65	0,001	0,61	0,001	0,64	0,001
LASP1	0,63	0,002	0,60	0,002	0,56	0,004
LATS2	0,85	0,002	1,30	0,000	0,92	0,001
LAX1	-2,11	0,000	-1,09	0,000	-1,36	0,000
LCP2	-0,68	0,003	-1,43	0,000	-0,87	0,001
LDHA	-0,88	0,009	-2,40	0,000	-1,15	0,003
LGALS1	-0,95	0,002	-1,09	0,001	-1,34	0,000
LGALS8	0,76	0,006	1,19	0,000	0,68	0,010
LGMN	0,48	0,009	0,61	0,002	0,62	0,003
LIG3	0,85	0,002	0,71	0,003	0,90	0,001
LIMD1	0,76	0,000	0,80	0,000	0,74	0,001
lime1	-0,76	0,004	-1,19	0,001	-0,81	0,003
LIN28A	-2,95	0,002	-6,91	0,000	-4,02	0,001
Lipo1	1,05	0,001	0,73	0,004	0,76	0,004
LMBRD2	1,88	0,001	2,32	0,000	2,01	0,001
LMNTD2	-1,95	0,001	-2,22	0,001	-2,52	0,001
LMO2	0,92	0,001	1,03	0,001	0,71	0,005

	MaxKO vs HET		MycKO vs HET		DKO vs HET	
Gene Symbol	**logFC**	**adj.P.Val**	**logFC**	**adj.P.Val**	**logFC**	**adj.P.Val**
LMO7	-1,95	0,001	-1,20	0,005	-1,37	0,003
lmtk3	-3,51	0,003	-2,72	0,005	-3,10	0,004
LNPEP	1,84	0,001	2,70	0,000	2,18	0,000
LOC101056073	-1,29	0,000	-1,59	0,000	-1,21	0,000
LOC102633156	-0,79	0,002	-0,89	0,001	-0,89	0,001
LOC102635638	-1,47	0,001	-1,30	0,001	-1,97	0,000
LONP1	-0,77	0,001	-1,13	0,000	-0,77	0,001
LPCAT1	0,63	0,001	0,43	0,003	0,37	0,008
LPCAT2	1,60	0,010	2,47	0,001	2,11	0,002
LPCAT4	-1,35	0,000	-1,43	0,000	-1,40	0,000
LPGAT1	0,50	0,007	0,63	0,002	0,53	0,005
LPIN2	0,59	0,007	0,99	0,000	0,74	0,002
LPP	1,02	0,000	0,43	0,009	0,85	0,000
LRBA	1,53	0,000	1,96	0,000	1,57	0,000
LRCH1	0,82	0,006	1,09	0,001	0,89	0,004
LRFN1	-2,50	0,003	-1,71	0,009	-1,91	0,007
LRIG2	0,81	0,008	1,24	0,001	0,78	0,009
lrp6	0,88	0,002	1,01	0,001	0,93	0,002
LRP8	-0,83	0,003	-0,81	0,002	-0,76	0,004
LRRC61	1,34	0,001	1,21	0,001	1,11	0,001
LRRC71	-2,67	0,001	-3,40	0,001	-2,66	0,001
LRRC8B	1,06	0,001	0,98	0,002	0,82	0,005
LRRK2	2,29	0,000	2,58	0,000	2,31	0,000
LSM4	-0,57	0,004	-1,03	0,000	-0,68	0,002
LSS	-0,83	0,001	-1,36	0,000	-0,94	0,000
LST1	-1,82	0,004	-1,57	0,006	-2,23	0,002
LTB	-1,67	0,000	-1,00	0,001	-1,54	0,000
LTBP3	-3,03	0,001	-3,69	0,000	-3,29	0,001
LTN1	0,67	0,001	0,74	0,000	0,76	0,001
LURAP1	-1,50	0,001	-1,72	0,000	-1,32	0,001
LXN	-1,32	0,008	-1,37	0,006	-1,34	0,008
LYN	0,87	0,000	1,06	0,000	0,78	0,001
LYSMD3	1,16	0,003	1,49	0,001	1,11	0,004
MAGED1	-1,82	0,001	-1,19	0,004	-1,31	0,003
MAK16	-0,53	0,004	-0,53	0,004	-0,48	0,007
MALSU1	-0,74	0,004	-0,91	0,001	-0,69	0,005
Man1a	0,61	0,001	0,76	0,000	0,54	0,001
MAN2A1	0,94	0,001	1,23	0,000	1,13	0,000
MAP2K2	-0,41	0,005	-0,36	0,008	-0,39	0,007
MAP3K1	0,61	0,005	0,90	0,001	0,54	0,010
MAP3K12	-1,35	0,004	-1,99	0,001	-1,70	0,002
MAP3K2	1,05	0,001	1,06	0,000	0,98	0,001
MAP3K3	0,98	0,000	1,05	0,000	0,95	0,000
MAP3K7	0,41	0,006	0,44	0,004	0,47	0,003
MAP3K9	0,88	0,006	1,10	0,001	0,85	0,007
MAPK8IP3	-0,62	0,004	-0,80	0,001	-0,73	0,002
MAPK9	0,50	0,006	0,56	0,003	0,48	0,007
MAPKAP1	0,65	0,003	0,57	0,004	0,63	0,003
march6	0,59	0,003	0,84	0,000	0,69	0,001
MARCH7	0,66	0,002	0,65	0,001	0,62	0,002
MARCKSL1	-0,73	0,004	-0,71	0,004	-0,62	0,009
MATR3	0,50	0,002	0,53	0,001	0,53	0,002
MBNL1	1,40	0,000	1,30	0,000	1,25	0,000
MCM4	0,37	0,006	0,37	0,005	0,54	0,001
MDC1	1,00	0,000	0,91	0,000	1,03	0,000
MDFIC	1,23	0,000	1,17	0,000	0,96	0,001
Mdn1	0,92	0,000	0,68	0,000	1,11	0,000

	MaxKO vs HET		MycKO vs HET		DKO vs HET	
Gene Symbol	**logFC**	**adj.P.Val**	**logFC**	**adj.P.Val**	**logFC**	**adj.P.Val**
MECP2	0,88	0,001	1,00	0,000	0,81	0,002
MED1	0,68	0,001	0,65	0,001	0,69	0,001
MED13	1,10	0,000	1,43	0,000	1,13	0,000
MED13L	1,30	0,005	1,18	0,006	1,12	0,009
MED14	1,00	0,001	1,22	0,000	1,11	0,000
MED23	0,60	0,002	0,68	0,001	0,65	0,002
MEGF9	1,24	0,008	1,75	0,001	1,48	0,003
MET	7,07	0,003	6,31	0,004	7,62	0,002
METRN	-1,18	0,000	-0,88	0,001	-0,98	0,001
METTL26	-0,83	0,005	-0,82	0,005	-1,10	0,002
MEX3C	0,74	0,002	0,64	0,002	0,67	0,002
Mfap1b	0,71	0,003	0,77	0,001	0,64	0,004
MFAP5	-3,43	0,002	-2,56	0,003	-2,74	0,003
MFGE8	-1,78	0,001	-0,91	0,007	-1,39	0,002
MFHAS1	0,80	0,000	0,55	0,002	0,60	0,002
MFN2	0,74	0,001	0,68	0,001	0,76	0,001
MFSD1	0,58	0,003	0,43	0,010	0,51	0,006
MFSD13A	-1,32	0,000	-1,63	0,000	-1,47	0,000
MGA	1,52	0,000	1,04	0,000	1,51	0,000
mgarp	-2,25	0,003	-8,18	0,002	-3,46	0,001
MGAT4B	-1,81	0,001	-1,04	0,005	-1,74	0,001
MGAT5	1,55	0,000	1,36	0,000	1,33	0,000
MGRN1	0,73	0,001	0,69	0,001	0,54	0,004
MGST2	-1,96	0,001	-2,36	0,000	-2,60	0,000
mia2	0,63	0,001	0,35	0,010	0,63	0,001
MICU2	0,97	0,000	0,48	0,008	0,88	0,000
MIER1	0,53	0,001	0,51	0,001	0,41	0,005
MIF	-1,21	0,001	-2,88	0,000	-1,55	0,000
MIGA1	-1,13	0,000	-0,98	0,001	-1,10	0,001
miip	-1,05	0,004	-0,91	0,006	-0,96	0,006
Mirt1	-1,57	0,003	-2,14	0,001	-2,36	0,001
MKL2	1,24	0,001	1,67	0,000	1,26	0,001
MKLN1	0,50	0,007	0,61	0,002	0,47	0,009
Mndal	0,38	0,008	0,57	0,001	0,43	0,005
mob1a	0,69	0,002	0,63	0,002	0,56	0,005
MON2	0,53	0,005	0,70	0,001	0,60	0,003
MORC3	0,67	0,001	0,82	0,000	0,59	0,002
MORF4L1	0,44	0,003	0,44	0,002	0,40	0,005
MPEG1	2,81	0,000	3,04	0,000	2,79	0,000
MPND	-0,51	0,006	-0,52	0,005	-0,54	0,005
mri1	-0,65	0,003	-0,90	0,001	-0,58	0,005
MRM2	-0,86	0,007	-1,03	0,003	-0,83	0,009
MRPL12	-0,88	0,001	-0,99	0,000	-0,67	0,002
MRPL14	-0,75	0,004	-1,14	0,000	-0,85	0,002
MRPL15	-0,58	0,003	-0,58	0,002	-0,47	0,008
MRPL28	-0,86	0,001	-0,86	0,001	-0,76	0,002
MRPL30	-0,80	0,003	-0,72	0,005	-0,71	0,006
MRPL45	-0,54	0,003	-0,53	0,002	-0,55	0,003
MRPS15	-0,84	0,000	-1,06	0,000	-0,92	0,000
MRPS16	-0,47	0,009	-0,66	0,002	-0,61	0,003
MRPS24	-0,82	0,001	-0,81	0,001	-0,75	0,001
MRPS26	-0,67	0,002	-0,66	0,002	-0,57	0,004
mrps6	-1,23	0,003	-1,23	0,002	-1,00	0,006
MRPS7	-0,79	0,001	-0,91	0,000	-0,73	0,001
MRS2	0,91	0,003	0,92	0,002	0,90	0,003
MS4A1	1,32	0,000	1,56	0,000	1,34	0,000
Ms4a4c	2,37	0,003	4,06	0,000	3,03	0,001
Ms4a6b	2,04	0,001	3,39	0,000	2,28	0,000

	MaxKO vs HET		MycKO vs HET		DKO vs HET	
Gene Symbol	**logFC**	**adj.P.Val**	**logFC**	**adj.P.Val**	**logFC**	**adj.P.Val**
Ms4a6c	2,64	0,002	3,97	0,000	2,90	0,001
MSL2	0,80	0,000	1,02	0,000	0,85	0,000
MSMO1	-0,73	0,001	-1,00	0,000	-0,91	0,000
MSN	1,09	0,000	1,02	0,000	1,03	0,000
MSRB1	-0,65	0,003	-0,75	0,001	-0,77	0,001
MSRB3	-1,90	0,006	-2,86	0,002	-2,36	0,003
Mt1	-3,62	0,000	-3,63	0,000	-2,61	0,000
Mt2	-4,30	0,002	-3,60	0,002	-2,67	0,004
MTA1	-0,74	0,001	-0,72	0,000	-0,69	0,001
MTMR1	0,56	0,003	0,53	0,003	0,55	0,003
MTMR14	-1,08	0,000	-0,94	0,000	-0,87	0,001
MTMR2	0,79	0,008	0,92	0,003	0,77	0,009
MTMR3	0,49	0,005	0,77	0,000	0,59	0,002
MTR	0,58	0,007	0,62	0,004	0,80	0,002
MTSS1	1,08	0,001	1,29	0,000	1,09	0,001
MUC1	-4,11	0,000	-2,74	0,000	-3,66	0,000
muc2	-2,59	0,010	-6,87	0,004	-6,17	0,005
MUC3A	-2,99	0,003	-2,28	0,005	-3,07	0,003
MVB12A	-0,80	0,006	-0,78	0,005	-0,77	0,006
MVD	-0,92	0,001	-1,81	0,000	-1,25	0,000
MVK	-0,91	0,001	-1,06	0,000	-1,21	0,000
MXD1	-1,75	0,000	-1,20	0,001	-1,34	0,001
MXI1	-1,01	0,006	-2,26	0,000	-1,48	0,002
MYADM	-3,31	0,000	-2,27	0,000	-2,38	0,000
MYC	0,69	0,005	-1,13	0,001	-1,30	0,000
MYCBP2	1,11	0,000	1,40	0,000	1,22	0,000
MYDGF	-0,69	0,002	-0,67	0,002	-0,48	0,009
MYH9	0,67	0,000	0,61	0,000	0,64	0,000
MYL12B	0,69	0,001	0,91	0,000	0,64	0,002
MYLK	-3,60	0,001	-4,91	0,000	-4,72	0,000
MYNN	0,62	0,008	0,61	0,007	0,63	0,007
MYO18A	0,82	0,003	1,03	0,001	0,71	0,006
MYO1H	-2,34	0,002	-3,11	0,001	-2,04	0,003
MYO9A	0,96	0,006	1,22	0,001	1,11	0,003
MYSM1	0,77	0,010	0,88	0,004	0,77	0,010
MZB1	-1,10	0,000	-0,63	0,003	-0,72	0,002
N4BP2	0,78	0,001	0,68	0,001	0,68	0,002
NAA10	-0,87	0,001	-0,74	0,001	-0,68	0,002
NACA	-0,70	0,001	-0,87	0,000	-0,75	0,001
NAPA	-0,42	0,004	-0,48	0,002	-0,41	0,004
NAPRT	-1,37	0,009	-1,90	0,002	-1,73	0,004
NAXD	-0,55	0,009	-0,83	0,001	-0,60	0,006
NBAS	0,82	0,001	1,10	0,000	1,06	0,000
NCAPH2	-0,40	0,005	-0,62	0,000	-0,47	0,002
NCEH1	1,13	0,002	1,14	0,001	1,20	0,002
NCKAP1L	0,65	0,001	0,57	0,001	0,63	0,001
nckipsd	-0,71	0,007	-0,82	0,003	-1,02	0,002
NCOA1	1,17	0,000	1,50	0,000	1,14	0,000
NCOA2	1,29	0,000	1,64	0,000	1,45	0,000
NCOA6	0,69	0,001	0,86	0,000	0,68	0,001
NCOA7	1,06	0,001	1,16	0,001	1,03	0,001
NCOR1	0,83	0,000	0,93	0,000	0,85	0,000
ND1	-1,04	0,001	-1,26	0,000	-1,16	0,000
ND2	-1,04	0,002	-1,53	0,000	-1,23	0,001
ND4	-0,85	0,001	-1,54	0,000	-1,17	0,000
ND4L	-0,85	0,002	-1,51	0,000	-1,13	0,001
ND5	-0,70	0,002	-1,45	0,000	-1,01	0,000

	MaxKO vs HET		MycKO vs HET		DKO vs HET	
Gene Symbol	**logFC**	**adj.P.Val**	**logFC**	**adj.P.Val**	**logFC**	**adj.P.Val**
ND6	-0,59	0,004	-1,29	0,000	-0,95	0,000
NDRG2	-3,50	0,003	-4,92	0,002	-3,64	0,003
NDST1	1,21	0,003	1,13	0,004	1,01	0,007
NDUFA1	-0,52	0,006	-0,89	0,000	-0,61	0,003
NDUFA13	-0,69	0,003	-0,69	0,002	-0,77	0,002
NDUFA2	-0,49	0,006	-0,62	0,002	-0,51	0,005
NDUFA6	-0,53	0,003	-0,50	0,004	-0,63	0,002
NDUFA7	-0,52	0,005	-0,69	0,001	-0,55	0,004
NDUFAB1	-0,56	0,004	-0,66	0,001	-0,49	0,007
NDUFB10	-0,59	0,003	-0,57	0,003	-0,63	0,003
NDUFB11	-0,84	0,000	-0,64	0,001	-0,65	0,001
NDUFB5	-0,43	0,007	-0,47	0,004	-0,41	0,009
NDUFB7	-0,67	0,002	-0,76	0,001	-0,58	0,005
NDUFB8	-0,64	0,002	-0,58	0,002	-0,55	0,003
NDUFB9	-0,58	0,003	-0,58	0,003	-0,52	0,005
NDUFS6	-0,86	0,001	-0,95	0,001	-0,71	0,003
NDUFS7	-0,57	0,003	-0,56	0,003	-0,54	0,004
NDUFV2	-0,46	0,005	-0,63	0,001	-0,50	0,004
NDUFV3	-1,42	0,000	-2,00	0,000	-1,69	0,000
NECTIN2	-2,06	0,008	-2,25	0,006	-2,01	0,009
NEDD1	0,56	0,008	0,59	0,005	0,60	0,006
NEDD9	1,19	0,000	1,17	0,000	1,09	0,000
NEIL1	-2,80	0,000	-2,40	0,000	-2,24	0,000
NEK7	1,03	0,000	1,36	0,000	1,08	0,000
NELFE	-0,69	0,003	-0,68	0,003	-0,57	0,007
NET1	-0,60	0,002	-0,66	0,001	-0,47	0,006
NEU1	-1,24	0,001	-1,03	0,001	-1,07	0,001
NEURL2	-1,52	0,002	-1,88	0,001	-2,04	0,001
NFATC1	1,27	0,000	1,80	0,000	1,42	0,000
NFATC3	0,56	0,002	0,80	0,000	0,58	0,002
NHLRC2	0,93	0,004	1,03	0,002	0,97	0,004
NIN	1,35	0,000	1,58	0,000	1,39	0,000
NINJ1	-0,79	0,005	-0,75	0,005	-0,79	0,005
NIPBL	0,87	0,001	1,26	0,000	0,97	0,001
NISCH	-0,45	0,009	-0,75	0,001	-0,57	0,003
NLGN2	-2,81	0,000	-3,27	0,000	-2,92	0,000
NLRC5	0,92	0,001	0,88	0,000	0,93	0,001
NME4	-1,35	0,003	-1,94	0,001	-1,19	0,005
NOC2L	-0,69	0,002	-0,66	0,002	-0,48	0,008
NOP56	-0,84	0,000	-0,96	0,000	-0,63	0,001
NOTCH2	1,26	0,002	1,27	0,001	1,17	0,003
NPAT	0,73	0,002	0,80	0,001	0,77	0,001
NPHP3	-1,69	0,001	-1,59	0,001	-1,67	0,001
NPM1	-0,79	0,001	-0,95	0,000	-0,59	0,002
NR1D2	3,02	0,001	2,41	0,001	3,11	0,000
NR2C2	1,71	0,001	1,88	0,000	1,70	0,001
NR3C1	0,99	0,000	1,61	0,000	1,20	0,000
NRBP1	0,51	0,003	0,67	0,001	0,47	0,005
NRIP1	0,87	0,001	1,06	0,000	0,91	0,001
NSDHL	-0,71	0,002	-1,10	0,000	-0,86	0,001
NSF	0,57	0,004	0,62	0,002	0,60	0,003
NSUN5	-0,89	0,001	-0,82	0,001	-0,78	0,002
NT5C	-0,75	0,003	-1,10	0,000	-0,86	0,002
NT5DC2	-1,12	0,001	-1,12	0,001	-1,05	0,001
NTN5	-2,52	0,000	-3,17	0,000	-3,14	0,000
NUDT14	-1,13	0,002	-1,12	0,001	-1,02	0,003
NUFIP2	0,53	0,007	0,54	0,005	0,59	0,004
NUMA1	0,67	0,002	0,70	0,001	0,69	0,002

	MaxKO vs HET		MycKO vs HET		DKO vs HET	
Gene Symbol	**logFC**	**adj.P.Val**	**logFC**	**adj.P.Val**	**logFC**	**adj.P.Val**
NUP153	0,75	0,000	0,78	0,000	0,83	0,000
NUP160	0,82	0,001	1,08	0,000	1,01	0,000
NUP205	0,61	0,001	0,48	0,002	0,68	0,000
NUP210L	-1,61	0,004	-1,51	0,004	-1,69	0,003
NUP214	0,52	0,002	0,41	0,005	0,60	0,001
NUP98	1,29	0,000	1,58	0,000	1,45	0,000
Nupl1	0,76	0,003	0,84	0,001	0,85	0,002
OAZ2	-0,51	0,008	-0,62	0,003	-0,63	0,003
OGFOD2	-0,78	0,007	-0,69	0,010	-0,74	0,008
OIT3	-1,34	0,007	-2,06	0,001	-1,54	0,005
olfml2a	5,61	0,003	4,66	0,006	5,94	0,002
Olfr56	1,75	0,005	1,59	0,006	1,91	0,003
OSBPL8	1,13	0,002	1,43	0,000	1,16	0,002
OSBPL9	0,68	0,001	0,72	0,000	0,57	0,002
OTUD1	2,15	0,001	2,56	0,000	2,14	0,001
OTUD4	0,71	0,001	0,60	0,001	0,74	0,001
OTUD5	-0,56	0,002	-0,59	0,001	-0,58	0,002
P4HB	-0,84	0,002	-0,89	0,001	-0,74	0,003
PACS1	1,23	0,000	1,08	0,000	0,99	0,001
PACSIN1	-1,20	0,001	-0,80	0,002	-0,69	0,005
PACSIN3	-2,38	0,001	-2,46	0,001	-2,64	0,001
PADI3	-3,40	0,003	-2,33	0,006	-2,06	0,010
PAFAH1B1	0,48	0,004	0,65	0,001	0,51	0,003
PAFAH1B3	-1,01	0,000	-0,73	0,001	-0,85	0,001
PAG1	1,23	0,003	1,17	0,003	1,07	0,006
PAICS	-0,47	0,003	-0,65	0,000	-0,38	0,008
PAK2	0,56	0,003	0,48	0,005	0,57	0,003
PALM	-1,94	0,000	-2,13	0,000	-2,02	0,000
PANK3	0,82	0,001	0,92	0,001	0,80	0,002
PARD3B	2,54	0,004	3,37	0,001	2,87	0,002
PARK7	-0,53	0,002	-0,49	0,002	-0,42	0,006
PARP11	0,73	0,008	0,91	0,002	0,76	0,006
PARP12	1,62	0,004	1,53	0,004	1,74	0,003
PARP14	1,05	0,001	1,48	0,000	1,27	0,000
PARP4	1,05	0,000	1,19	0,000	1,07	0,000
PARP9	0,57	0,001	0,36	0,009	0,48	0,003
PATJ	1,11	0,003	1,54	0,000	1,40	0,001
PAX5	1,63	0,000	1,68	0,000	1,61	0,000
PBRM1	0,94	0,000	1,32	0,000	1,10	0,000
PCBP4	-0,88	0,001	-0,82	0,001	-1,05	0,001
PCED1B	-0,45	0,008	-0,50	0,005	-0,60	0,002
PCGF2	-2,08	0,003	-3,19	0,001	-2,67	0,002
PCM1	0,76	0,001	0,79	0,001	0,74	0,002
PCMTD1	0,55	0,006	1,42	0,000	0,61	0,004
PCSK4	-1,84	0,006	-2,42	0,002	-1,93	0,005
PCYOX1L	-1,88	0,002	-1,98	0,002	-1,80	0,003
PCYT1A	0,75	0,003	0,86	0,001	0,81	0,002
PCYT2	-1,13	0,000	-1,57	0,000	-1,34	0,000
PDCD10	0,46	0,005	0,40	0,007	0,40	0,008
PDE3B	0,83	0,001	1,12	0,000	1,01	0,000
PDK1	-0,98	0,002	-2,27	0,000	-1,28	0,001
PDLIM5	0,64	0,005	0,76	0,001	0,73	0,002
PDPK1	0,66	0,002	0,67	0,002	0,62	0,003
PDPR	2,76	0,000	1,78	0,000	2,60	0,000
PDS5A	0,42	0,008	0,48	0,003	0,44	0,007
PDS5B	0,86	0,001	0,95	0,000	0,91	0,000
PDZD8	0,75	0,003	0,92	0,001	0,83	0,002

	MaxKO vs HET		MycKO vs HET		DKO vs HET	
Gene Symbol	**logFC**	**adj.P.Val**	**logFC**	**adj.P.Val**	**logFC**	**adj.P.Val**
PEAR1	-1,47	0,000	-1,89	0,000	-1,75	0,000
PEBP1	-0,61	0,002	-0,96	0,000	-0,59	0,002
PECAM1	1,35	0,001	1,91	0,000	1,32	0,002
Peg13	2,29	0,001	2,89	0,000	2,38	0,001
PFKM	-1,33	0,001	-1,86	0,000	-1,46	0,000
PGGT1B	0,98	0,001	0,85	0,001	0,95	0,001
PGK1	-1,16	0,005	-2,68	0,000	-1,53	0,002
PGLYRP2	-1,36	0,001	-1,09	0,002	-1,31	0,001
PGM2	-0,94	0,004	-2,05	0,000	-1,33	0,001
PGP	-0,95	0,007	-0,89	0,008	-1,02	0,006
PHC3	0,76	0,001	0,81	0,001	0,72	0,002
Phf11a	1,45	0,006	1,63	0,002	1,78	0,002
Phf11b	1,39	0,000	1,78	0,000	1,56	0,000
Phf11d	1,43	0,005	1,71	0,001	1,65	0,002
PHF2	0,54	0,001	0,56	0,001	0,45	0,004
PHF20	0,63	0,001	0,57	0,001	0,58	0,001
PHF20L1	0,52	0,003	0,60	0,001	0,50	0,003
PHF6	0,62	0,002	0,48	0,006	0,45	0,010
PHF8	0,88	0,001	0,87	0,000	0,87	0,001
PHIP	1,57	0,001	2,09	0,000	1,72	0,000
PHKG2	-0,46	0,009	-0,63	0,002	-0,55	0,004
PHLDA3	-1,57	0,001	-1,44	0,001	-1,21	0,001
PHLPP1	0,72	0,008	1,18	0,000	0,96	0,002
PHLPP2	0,60	0,005	0,59	0,004	0,64	0,003
PHTF2	0,74	0,006	1,04	0,001	0,81	0,004
PHYH	0,72	0,003	0,83	0,001	0,71	0,003
PIAS1	0,71	0,004	1,04	0,000	0,70	0,004
PIDD1	-0,67	0,003	-0,84	0,001	-0,58	0,005
PIGK	0,61	0,008	0,82	0,002	0,67	0,005
Pigyl	-0,74	0,006	-0,77	0,005	-0,83	0,004
pik3ap1	1,18	0,002	1,45	0,001	1,23	0,002
PIK3C2A	1,23	0,000	1,42	0,000	1,27	0,000
PIK3R1	0,65	0,001	0,75	0,000	0,56	0,002
PIK3R2	-0,43	0,007	-0,47	0,004	-0,60	0,002
PIK3R4	0,93	0,000	0,45	0,007	0,67	0,001
PIK3R5	-1,52	0,000	-1,24	0,000	-1,02	0,001
pik3r6	-2,26	0,002	-1,66	0,004	-1,69	0,004
PIKFYVE	0,93	0,000	1,16	0,000	0,93	0,000
PIM2	-1,48	0,004	-1,22	0,007	-1,34	0,006
PIM3	-1,08	0,000	-1,12	0,000	-1,06	0,000
PIP4K2A	0,84	0,001	1,01	0,000	0,74	0,002
PITPNM1	-0,59	0,001	-0,38	0,005	-0,56	0,001
PITPNM2	0,40	0,007	0,50	0,002	0,51	0,002
PITRM1	0,53	0,004	1,05	0,000	0,93	0,000
PJA2	0,63	0,003	0,86	0,000	0,64	0,003
PKD1	0,72	0,003	1,21	0,000	0,89	0,001
PKN3	-1,53	0,004	-1,47	0,004	-1,98	0,002
PLA2G12A	-1,34	0,001	-1,63	0,000	-1,32	0,001
PLAC8	1,68	0,001	1,63	0,001	1,52	0,001
PLCD1	-1,42	0,003	-3,44	0,000	-2,43	0,001
PLCXD1	-2,02	0,001	-3,04	0,000	-2,49	0,001
PLEK	0,51	0,010	0,68	0,002	0,66	0,003
PLEKHA2	0,51	0,001	0,37	0,004	0,47	0,002
PLEKHM2	-1,57	0,000	-1,80	0,000	-1,53	0,000
PLPP2	-2,15	0,001	-1,96	0,001	-2,20	0,001
PLXNB2	-1,55	0,001	-1,81	0,000	-1,64	0,001
PLXND1	1,12	0,004	2,07	0,000	1,41	0,001
PMEPA1	0,65	0,001	0,52	0,002	0,40	0,009

	MaxKO vs HET		MycKO vs HET		DKO vs HET	
Gene Symbol	**logFC**	**adj.P.Val**	**logFC**	**adj.P.Val**	**logFC**	**adj.P.Val**
PMM1	-1,28	0,000	-1,49	0,000	-1,03	0,000
pmvk	-1,04	0,000	-1,10	0,000	-1,09	0,000
pnkd	-1,44	0,000	-1,44	0,000	-1,38	0,000
PNPLA8	0,79	0,001	1,08	0,000	0,74	0,002
POGK	1,92	0,000	0,52	0,005	1,60	0,000
POLA1	0,84	0,000	0,73	0,001	0,87	0,000
POLE2	-0,79	0,005	-1,18	0,001	-0,71	0,008
POLR1D	-0,91	0,000	-0,92	0,000	-0,84	0,000
POLR2A	0,61	0,001	0,39	0,004	0,54	0,001
POLR2B	0,53	0,002	0,54	0,002	0,58	0,002
POLR2F	-0,56	0,006	-0,73	0,001	-0,58	0,005
POLR2G	0,56	0,007	0,68	0,002	0,74	0,002
POLR3B	0,88	0,002	0,61	0,009	0,89	0,002
POP5	-1,04	0,006	-1,01	0,006	-1,06	0,006
POU2F2	1,03	0,000	1,28	0,000	0,97	0,000
POU6F1	0,86	0,002	1,29	0,000	0,94	0,001
PPAN	-1,15	0,002	-1,33	0,001	-0,92	0,004
PPARD	-1,22	0,001	-1,10	0,001	-1,22	0,001
PPCDC	-0,96	0,002	-1,15	0,001	-1,03	0,002
ppfia1	0,48	0,005	0,60	0,001	0,52	0,004
PPFIA3	-2,54	0,006	-2,64	0,005	-3,20	0,004
PPHLN1	0,54	0,005	0,49	0,006	0,58	0,003
PPIB	-0,83	0,000	-0,72	0,000	-0,69	0,000
PPIP5K2	1,03	0,000	0,96	0,000	1,02	0,000
PPM1J	-2,73	0,002	-2,44	0,002	-2,91	0,001
PPM1L	1,28	0,004	1,92	0,000	1,50	0,002
PPP1R10	-0,66	0,009	-0,65	0,008	-0,65	0,009
PPP1R12A	1,33	0,000	1,54	0,000	1,37	0,000
PPP1R12C	-0,49	0,005	-0,61	0,001	-0,62	0,002
PPP1R14B	-0,72	0,004	-1,31	0,000	-0,67	0,005
PPP1R15B	0,45	0,005	0,49	0,002	0,51	0,002
PPP3CA	0,99	0,003	0,97	0,002	0,88	0,005
PPP3CB	0,49	0,003	0,39	0,007	0,40	0,008
PPT1	0,54	0,005	0,97	0,000	0,62	0,003
PPTC7	0,54	0,003	0,47	0,004	0,41	0,010
PRADC1	-0,78	0,006	-0,92	0,002	-0,77	0,006
PRDM2	0,44	0,004	0,64	0,001	0,40	0,007
PRDX2	-0,72	0,001	-0,96	0,000	-0,77	0,001
PRDX5	-0,49	0,006	-0,65	0,001	-0,49	0,006
PRDX6	-0,71	0,001	-0,90	0,000	-0,56	0,003
PREB	-0,71	0,001	-0,62	0,001	-0,59	0,002
PRELID1	-0,90	0,001	-1,75	0,000	-1,20	0,000
PREX1	-0,43	0,003	-0,56	0,001	-0,69	0,000
PRKACB	1,03	0,001	0,97	0,001	0,98	0,001
PRKCA	0,83	0,004	1,15	0,001	0,82	0,005
PRKCB	0,80	0,001	1,31	0,000	0,80	0,001
PRKCE	1,74	0,000	1,73	0,000	1,67	0,000
prkcg	-3,35	0,001	-2,42	0,001	-2,49	0,001
PRKD3	1,03	0,000	0,84	0,000	0,90	0,000
PRKDC	0,55	0,005	0,53	0,006	0,63	0,003
PRPF4B	0,49	0,003	0,58	0,001	0,47	0,004
PRPF8	0,71	0,000	0,78	0,000	0,80	0,000
PRR14L	0,79	0,005	1,06	0,001	0,74	0,007
PRR29	-2,32	0,009	-3,79	0,002	-2,85	0,005
PRR36	-2,20	0,009	-2,34	0,007	-2,75	0,006
PRRC2C	0,85	0,000	0,90	0,000	0,89	0,000
PSMB1	-0,52	0,003	-0,57	0,001	-0,52	0,003

	MaxKO vs HET		MycKO vs HET		DKO vs HET	
Gene Symbol	**logFC**	**adj.P.Val**	**logFC**	**adj.P.Val**	**logFC**	**adj.P.Val**
PSMB5	-0,61	0,003	-0,71	0,001	-0,53	0,006
Psme2b	2,49	0,002	3,15	0,000	2,71	0,001
PSRC1	-1,73	0,000	-2,02	0,000	-1,75	0,000
PTBP3	0,70	0,000	0,73	0,000	0,70	0,000
PTGS1	-2,60	0,002	-3,63	0,001	-3,46	0,001
PTPN11	0,40	0,008	0,49	0,002	0,51	0,003
PTPN12	0,68	0,008	1,12	0,000	0,84	0,003
PTPN22	0,83	0,001	0,92	0,000	0,95	0,000
PTPN3	-2,13	0,001	-1,80	0,001	-1,76	0,001
PTPN4	1,13	0,003	1,32	0,001	1,25	0,002
PTPRC	1,22	0,000	1,40	0,000	1,16	0,000
PTPRJ	2,05	0,000	2,21	0,000	1,88	0,001
PUM2	0,68	0,001	0,77	0,000	0,67	0,001
PURB	0,92	0,000	0,81	0,000	0,83	0,000
PXK	0,50	0,005	0,76	0,001	0,61	0,002
PXN	0,90	0,001	1,18	0,000	0,95	0,001
PYGL	-2,26	0,002	-3,49	0,001	-3,64	0,001
Qk	0,69	0,002	0,86	0,000	0,75	0,001
R3HDM2	0,60	0,002	0,84	0,000	0,64	0,001
RAB10	0,54	0,005	0,50	0,005	0,54	0,005
RAB24	-0,60	0,006	-0,93	0,001	-0,75	0,002
RAB26	-2,89	0,004	-2,92	0,004	-3,14	0,003
RAB27A	-1,04	0,000	-1,48	0,000	-1,23	0,000
RAB30	-1,09	0,003	-0,80	0,009	-1,08	0,003
RAB5B	0,83	0,003	0,97	0,001	0,70	0,006
RAB5C	0,48	0,002	0,41	0,004	0,40	0,005
RAB8B	0,71	0,002	0,77	0,001	0,68	0,002
RABGAP1	0,62	0,003	0,59	0,004	0,62	0,003
RABGGTB	-0,68	0,006	-0,83	0,002	-0,84	0,002
RACK1	-0,90	0,000	-1,15	0,000	-0,94	0,000
RAD21	0,45	0,002	0,37	0,005	0,40	0,004
RAD54L2	0,88	0,004	0,93	0,002	0,86	0,004
RALGAPA1	0,76	0,001	0,86	0,000	0,77	0,001
RALGAPA2	0,89	0,007	1,58	0,000	1,26	0,001
RALGAPB	0,65	0,001	0,82	0,000	0,70	0,001
RANBP2	0,86	0,000	1,11	0,000	1,02	0,000
RANBP6	0,66	0,004	0,82	0,001	0,67	0,004
RAP1B	0,71	0,002	0,91	0,000	0,70	0,002
RAP1GAP	-2,00	0,000	-3,06	0,000	-2,33	0,000
RAP2C	0,69	0,001	0,65	0,001	0,67	0,002
RAPGEF2	0,84	0,010	1,48	0,000	0,89	0,008
RAPGEF5	2,06	0,001	2,37	0,000	1,95	0,001
RAPGEF6	0,92	0,001	1,03	0,000	1,00	0,001
RARA	-0,89	0,002	-1,41	0,000	-1,34	0,000
RASA1	0,55	0,005	0,53	0,005	0,50	0,008
RASD1	-3,34	0,003	-3,30	0,003	-3,26	0,003
RASGRP1	1,14	0,000	1,10	0,000	0,91	0,001
RASGRP3	1,53	0,000	2,14	0,000	1,63	0,000
RASGRP4	-1,09	0,004	-1,79	0,000	-1,54	0,001
RASIP1	-2,02	0,002	-1,16	0,009	-1,22	0,008
RASSF6	-2,12	0,006	-2,19	0,005	-2,44	0,004
RB1	0,85	0,000	1,03	0,000	0,82	0,000
RBL1	0,99	0,001	1,18	0,000	1,06	0,000
RBL2	0,51	0,003	0,66	0,001	0,52	0,003
RBM26	0,63	0,002	0,89	0,000	0,79	0,001
RBM27	0,45	0,009	0,63	0,001	0,56	0,003
RBMX	0,83	0,005	1,09	0,001	0,88	0,004
RCN2	0,74	0,003	0,84	0,001	0,76	0,002

	MaxKO vs HET		MycKO vs HET		DKO vs HET	
Gene Symbol	**logFC**	**adj.P.Val**	**logFC**	**adj.P.Val**	**logFC**	**adj.P.Val**
RDX	0,45	0,005	0,68	0,001	0,63	0,001
REEP3	0,90	0,001	0,88	0,000	0,84	0,001
RELL2	-2,13	0,003	-2,64	0,001	-1,85	0,004
REV3L	1,20	0,000	1,45	0,000	1,31	0,000
RFK	0,93	0,001	1,11	0,000	0,79	0,003
RFNG	-0,58	0,007	-0,63	0,004	-0,71	0,003
RFX5	0,99	0,001	1,20	0,000	1,07	0,001
RFX7	0,42	0,005	0,56	0,001	0,44	0,004
RGL2	-0,59	0,008	-0,69	0,003	-0,71	0,004
RGS1	-1,86	0,006	-1,55	0,009	-1,78	0,006
RGS11	-2,21	0,007	-8,02	0,006	-3,82	0,003
RHBDF1	-2,52	0,000	-1,23	0,001	-1,87	0,000
RHOA	0,53	0,001	0,48	0,001	0,42	0,003
RIF1	0,70	0,006	1,00	0,001	1,01	0,001
rilpl2	-0,87	0,000	-0,99	0,000	-0,82	0,000
RINL	-0,96	0,006	-0,93	0,006	-1,08	0,004
Rn18s-rs5	-1,42	0,002	-0,99	0,006	-1,37	0,002
RNASEH2A	-0,65	0,003	-0,72	0,001	-0,58	0,005
RNF115	0,50	0,006	0,48	0,006	0,50	0,006
rnf126	-0,62	0,002	-0,73	0,001	-0,64	0,002
RNF139	0,87	0,005	1,03	0,002	0,83	0,006
RNF144A	1,56	0,008	1,97	0,002	1,54	0,009
RNF183	-3,18	0,000	-5,37	0,000	-4,91	0,000
RNF20	0,50	0,002	0,46	0,002	0,45	0,004
RNF213	1,73	0,001	2,19	0,000	2,23	0,000
RNF38	0,68	0,003	0,87	0,001	0,71	0,003
RNF44	0,62	0,002	0,48	0,006	0,58	0,003
rnr1	-1,69	0,002	-1,61	0,002	-1,82	0,001
rnr2	-1,35	0,007	-1,40	0,005	-1,41	0,006
ROCK1	0,67	0,004	0,84	0,001	0,68	0,003
ROCK2	0,55	0,004	0,86	0,000	0,62	0,002
ROMO1	-0,64	0,007	-0,58	0,009	-0,65	0,006
RP2	0,57	0,009	1,08	0,000	0,60	0,007
RPGRIP1	-2,26	0,000	-2,62	0,000	-2,02	0,000
RPL10	-1,36	0,003	-2,00	0,000	-1,31	0,004
RPL10A	-1,19	0,000	-1,48	0,000	-1,23	0,000
Rpl10-ps3	-0,53	0,009	-0,55	0,006	-0,54	0,008
RPL11	-1,01	0,000	-1,17	0,000	-1,05	0,000
RPL12	-0,60	0,002	-1,19	0,000	-0,64	0,001
RPL13	-0,94	0,000	-1,28	0,000	-1,04	0,000
RPL13A	-0,82	0,000	-1,09	0,000	-1,02	0,000
RPL14	-1,06	0,000	-1,23	0,000	-1,00	0,000
RPL15	-0,83	0,000	-1,11	0,000	-0,93	0,000
RPL17	-0,96	0,000	-1,26	0,000	-1,10	0,000
RPL18	-1,19	0,000	-1,45	0,000	-1,23	0,000
RPL18A	-1,21	0,000	-1,25	0,000	-1,20	0,000
RPL19	-1,03	0,000	-1,13	0,000	-1,02	0,000
RPL21	-0,89	0,000	-1,00	0,000	-0,95	0,000
RPL22	-0,99	0,000	-1,24	0,000	-1,05	0,000
RPL22L1	-1,07	0,000	-1,68	0,000	-1,27	0,000
RPL23	-0,87	0,000	-1,09	0,000	-1,01	0,000
RPL23A	-1,05	0,000	-1,13	0,000	-1,06	0,000
RPL24	-1,26	0,000	-1,37	0,000	-1,23	0,000
RPL26	-1,15	0,000	-1,39	0,000	-1,27	0,000
RPL27	-1,23	0,001	-1,38	0,000	-1,15	0,001
RPL27A	-1,09	0,000	-1,22	0,000	-1,15	0,000
Rpl27-ps3	-1,00	0,000	-1,28	0,000	-1,05	0,000

	MaxKO vs HET		MycKO vs HET		DKO vs HET	
Gene Symbol	**logFC**	**adj.P.Val**	**logFC**	**adj.P.Val**	**logFC**	**adj.P.Val**
RPL28	-1,27	0,000	-1,50	0,000	-1,35	0,000
RPL3	-1,04	0,000	-1,35	0,000	-1,04	0,000
RPL30	-0,65	0,000	-0,82	0,000	-0,69	0,000
RPL31	-0,89	0,000	-1,13	0,000	-1,11	0,000
RPL32	-1,29	0,000	-1,51	0,000	-1,35	0,000
RPL34	-1,01	0,000	-1,20	0,000	-1,04	0,000
RPL35	-1,05	0,000	-1,27	0,000	-1,15	0,000
RPL35A	-0,94	0,000	-1,11	0,000	-1,09	0,000
RPL36	-1,27	0,000	-1,42	0,000	-1,34	0,000
RPL36A	-0,89	0,000	-1,34	0,000	-1,04	0,000
RPL36AL	-1,01	0,000	-1,13	0,000	-0,91	0,000
RPL37	-1,12	0,000	-1,23	0,000	-1,23	0,000
RPL37A	-0,77	0,000	-0,95	0,000	-0,98	0,000
RPL38	-0,94	0,000	-1,08	0,000	-1,00	0,000
RPL39	-0,61	0,001	-1,09	0,000	-0,90	0,000
RPL4	-0,81	0,000	-1,04	0,000	-0,77	0,000
RPL41	-0,92	0,000	-1,36	0,000	-1,11	0,000
RPL5	-0,87	0,000	-1,25	0,000	-0,94	0,000
RPL6	-0,90	0,000	-1,14	0,000	-1,00	0,000
RPL7	-0,86	0,000	-1,06	0,000	-0,93	0,000
RPL7A	-0,80	0,000	-0,97	0,000	-0,84	0,000
RPL8	-0,87	0,000	-1,18	0,000	-0,96	0,000
RPL9	-0,80	0,000	-0,93	0,000	-0,89	0,000
RPLP0	-1,04	0,000	-1,43	0,000	-0,79	0,001
RPLP1	-0,76	0,000	-1,00	0,000	-0,79	0,000
RPLP2	-0,82	0,000	-1,27	0,000	-0,92	0,000
RPP25L	-0,74	0,008	-0,69	0,010	-0,85	0,005
RPRD1B	0,60	0,002	0,64	0,001	0,58	0,003
RPRD2	0,75	0,001	0,87	0,000	0,71	0,002
RPS10	-0,90	0,000	-1,27	0,000	-1,04	0,000
RPS11	-0,68	0,001	-0,98	0,000	-0,71	0,001
RPS12	-1,28	0,000	-1,36	0,000	-1,50	0,000
Rps12-ps3	-0,99	0,000	-1,23	0,000	-0,94	0,000
RPS13	-0,93	0,000	-1,17	0,000	-0,92	0,000
RPS14	-0,98	0,000	-1,17	0,000	-1,09	0,000
RPS15	-0,78	0,000	-1,01	0,000	-0,97	0,000
rps15a	-0,88	0,000	-1,06	0,000	-1,03	0,000
RPS16	-0,93	0,000	-1,13	0,000	-0,97	0,000
RPS17	-0,92	0,000	-1,22	0,000	-1,08	0,000
RPS18	-1,18	0,000	-1,56	0,000	-1,26	0,000
RPS19	-1,02	0,000	-1,49	0,000	-1,09	0,000
RPS2	-0,82	0,000	-1,26	0,000	-0,88	0,000
RPS20	-0,89	0,000	-1,18	0,000	-0,97	0,000
RPS21	-0,64	0,001	-0,86	0,000	-0,78	0,000
rps23	-0,87	0,000	-1,09	0,000	-0,91	0,000
RPS24	-0,61	0,001	-0,72	0,000	-0,73	0,001
RPS25	-0,86	0,001	-0,93	0,000	-0,86	0,001
RPS26	-1,18	0,000	-1,29	0,000	-1,24	0,000
RPS27A	-1,25	0,000	-1,49	0,000	-1,25	0,000
RPS27L	-1,21	0,000	-1,13	0,000	-0,88	0,001
RPS28	-0,99	0,000	-1,33	0,000	-1,13	0,000
RPS29	-0,51	0,002	-0,81	0,000	-0,75	0,000
RPS3	-0,89	0,000	-1,29	0,000	-1,00	0,000
Rps3a1	-0,70	0,000	-1,02	0,000	-0,82	0,000
RPS4X	-0,73	0,000	-1,17	0,000	-0,91	0,000
RPS5	-1,01	0,000	-1,22	0,000	-1,01	0,000
RPS6	-0,97	0,000	-1,20	0,000	-1,02	0,000
RPS6KA3	0,95	0,001	1,36	0,000	1,10	0,000

	MaxKO vs HET		MycKO vs HET		DKO vs HET	
Gene Symbol	**logFC**	**adj.P.Val**	**logFC**	**adj.P.Val**	**logFC**	**adj.P.Val**
RPS7	-0,75	0,000	-0,91	0,000	-0,85	0,000
RPS8	-0,90	0,000	-1,22	0,000	-1,03	0,000
RPS9	-0,79	0,000	-1,02	0,000	-0,83	0,000
RPSA	-1,19	0,000	-1,50	0,000	-1,19	0,000
RRAGA	0,73	0,003	0,56	0,009	0,65	0,005
RRAS	-1,62	0,001	-0,77	0,009	-1,55	0,001
RRM2B	1,46	0,001	1,71	0,000	1,37	0,002
RRP1	-0,42	0,003	-0,55	0,001	-0,40	0,004
RRP1B	-0,75	0,002	-0,96	0,000	-0,54	0,008
RRP7A	-0,48	0,005	-0,79	0,000	-0,49	0,005
RSBN1L	0,79	0,002	1,02	0,000	0,80	0,002
Rsph3a	-0,81	0,005	-0,94	0,002	-0,91	0,003
RSRP1	-0,54	0,001	-0,49	0,002	-0,62	0,001
rtf1	0,58	0,001	0,54	0,001	0,51	0,002
RTP4	2,15	0,006	2,95	0,001	2,56	0,002
rubcn	0,74	0,002	0,98	0,000	0,65	0,004
RUBCNL	0,81	0,003	1,40	0,000	0,85	0,003
RUFY1	0,70	0,003	0,67	0,003	0,57	0,008
RXRA	1,75	0,001	1,65	0,001	1,64	0,001
RYR2	2,27	0,001	3,14	0,000	2,47	0,000
S1PR3	1,12	0,009	2,48	0,000	1,23	0,006
SAFB2	-0,77	0,001	-0,72	0,001	-0,92	0,000
SAMD11	-2,78	0,002	-1,57	0,007	-2,49	0,002
SAMD9L	1,72	0,000	2,34	0,000	1,83	0,000
SAMHD1	0,74	0,003	0,60	0,006	0,57	0,009
SAPCD2	-0,99	0,002	-1,01	0,002	-0,73	0,008
SARS	-0,62	0,002	-0,55	0,002	-0,50	0,005
SAV1	0,69	0,005	0,65	0,005	0,73	0,004
SBK1	1,87	0,000	1,56	0,000	1,51	0,000
sbno1	0,57	0,001	0,47	0,002	0,55	0,001
SCAF11	0,57	0,002	0,78	0,000	0,57	0,002
scaf8	0,58	0,003	0,60	0,002	0,57	0,003
SCAND1	-0,49	0,004	-0,59	0,001	-0,62	0,002
SCAPER	1,17	0,007	1,39	0,002	1,31	0,004
SCARB1	-0,77	0,004	-1,35	0,000	-0,88	0,002
Scd1	0,57	0,002	0,75	0,000	0,60	0,001
Scd2	-1,24	0,002	-2,11	0,000	-1,33	0,002
SCFD1	0,50	0,004	0,55	0,002	0,69	0,001
SDC3	1,46	0,008	1,71	0,003	1,68	0,004
SEC16A	0,36	0,008	0,67	0,000	0,62	0,001
SEC23IP	0,53	0,003	0,59	0,002	0,55	0,003
SEC31A	0,62	0,001	0,70	0,000	0,74	0,000
SEC61B	-0,89	0,002	-0,65	0,006	-0,65	0,007
SEC61G	-0,92	0,001	-1,06	0,000	-0,71	0,003
SECISBP2L	1,15	0,000	1,26	0,000	1,00	0,000
SELPLG	-0,90	0,000	-0,79	0,000	-0,69	0,001
SEMA6B	-1,82	0,002	-2,13	0,001	-2,26	0,001
SENP1	0,61	0,001	0,73	0,000	0,65	0,001
SENP5	0,86	0,003	1,09	0,001	0,94	0,002
SEP06	0,50	0,008	0,87	0,000	0,51	0,007
SERP1	0,58	0,002	0,99	0,000	0,79	0,001
Serpina3f	2,16	0,000	2,59	0,000	2,28	0,000
Serpina3g	1,16	0,000	0,91	0,001	0,81	0,002
Serpinb1a	2,31	0,002	3,29	0,000	2,63	0,001
SESN1	0,79	0,009	1,33	0,000	0,89	0,005
SESN3	0,78	0,001	1,09	0,000	0,76	0,001
SETBP1	1,37	0,000	1,49	0,000	1,45	0,000

	MaxKO vs HET		MycKO vs HET		DKO vs HET	
Gene Symbol	**logFC**	**adj.P.Val**	**logFC**	**adj.P.Val**	**logFC**	**adj.P.Val**
SETD1B	0,49	0,005	0,63	0,001	0,50	0,004
SETD2	0,91	0,000	0,95	0,000	0,88	0,000
SETX	0,40	0,006	0,88	0,000	0,49	0,002
SF3B1	0,51	0,003	0,47	0,003	0,49	0,003
sfmbt1	0,90	0,001	1,11	0,000	1,07	0,001
SFN	-1,69	0,003	-2,06	0,001	-2,03	0,002
SFT2D2	-0,59	0,001	-0,53	0,002	-0,44	0,005
SGIP1	-1,51	0,003	-1,54	0,002	-1,37	0,004
SGMS1	1,22	0,003	1,78	0,000	1,39	0,002
SGPL1	1,21	0,001	1,20	0,001	1,16	0,001
sgpp1	0,62	0,002	0,61	0,002	0,56	0,004
SH2B1	-0,96	0,006	-0,87	0,008	-0,96	0,007
SH2D2A	-1,24	0,001	-0,88	0,002	-0,87	0,002
SH3BGRL	0,93	0,000	0,95	0,000	0,93	0,000
SH3KBP1	1,00	0,000	1,30	0,000	1,00	0,000
SHANK1	1,80	0,002	1,66	0,002	1,42	0,006
SHB	-2,54	0,000	-2,49	0,000	-2,66	0,000
SHFM1	-0,55	0,003	-0,80	0,000	-0,56	0,003
SHPRH	0,83	0,001	0,85	0,000	0,77	0,001
SIGIRR	-1,22	0,000	-1,41	0,000	-1,26	0,000
SIGMAR1	-0,95	0,004	-1,08	0,002	-0,76	0,009
SIK3	0,44	0,006	0,48	0,003	0,42	0,007
SIRT1	0,65	0,003	0,79	0,001	0,67	0,003
SKAP1	2,55	0,010	3,52	0,001	2,61	0,009
SKIL	1,23	0,003	1,76	0,000	1,50	0,001
SLA	1,70	0,000	1,46	0,001	1,36	0,001
SLAIN2	0,67	0,003	0,92	0,000	0,78	0,001
SLC10A3	1,09	0,002	0,75	0,009	0,85	0,006
SLC12A2	0,70	0,005	1,08	0,000	1,05	0,001
SLC12A5	-2,48	0,004	-3,10	0,002	-2,79	0,003
SLC12A6	1,01	0,000	1,23	0,000	0,98	0,000
slc1a5	-0,98	0,000	-1,13	0,000	-0,82	0,001
SLC22A17	-2,19	0,001	-1,59	0,001	-2,01	0,001
SLC23A2	0,85	0,001	0,85	0,001	0,95	0,001
SLC25A1	-0,89	0,000	-1,34	0,000	-0,95	0,000
SLC25A10	-0,70	0,004	-0,71	0,003	-0,71	0,003
SLC25A16	1,08	0,007	1,07	0,006	1,13	0,006
SLC25A30	1,14	0,006	1,01	0,009	1,13	0,006
SLC25A4	-0,57	0,001	-0,70	0,000	-0,50	0,002
SLC28A2	0,60	0,003	0,83	0,000	0,69	0,002
SLC2A3	-0,83	0,010	-1,63	0,000	-1,12	0,003
SLC30A5	0,41	0,007	0,52	0,002	0,49	0,003
SLC31A1	-1,13	0,000	-0,91	0,001	-0,97	0,001
SLC38A1	0,64	0,001	0,53	0,003	0,73	0,001
SLC39A9	0,66	0,004	0,72	0,002	0,71	0,003
SLC43A3	-0,84	0,001	-0,71	0,001	-0,56	0,005
SLC9A5	-1,10	0,002	-1,47	0,000	-1,45	0,001
SLC9A7	1,31	0,001	1,63	0,000	1,42	0,001
SLCO4A1	-3,08	0,000	-2,16	0,000	-2,42	0,001
Slfn2	0,71	0,001	0,83	0,000	0,69	0,001
SLFN5	3,01	0,001	2,52	0,002	2,85	0,002
Slfn8	1,78	0,000	1,99	0,000	1,74	0,000
SLIT3	3,78	0,001	3,04	0,001	2,76	0,003
SLMAP	0,84	0,000	0,81	0,000	0,81	0,001
SMAD2	0,57	0,003	0,58	0,002	0,62	0,002
SMARCA5	0,49	0,005	0,51	0,003	0,57	0,003
SMARCC1	0,74	0,000	0,47	0,003	0,73	0,000
SMARCC2	0,41	0,005	0,36	0,008	0,36	0,009

	MaxKO vs HET		MycKO vs HET		DKO vs HET	
Gene Symbol	**logFC**	**adj.P.Val**	**logFC**	**adj.P.Val**	**logFC**	**adj.P.Val**
SMARCD3	-2,53	0,001	-2,44	0,000	-2,61	0,001
SMC2	0,63	0,001	0,45	0,002	0,62	0,001
SMC6	0,70	0,001	0,70	0,000	0,65	0,001
SMCHD1	0,70	0,001	1,04	0,000	0,81	0,000
SMCO4	-0,99	0,003	-1,19	0,001	-1,08	0,002
SMCR8	0,93	0,000	1,23	0,000	1,00	0,000
smek2	0,66	0,001	0,58	0,001	0,65	0,001
SMG1	0,91	0,000	1,32	0,000	0,99	0,000
SMIM14	1,65	0,000	1,96	0,000	1,56	0,000
SMIM3	-0,78	0,006	-1,86	0,000	-1,26	0,001
SMO	-1,87	0,001	-2,06	0,000	-2,43	0,000
SMOX	-2,77	0,001	-2,43	0,001	-2,63	0,001
SMYD2	-2,10	0,001	-1,62	0,001	-1,41	0,002
SNAP29	1,22	0,000	1,11	0,000	1,01	0,000
Snhg15	-1,42	0,001	-1,90	0,000	-1,43	0,001
SNHG5	-0,70	0,005	-0,88	0,002	-0,71	0,005
SNHG6	-1,05	0,006	-1,39	0,002	-1,06	0,006
SNN	1,26	0,000	1,59	0,000	1,21	0,000
SNRNP200	0,81	0,001	0,81	0,001	0,89	0,001
SNRNP25	-0,67	0,002	-0,75	0,001	-0,65	0,002
SNRNP48	-0,61	0,006	-0,66	0,003	-0,58	0,007
SNRNP70	-0,47	0,002	-0,56	0,001	-0,48	0,001
SNRPD1	-0,65	0,003	-0,65	0,002	-0,53	0,007
SNRPD2	-0,74	0,001	-0,80	0,000	-0,61	0,001
SNRPE	-0,60	0,001	-0,95	0,000	-0,73	0,001
SNRPF	-1,06	0,000	-0,98	0,000	-0,95	0,000
SNRPG	-0,74	0,003	-1,00	0,001	-0,71	0,003
SNX13	0,71	0,003	0,86	0,001	0,58	0,008
SNX19	0,51	0,004	0,61	0,001	0,50	0,005
SNX27	0,95	0,000	0,88	0,000	0,95	0,000
SNX29	1,57	0,000	1,40	0,000	1,43	0,000
SNX30	0,92	0,005	1,23	0,001	0,90	0,005
SNX9	0,64	0,001	0,64	0,001	0,63	0,001
SOCS1	0,74	0,002	0,90	0,001	0,53	0,009
SOCS4	0,86	0,003	0,95	0,001	0,84	0,003
SOCS7	0,95	0,002	1,15	0,001	0,87	0,003
SOD1	-0,68	0,001	-0,60	0,001	-0,53	0,002
SON	0,79	0,001	0,95	0,000	0,82	0,001
SORL1	2,10	0,000	2,83	0,000	2,40	0,000
SOS2	0,75	0,003	0,81	0,002	0,69	0,005
SP1	0,75	0,001	0,61	0,002	0,59	0,002
SP100	0,79	0,000	0,64	0,001	0,72	0,001
SP3	0,66	0,001	0,92	0,000	0,74	0,001
SP4	1,54	0,002	1,99	0,000	1,54	0,002
SPAG9	0,99	0,001	1,23	0,000	0,97	0,001
SPAST	0,59	0,006	0,55	0,007	0,54	0,009
SPATA5	0,94	0,002	0,68	0,007	0,93	0,002
SPECC1	2,21	0,003	4,00	0,000	2,81	0,001
SPECC1L	0,97	0,001	1,27	0,000	1,00	0,000
SPNS2	3,09	0,001	3,33	0,000	2,70	0,001
SPPL2A	0,64	0,002	0,46	0,006	0,60	0,002
SPRED1	0,83	0,004	0,80	0,004	0,82	0,005
SPRED3	-1,39	0,004	-2,01	0,001	-1,95	0,001
SPRTN	1,08	0,006	1,36	0,001	1,28	0,003
spryd3	0,83	0,003	0,73	0,005	0,75	0,005
SPSB1	-1,22	0,001	-2,58	0,000	-1,95	0,000
SPTAN1	0,71	0,000	0,58	0,000	0,63	0,000

	MaxKO vs HET		MycKO vs HET		DKO vs HET	
Gene Symbol	**logFC**	**adj.P.Val**	**logFC**	**adj.P.Val**	**logFC**	**adj.P.Val**
SPTBN1	0,81	0,000	0,83	0,000	0,83	0,000
SRCAP	1,41	0,001	1,88	0,000	1,53	0,001
SRP9	-0,56	0,002	-0,50	0,003	-0,47	0,005
SRPK3	1,36	0,003	1,74	0,001	1,25	0,004
SSFA2	0,71	0,008	0,98	0,001	0,82	0,004
SSH2	1,14	0,001	1,61	0,000	1,31	0,000
SSR4	-0,98	0,000	-0,78	0,000	-0,79	0,000
ST14	-1,55	0,000	-1,17	0,001	-1,05	0,001
ST3GAL1	1,06	0,000	1,03	0,000	0,87	0,001
ST6GALNAC6	-1,92	0,002	-2,17	0,001	-2,19	0,001
STAC2	-0,90	0,009	-1,23	0,002	-0,99	0,006
STAG1	0,91	0,000	1,03	0,000	1,00	0,000
STAG2	0,94	0,000	1,12	0,000	0,97	0,000
STAG3	2,60	0,000	-1,92	0,002	2,00	0,000
STAM2	0,77	0,003	0,78	0,003	0,80	0,003
STARD10	-0,91	0,003	-0,74	0,006	-1,05	0,002
STAT1	1,32	0,000	1,49	0,000	1,33	0,000
STAT2	0,52	0,006	0,66	0,002	0,56	0,005
STAT4	-0,50	0,005	-0,75	0,001	-0,45	0,008
STIM1	0,60	0,003	0,65	0,001	0,66	0,002
STK10	0,80	0,000	0,52	0,002	0,60	0,002
STK11	-0,56	0,003	-0,75	0,000	-0,66	0,001
STK17B	0,56	0,002	0,82	0,000	0,58	0,002
STK26	0,71	0,005	1,18	0,000	0,98	0,001
STK4	0,86	0,000	0,88	0,000	0,88	0,000
STOML2	-0,65	0,002	-0,66	0,002	-0,51	0,007
STRN	0,86	0,001	0,98	0,000	0,86	0,001
stx1a	-1,04	0,007	-1,50	0,002	-1,47	0,002
STXBP2	-0,51	0,002	-0,71	0,000	-0,64	0,001
SUB1	-0,79	0,001	-0,94	0,000	-0,81	0,001
SUCO	0,72	0,004	1,17	0,000	0,86	0,002
SUMF1	0,91	0,002	0,90	0,002	0,83	0,004
SUMO1	-0,59	0,002	-0,71	0,001	-0,62	0,002
SUN2	0,70	0,001	0,81	0,000	0,62	0,002
Supt16	0,70	0,001	0,54	0,001	0,68	0,001
Supt4a	-0,76	0,002	-0,88	0,001	-0,74	0,002
SUZ12	0,79	0,000	0,70	0,000	0,73	0,000
SWAP70	0,51	0,005	0,81	0,000	0,55	0,004
SYDE2	-1,63	0,006	-1,84	0,003	-1,59	0,006
SYK	1,09	0,000	1,05	0,000	0,78	0,001
syne3	1,26	0,000	1,12	0,001	1,22	0,001
SYNRG	0,96	0,000	1,15	0,000	0,94	0,000
Sypl	1,29	0,000	1,52	0,000	1,24	0,000
TAB3	0,73	0,008	1,06	0,001	0,85	0,004
TACC1	0,90	0,001	0,73	0,002	0,79	0,001
TAF3	0,53	0,008	0,60	0,004	0,58	0,006
TAF9B	1,35	0,001	1,12	0,001	1,12	0,001
Tagap1	-0,64	0,002	-0,49	0,005	-0,66	0,002
TAOK3	0,73	0,001	0,56	0,002	0,63	0,002
TAP1	0,42	0,006	0,52	0,002	0,45	0,004
TAPBP	0,82	0,000	0,98	0,000	0,90	0,000
TAPBPL	0,55	0,005	0,66	0,002	0,69	0,002
TAX1BP1	0,43	0,007	0,63	0,001	0,43	0,007
TBC1D2	-1,20	0,007	-1,41	0,004	-1,13	0,009
TBC1D4	-2,16	0,001	-1,64	0,002	-1,76	0,002
TBC1D5	1,12	0,001	1,01	0,001	0,92	0,002
TBL1XR1	0,86	0,003	1,13	0,000	0,90	0,002
TBXA2R	-2,59	0,002	-1,46	0,010	-2,30	0,003

	MaxKO vs HET		MycKO vs HET		DKO vs HET	
Gene Symbol	**logFC**	**adj.P.Val**	**logFC**	**adj.P.Val**	**logFC**	**adj.P.Val**
TCF12	1,11	0,000	1,33	0,000	1,25	0,000
tcf20	0,78	0,001	0,99	0,000	0,79	0,001
TCF3	-0,74	0,001	-0,75	0,001	-0,81	0,001
TCIRG1	-0,86	0,001	-0,56	0,004	-0,89	0,001
TCP1	-0,59	0,001	-0,75	0,000	-0,50	0,002
TDRD7	1,11	0,003	1,31	0,001	0,97	0,005
TECR	-0,65	0,001	-0,63	0,001	-0,65	0,001
TGFBR2	1,12	0,001	1,68	0,000	1,26	0,000
TGFBRAP1	0,99	0,001	1,04	0,000	1,06	0,001
Tgoln1	0,68	0,001	0,61	0,001	0,65	0,001
TGS1	0,62	0,002	0,54	0,004	0,55	0,004
Tgtp1	2,79	0,001	3,08	0,001	2,90	0,001
Tgtp2	2,87	0,001	3,17	0,000	2,94	0,001
tha1	-1,47	0,002	-3,62	0,000	-2,52	0,000
THADA	0,99	0,001	0,94	0,001	1,16	0,001
THOC2	0,61	0,001	0,64	0,001	0,56	0,002
THOC7	-0,50	0,009	-0,67	0,002	-0,59	0,004
THRAP3	0,66	0,004	0,69	0,003	0,70	0,003
TIMM13	-0,64	0,004	-0,95	0,000	-0,67	0,003
TIMM44	-0,48	0,004	-0,62	0,001	-0,47	0,005
TJP2	-0,72	0,004	-0,74	0,003	-0,59	0,008
TK1	-0,55	0,001	-0,95	0,000	-0,65	0,001
TKT	-0,71	0,001	-0,93	0,000	-0,62	0,001
TLE2	-1,51	0,001	-1,90	0,000	-2,05	0,000
TLE3	0,90	0,001	0,60	0,005	0,62	0,005
TLK1	0,76	0,003	0,83	0,001	0,77	0,003
TLN1	0,54	0,001	0,61	0,000	0,56	0,001
TLR1	0,71	0,002	0,94	0,000	0,60	0,004
TLR7	1,08	0,000	0,95	0,000	1,00	0,000
TLR9	2,04	0,000	2,61	0,000	1,96	0,000
TM9SF2	0,54	0,005	0,60	0,002	0,61	0,003
TMBIM1	-1,71	0,002	-1,93	0,001	-1,64	0,002
TMCC3	1,65	0,003	2,29	0,000	1,75	0,002
TMEM108	-2,62	0,000	-1,67	0,000	-2,12	0,000
TMEM123	1,03	0,000	1,16	0,000	0,98	0,000
TMEM131	0,92	0,001	0,57	0,004	0,65	0,003
tmem141	-3,31	0,007	-2,64	0,010	-3,13	0,007
TMEM147	-0,50	0,008	-0,59	0,003	-0,49	0,008
TMEM160	-0,83	0,001	-0,80	0,000	-0,68	0,001
TMEM167B	0,75	0,004	0,88	0,001	0,75	0,004
TMEM168	0,89	0,003	1,08	0,001	0,91	0,003
TMEM171	-3,34	0,003	-3,33	0,002	-2,54	0,005
TMEM176A	-2,22	0,000	-2,35	0,000	-2,09	0,000
TMEM176B	-2,15	0,001	-2,24	0,000	-1,83	0,001
TMEM184B	0,73	0,001	0,49	0,007	0,72	0,001
TMEM205	-1,68	0,010	-1,86	0,006	-1,68	0,010
TMEM208	-0,57	0,006	-0,55	0,006	-0,58	0,006
TMEM209	0,93	0,001	0,80	0,002	0,96	0,001
TMEM230	0,67	0,009	0,65	0,008	0,66	0,009
TMEM238	-1,66	0,003	-1,51	0,003	-1,30	0,007
TMEM256	-1,06	0,000	-0,89	0,000	-1,06	0,000
TMEM259	-0,65	0,002	-0,60	0,002	-0,72	0,001
TMEM260	1,60	0,002	1,24	0,007	1,43	0,004
TMSB10	-0,72	0,005	-1,05	0,001	-0,91	0,002
TMSB4X	-0,44	0,006	-0,66	0,001	-0,71	0,001
TNFRSF13B	1,09	0,000	1,36	0,000	1,12	0,000
Tnfrsf26	-1,06	0,002	-0,98	0,003	-1,06	0,002

	MaxKO vs HET		MycKO vs HET		DKO vs HET	
Gene Symbol	**logFC**	**adj.P.Val**	**logFC**	**adj.P.Val**	**logFC**	**adj.P.Val**
TNFSF14	-3,32	0,001	-2,59	0,001	-2,76	0,001
TNFSF15	3,96	0,009	3,98	0,007	3,97	0,009
TNFSF9	-1,78	0,001	-2,41	0,000	-1,93	0,001
TNIP2	-0,87	0,002	-1,12	0,000	-1,09	0,001
TNKS	1,84	0,000	1,95	0,000	1,96	0,000
TNKS2	0,49	0,002	0,52	0,001	0,53	0,002
TNNT1	-1,97	0,005	-2,45	0,002	-1,59	0,010
TNP2	-1,54	0,007	-2,49	0,001	-2,23	0,002
TNRC18	0,50	0,008	0,52	0,006	0,51	0,008
TNRC6B	0,82	0,004	1,29	0,000	0,93	0,002
TNRC6C	0,72	0,001	0,87	0,000	0,75	0,001
TOMM20	-0,63	0,002	-0,59	0,002	-0,47	0,007
TOP2B	0,73	0,001	0,75	0,000	0,68	0,001
TOR1AIP1	0,97	0,000	1,19	0,000	0,99	0,000
TPGS1	-0,70	0,004	-0,67	0,004	-0,75	0,003
TPI1	-1,04	0,009	-3,21	0,000	-1,55	0,002
TPP1	0,61	0,002	0,87	0,000	0,65	0,001
TPR	0,50	0,002	0,46	0,002	0,51	0,002
TRABD	-0,73	0,001	-0,63	0,002	-0,69	0,002
TRAF3	0,88	0,002	0,98	0,001	0,77	0,004
TRAFD1	0,78	0,001	0,79	0,001	0,76	0,002
TRAK2	0,78	0,005	1,01	0,001	0,81	0,004
TRAPPC10	0,53	0,004	0,55	0,002	0,53	0,004
TRAPPC5	-0,57	0,008	-0,63	0,004	-0,59	0,007
TRAPPC6A	-0,99	0,001	-2,08	0,000	-1,22	0,001
TRAPPC8	0,69	0,006	0,88	0,001	0,74	0,004
TRAPPC9	0,83	0,002	0,84	0,001	0,73	0,003
Trbc2	2,51	0,004	3,31	0,001	2,76	0,002
Trim12c	1,04	0,001	1,13	0,000	1,04	0,001
TRIM14	1,67	0,000	1,50	0,000	1,56	0,000
TRIM21	1,27	0,001	1,38	0,000	1,12	0,001
TRIM26	0,56	0,003	0,50	0,004	0,48	0,006
Trim30a	0,88	0,000	1,13	0,000	1,13	0,000
Trim30c	3,42	0,002	2,86	0,003	3,09	0,003
TRIM44	0,88	0,000	0,55	0,004	0,87	0,000
TRIM46	-2,34	0,000	-3,02	0,000	-2,88	0,000
TRIM56	0,79	0,001	1,09	0,000	0,73	0,001
TRIP11	0,66	0,007	0,90	0,001	0,73	0,005
TRIP12	0,76	0,000	0,76	0,000	0,71	0,000
Trp53bp1	0,74	0,001	0,58	0,001	0,73	0,001
TRPM4	-1,51	0,002	-1,91	0,001	-1,95	0,001
TRPM7	0,55	0,005	0,70	0,001	0,63	0,003
TSC1	0,69	0,002	0,77	0,001	0,72	0,002
TSC22D2	0,78	0,003	1,02	0,001	0,91	0,002
TSEN54	-0,78	0,006	-1,06	0,001	-0,77	0,007
TTBK2	1,33	0,001	1,72	0,000	1,48	0,000
ttc21a	-1,47	0,000	-3,33	0,000	-1,60	0,000
TTC3	0,91	0,002	1,01	0,001	0,94	0,002
TTC37	1,05	0,003	1,25	0,001	1,14	0,002
TTC39B	0,98	0,004	1,00	0,003	0,87	0,008
ttc41	-2,23	0,001	-1,55	0,003	-1,45	0,004
Ttc7	0,82	0,001	0,91	0,000	0,87	0,000
TTLL3	-1,09	0,006	-1,42	0,002	-1,29	0,003
ttll5	0,71	0,004	0,75	0,002	0,72	0,004
TUBB4A	-1,84	0,007	-1,86	0,006	-1,99	0,006
TUBB6	-1,75	0,000	-1,02	0,002	-0,79	0,008
TUFM	-0,70	0,002	-0,83	0,001	-0,61	0,004
TUT1	-0,55	0,010	-0,78	0,002	-0,58	0,008

	MaxKO vs HET		MycKO vs HET		DKO vs HET	
Gene Symbol	**logFC**	**adj.P.Val**	**logFC**	**adj.P.Val**	**logFC**	**adj.P.Val**
TYRO3	-2,21	0,001	-2,11	0,001	-2,15	0,001
U2AF1	-0,66	0,001	-0,79	0,000	-0,56	0,002
U2SURP	0,42	0,005	0,36	0,010	0,42	0,005
UBA52	-1,52	0,000	-1,54	0,000	-1,54	0,000
UBA6	0,59	0,005	0,62	0,003	0,65	0,003
uba7	0,82	0,003	1,14	0,000	0,82	0,003
UBAP2L	0,64	0,000	0,45	0,002	0,61	0,001
UBASH3B	1,27	0,000	1,34	0,000	1,06	0,000
UBE2C	-0,49	0,004	-0,80	0,000	-0,47	0,005
UBE3A	0,81	0,001	1,05	0,000	0,85	0,001
UBQLN2	0,48	0,009	0,70	0,001	0,58	0,004
UBR1	0,79	0,001	1,05	0,000	0,89	0,001
UBR4	0,65	0,001	0,92	0,000	0,86	0,000
UBR5	0,84	0,000	0,84	0,000	0,91	0,000
UBXN11	-0,78	0,010	-1,36	0,001	-0,98	0,004
UBXN2A	0,82	0,002	0,94	0,001	0,95	0,001
UCHL5	-0,78	0,005	-0,74	0,005	-0,73	0,007
UCK2	-1,43	0,001	-1,16	0,002	-0,96	0,005
UHMK1	1,03	0,000	0,78	0,000	0,87	0,000
ULK2	0,92	0,002	0,89	0,002	0,76	0,005
UNC13A	-2,59	0,001	-3,11	0,000	-2,47	0,001
unc93b1	0,58	0,004	1,18	0,000	0,66	0,002
UPRT	1,77	0,006	1,92	0,003	2,06	0,003
Uqcr10	-0,61	0,002	-0,64	0,001	-0,60	0,002
Uqcrh	-0,69	0,001	-0,87	0,000	-0,80	0,000
Uqcrq	-0,63	0,002	-0,67	0,001	-0,58	0,003
URB1	0,50	0,005	0,44	0,008	0,74	0,001
USB1	0,77	0,005	0,93	0,001	0,78	0,005
USE1	-0,46	0,006	-0,41	0,009	-0,58	0,002
USF3	0,99	0,000	1,07	0,000	0,93	0,001
USMG5	-0,65	0,002	-0,80	0,000	-0,66	0,001
USP1	0,52	0,005	0,45	0,008	0,55	0,004
USP11	1,10	0,001	1,18	0,001	1,10	0,001
USP12	0,79	0,001	0,92	0,000	0,75	0,002
USP22	0,68	0,003	0,77	0,001	0,83	0,001
USP24	0,91	0,000	1,14	0,000	1,00	0,000
USP25	1,15	0,000	1,29	0,000	1,09	0,000
USP31	1,15	0,008	1,25	0,005	1,27	0,005
USP32	0,97	0,001	1,22	0,000	0,94	0,001
USP34	1,06	0,000	1,37	0,000	1,20	0,000
USP35	-1,09	0,002	-0,78	0,007	-1,47	0,001
USP45	0,94	0,001	0,86	0,001	0,92	0,001
USP47	0,43	0,006	0,60	0,001	0,53	0,002
USP8	0,62	0,003	0,73	0,001	0,69	0,002
USP9X	0,77	0,001	1,05	0,000	0,87	0,000
UTP20	0,98	0,000	0,51	0,003	0,99	0,000
vash1	2,04	0,002	2,43	0,001	2,06	0,002
VCPIP1	0,84	0,001	1,02	0,000	0,85	0,001
VCPKMT	-0,79	0,010	-0,78	0,009	-0,86	0,007
VDAC1	-0,52	0,004	-0,74	0,001	-0,50	0,005
VDR	-1,87	0,001	-2,21	0,001	-2,00	0,001
VEGFA	-2,19	0,003	-2,54	0,001	-2,20	0,003
VEGFB	-0,75	0,005	-0,94	0,002	-0,83	0,003
VEZF1	0,78	0,003	1,10	0,000	0,81	0,003
VPREB3	-1,55	0,000	-1,55	0,000	-1,90	0,000
VPS13A	1,10	0,001	1,29	0,000	1,15	0,000
VPS13B	1,20	0,000	1,28	0,000	1,22	0,000

	MaxKO vs HET		MycKO vs HET		DKO vs HET	
Gene Symbol	**logFC**	**adj.P.Val**	**logFC**	**adj.P.Val**	**logFC**	**adj.P.Val**
VPS13C	1,20	0,000	1,63	0,000	1,43	0,000
VPS13D	0,82	0,000	1,25	0,000	0,90	0,000
VPS33A	0,65	0,002	0,56	0,004	0,61	0,003
VPS4B	0,64	0,001	0,56	0,001	0,57	0,002
VPS8	0,64	0,006	0,75	0,002	0,74	0,003
Vsir	-0,80	0,004	-0,69	0,007	-0,68	0,008
VWA5A	1,19	0,001	1,03	0,002	1,19	0,001
VWA8	0,69	0,003	0,70	0,003	0,71	0,003
WAC	0,57	0,001	0,73	0,000	0,56	0,001
WAPL	0,40	0,008	0,37	0,010	0,40	0,008
WASF2	0,87	0,001	0,93	0,001	0,84	0,001
WBSCR27	-1,38	0,001	-2,77	0,000	-1,60	0,001
WDFY2	2,57	0,001	2,27	0,001	2,40	0,001
WDFY4	0,85	0,000	0,60	0,002	0,74	0,001
WDR44	1,05	0,002	1,31	0,001	1,11	0,002
WDR7	1,15	0,001	0,97	0,001	1,00	0,001
WDR81	0,88	0,000	0,44	0,007	0,68	0,001
WDSUB1	1,10	0,006	1,17	0,004	1,18	0,005
WDTC1	1,12	0,000	0,97	0,000	0,98	0,000
WHAMM	-0,73	0,007	-0,67	0,008	-0,80	0,005
whsc1l1	0,57	0,002	0,73	0,000	0,58	0,002
WNK1	0,68	0,001	1,05	0,000	0,82	0,001
XBP1	-1,48	0,000	-0,89	0,002	-0,89	0,002
XIAP	1,09	0,000	1,08	0,000	1,02	0,000
XPO4	1,24	0,005	1,63	0,001	1,64	0,001
XRCC1	-0,79	0,001	-1,02	0,000	-0,74	0,002
XRCC5	0,75	0,007	0,98	0,001	1,09	0,001
XRN1	1,05	0,005	1,17	0,002	1,10	0,004
XRN2	0,71	0,001	0,45	0,006	0,75	0,001
XYLT2	-1,04	0,001	-1,01	0,001	-1,15	0,001
YBX3	-1,27	0,000	-0,68	0,001	-0,62	0,002
YDJC	-2,18	0,000	-1,63	0,001	-1,47	0,001
YIPF3	-0,61	0,002	-0,60	0,001	-0,60	0,002
YLPM1	0,50	0,003	0,55	0,002	0,52	0,003
YME1L1	0,50	0,007	0,57	0,003	0,56	0,004
YTHDC2	0,77	0,001	0,93	0,000	0,87	0,001
YWHAZ	0,37	0,006	0,38	0,004	0,39	0,005
ZBP1	1,26	0,001	1,33	0,000	1,31	0,000
zbtb18	0,89	0,000	0,70	0,000	0,63	0,001
ZBTB33	0,94	0,000	0,83	0,001	0,94	0,000
ZBTB37	1,47	0,004	1,86	0,001	1,61	0,003
ZBTB4	1,26	0,001	1,56	0,000	1,13	0,001
ZBTB41	1,02	0,002	1,12	0,001	1,09	0,002
ZBTB43	0,70	0,006	0,79	0,003	0,70	0,006
ZBTB46	-1,55	0,002	-1,58	0,002	-1,50	0,003
ZBTB6	0,75	0,008	0,89	0,003	0,77	0,008
ZC3HAV1	0,85	0,000	0,85	0,000	0,85	0,000
ZCCHC11	1,01	0,000	1,23	0,000	1,07	0,000
ZCCHC2	0,81	0,006	1,09	0,001	0,98	0,002
ZCCHC6	0,90	0,000	1,18	0,000	0,88	0,000
ZDHHC20	0,65	0,002	0,66	0,001	0,54	0,004
ZDHHC5	0,52	0,004	0,55	0,002	0,52	0,004
ZEB2	1,88	0,003	1,88	0,002	1,68	0,005
ZFAND2B	-0,66	0,005	-0,65	0,005	-0,77	0,003
ZFP106	0,37	0,006	0,43	0,002	0,46	0,002
Zfp110	0,63	0,002	0,67	0,001	0,72	0,001
Zfp148	0,57	0,003	0,74	0,001	0,48	0,007
Zfp236	0,73	0,002	1,11	0,000	0,82	0,001

	MaxKO vs HET		MycKO vs HET		DKO vs HET	
Gene Symbol	**logFC**	**adj.P.Val**	**logFC**	**adj.P.Val**	**logFC**	**adj.P.Val**
Zfp280d	0,56	0,003	0,67	0,001	0,65	0,001
Zfp281	0,69	0,004	1,05	0,000	0,67	0,004
Zfp292	0,84	0,002	0,70	0,003	0,67	0,005
Zfp318	0,87	0,003	1,04	0,001	0,86	0,003
Zfp395	-0,77	0,006	-1,22	0,001	-1,07	0,002
Zfp397	0,68	0,005	0,72	0,003	0,65	0,006
Zfp407	0,98	0,001	1,10	0,001	0,91	0,002
Zfp445	0,92	0,002	1,01	0,001	0,95	0,002
Zfp473	-1,33	0,008	-1,47	0,005	-1,63	0,004
Zfp507	1,04	0,001	1,05	0,000	1,05	0,001
Zfp541	-4,58	0,003	-4,68	0,002	-3,18	0,005
ZFP57	-3,43	0,007	-4,33	0,004	-3,07	0,009
Zfp597	1,01	0,001	1,01	0,001	0,91	0,002
Zfp608	0,58	0,001	1,07	0,000	0,60	0,001
Zfp609	0,77	0,003	0,70	0,004	0,79	0,002
Zfp651	-2,06	0,002	-1,45	0,005	-1,32	0,008
Zfp692	-1,06	0,001	-1,06	0,000	-1,10	0,001
Zfp831	1,44	0,004	1,74	0,001	1,40	0,004
Zfp871	1,89	0,001	1,97	0,001	1,96	0,001
ZFP91	0,62	0,002	0,62	0,002	0,57	0,004
ZFR	0,48	0,004	0,49	0,003	0,42	0,007
ZHX1	0,78	0,001	0,72	0,001	0,61	0,003
ZKSCAN8	1,34	0,007	1,31	0,007	1,36	0,007
ZMAT3	-1,33	0,002	-1,30	0,001	-1,10	0,003
ZMYM2	0,53	0,006	0,85	0,000	0,57	0,005
ZMYND11	0,56	0,004	0,52	0,005	0,48	0,008
ZNFX1	1,02	0,001	1,07	0,000	1,07	0,000
ZNRF2	0,97	0,000	0,57	0,002	0,75	0,001
ZXDB	0,65	0,008	0,76	0,003	0,80	0,003
ZYG11B	0,53	0,004	0,56	0,003	0,54	0,004
ZZEF1	0,86	0,001	0,91	0,000	0,97	0,000